Title
Neural Regulation of Hunger and Thirst in Drosophila melanogaster

Author
Jourjine, Nicholas

Publication Date
2018

Peer reviewed|Thesis/dissertation

Neural Regulation of Hunger and Thirst in *Drosophila melanogaster*

By

Nicholas W. Jourjine

A dissertation submitted in partial satisfaction of the

requirements for the degree of

Doctor of Philosophy

in

Molecular and Cell Biology

in the

Graduate Division

of the

University of California, Berkeley

Committee in charge:

Professor Kristin Scott, Chair
Professor Diana Bautista
Professor Neil Tsutsui
Professor Marla Feller

Spring 2018

ABSTRACT

Neural Regulation of Hunger and Thirst in *Drosophila melanogaster*

By

Nicholas W. Jourjine

Doctor of Philosophy in Molecular and Cell Biology

University of California, Berkeley

Professor Kristin Scott, Chair

Eating food and drinking water are fundamental requirements for animal survival. Understanding how animal nervous systems regulate these behaviors has been a focus of neuroscience research for over a century. Until recently, however, a lack of experimental tools has made it challenging to identify the molecules and neurons that orchestrate food and water ingestion behaviors. Here, I use the fruit fly *Drosophila melanogaster* as a model to identify such molecules and neurons. I find that a group of four neurons regulates both food and water ingestion in *Drosophila*, and that they accomplish this by co-expression of molecules that confer on them sensitivity to internal signals of both hunger and thirst.

In the first part of this dissertation (chapter 2), I describe the discovery of a novel group of neurons in the *Drosophila* brain, and show that they are regulators of both food and water ingestion. This work is presented in the form of a published co-first author manuscript. Using genetic tools, behavioral assays, and calcium imaging, I show, together with co-authors Brendan Mullaney and Kevin Mann, that these neurons, which we name ISNs (Interoceptive SEZ Neurons), are sensitive both to an internal signal of nutrient deprivation, the glucagon-like peptide adipokinetic hormone (AKH), and an internal signal of water abundance, extracellular osmolality. We further show that this dual sensitivity arises because ISNs co-express a G-protein coupled receptor, the adipokinetic hormone receptor (AKHR), and a conserved TRPV channel, Nanchung (Nan), which act as molecular sensors of AKH and osmolality, respectively. Finally, we show that ISN activity is sufficient to regulate both sugar and water consumption in a manner that promotes homeostasis.

In the second part of this dissertation (chapter 3), I use a combination of behavioral genetics and calcium imaging to characterize neural circuits downstream of ISNs. I show that ISNs likely express and release the peptide dILP-3, an insulin-like peptide, and determine the anatomy of neurons post-synaptic to ISNs. Finally, I use large-scale calcium imaging to characterize how AKH (and, by extension, ISN activity) modulates neural responses to the taste of sugar and water.

In the final part of this dissertation (chapter 4), I place the above results in the context of mammalian studies of food and water ingestion. I argue that understanding how nervous systems regulate the ingestion of food and water will require a deeper understanding of the interactions between neural regulators of these behaviors. This work is presented as a published first author manuscript.

TABLE OF CONTENTS

ACKNOWLEDGEMENTS

This work would not have been possible without years of support, advice, and resources provided by my dissertation adviser, Kristin Scott. Thank you. I could not have asked for a better scientific mentor. It also would not have been possible without the daily conversation (scientific and otherwise), parties (scientific and otherwise), and birthday cakes (mostly non-scientific) of all the members of the Scott lab 2012-2018: Allan-Hermann Pool, Rob Thistle, Kevin Mann, Heesoo Kim, Hyesoo Youn, Ben Kallman, Allen Wang, Colleen Kirkhart, Samantha Cheung, Dave Harris, Justine Chia, Stefanie Engert, Molly Kirk, Meghan Laturney, Sarah Leinwand, Salil Bidaye, Zepeng Yao, Christoph Scheper, Phil Shiu, and Carolina Reisenman. I would especially like to thank Brendan Mullaney, who collaborated on key elements of this dissertation, and who helped guide me through some of the most challenging times of my PhD. Several excellent rotation students also contributed to the work presented here: Justine Chia, Dan Kramer, Melissa Metcalf, Amanda González-Segarra, and Hayley Bounds. Finally, and most importantly, I would like to thank my parents: my mom for showing me the beauty of the natural world, and my dad for showing me the beauty of studying it.

I would like to dedicate this dissertation to my parents, who taught me about art and science, and to Helen Kurkjian, who is my colleague and my love.

Chapter 1: Introduction

Homeostasis and animal behavior

Living things maintain a stable internal environment despite changes in the external world. This fundamental property, which the physiologist Walter Cannon termed "homeostasis" in 1936, is a central concept in the biological sciences, and understanding the mechanisms that give rise to homeostasis has been a major goal of biological research since antiquity (*1*).

One of the key results of this research is that homeostasis is an emergent property of complex interactions between molecules, cells, and the environment (*2*). For example**,** unicellular organisms maintain their internal chemical environment via stable feedback loops involving transcription factors and signaling molecules. Likewise, plants maintain nutrient homeostasis via stable feedback loops between photosynthetic cells in shoots and non-photosynthetic cells in roots (*4*).

Similar systems of feedback loops are also an essential aspect of homeostasis among multicellular animals. Animals with nervous systems are unique, however, in that homeostasis also requires neural circuits to organize and direct animal behavior. These behaviors are in some cases highly specialized. For example, to maintain stable body temperature, cold-blooded animals depend on nervous systems to drive the exploration of temperature gradients in their environment. Likewise, to maintain internal oxygen homeostasis, aquatic vertebrates depend on nervous systems to explore regions with sufficient levels of dissolved oxygen, and to reduce movement when oxygen levels are low (*5*). Nearly all animals, however, depend on nervous systems to regulate two ancient and essential homeostatic behaviors: the ingestion of food and the ingestion of water. In the absence of these behaviors, sugars metabolized by cells and water lost to evaporation cannot be replenished, metabolic homeostasis is lost, and death quickly ensues. Thus, food and water ingestion are essential behaviors for metabolic homeostasis and animal survival.

To regulate food and water ingestion in a manner that promotes metabolic homeostasis, nervous systems must not only be able to detect levels of multiple internal nutrients (e.g. water and glucose), but also use information about those levels to regulate appropriate ingestive behaviors. Understanding the mechanisms by which nervous systems accomplish this task is a major unanswered question in neuroscience. In this chapter, I briefly review the history of research into the neural regulation food and water ingestion, outline recent discoveries in the field, and motivate the central questions of this dissertation: what are the molecular mechanisms by which nervous systems detect internal signals of metabolic need? How do they use those signals to organize and direct behavior?

Homeostatic models of animal behavior

In the late 19th and early 20th centuries, the physiologists Claude Bernard and Walter Cannon used principles from engineering control theory to described homeostatic behaviors as feedback loops between nervous system components that monitored an animal's internal state and components that directed behaviors influencing those states (*6*-*8*). At the core of these models was the notion that organisms maintained key internal variables, such as blood osmolality and sugar abundance, at a "set point" compatible with survival. Thus, a central function of the nervous system in these models was to detect deviations in set points and generate behaviors that resulted in those deviations being corrected.

These simple homeostatic models were later extended by behavioral neuroscientists such as Konrad Lorenz, and behavioral psychologists such as Edward Tolman and Clark Hull (*9-11*). Specifically, the models proposed by these scientists sought to incorporate the notion of motivation or "drive" to explain purposive, goal-directed behaviors such as eating food and drinking water. According to these models, drives were the psychological states, such as thirst and hunger, that organized and gave purpose to these behaviors. Drives depended on internal physiological variables (as, for example, thirst depends on blood osmolality), but they were also distinct from those variables because, as psychological states, they resulted from the integration of information about multiple aspects of internal state as well as the external world (*12*). For example, the drive to ingest water might depend not just on an organism's blood osmolality, but also its body temperature, internal sugar abundance, or whether it is experiencing other psychological states such as fear or hunger. Thus, unlike earlier models of homeostatic behavior, drive models emphasized the need for the nervous system to integrate information about multiple internal variables, then use that information to produce a behavioral output.

Molecular and cellular mechanisms underlying homeostatic behaviors

The homeostatic models of animal behavior described above motivated a search for biological mechanisms that could implement the error detection, negative feedback loops, and information integration these models required. This search quickly led to the discovery of numerous molecular signals of physiological state that acted on the nervous system to influence behavior. These signals included direct readouts of metabolic processes, such as glucose and amino acids, as well as indirect signals, such as the neuropeptide CCK, which is secreted by the gut and functions as a signal of food satiety (*13*). Some of these signals were shown to interact with each other in complex and surprising ways. For example, the release of vasopressin, a neuropeptide that strongly promotes water ingestion, was shown to be caused by CCK, the gut peptide mentioned above that functions to suppress appetite (*14*). In addition to peptides and metabolites, many physical properties of an organism's internal environment were found to be directly sensed by the nervous system. For example, Bourque and colleagues showed that neurons in the mammalian hypothalamus are acutely sensitive to changes in blood osmolality, and that the mechanism underlying this sensitivity involves mechanosensitive ion channels (*15*).

Thus, signals of internal metabolic state include multiple neuropeptides, diverse chemical metabolites, and physical properties of the extracellular environment, and these signals can interact with each other in complex ways. How do nervous systems integrate and weigh these diverse signals to produce organized, goal-directed behavioral outputs? Early studies sought to answer this question with experiments in which specific brain regions were ablated or electrically stimulated and the effect on homeostatic behaviors was observed (*16*). These studies identified specific regions in the hypothalamus, a conserved mammalian forebrain region, as being necessary and sufficient to generate either food or water ingestion behavior. These results led to the hypothesis that the hypothalamus was the anatomical location of at least some of the biological drives proposed by Lorenz, Hull, and others (*16*).

However, the manipulations carried out in these studies lacked cell type specificity, and the behavioral phenotypes they produced were often difficult to interpret. Advances in genetic tools to manipulate and monitor neural activity have overcome these limitations in the last several decades. While in many cases these tools have corroborated early studies (for example, the claim that the hypothalamus plays a key role in regulating food and water ingestion), they

have also led to surprising insights with implications for the kinds of homeostatic control models animal nervous systems implement. For example, as I describe in detail in chapter 4, Knight and colleagues have used *in vivo* calcium imaging in behaving animals to show that the sight or smell of food is sufficient to rapidly modulate activity in internal sensors of nutrient abundance prior to any nutrients actually being ingested (*17*). Thus, models of animal behavior proposed by Lorenz, Hull, and others will likely need to be updated to incorporate these anticipatory mechanisms.

A current challenge in neuroscience is to understand how nervous systems integrate information about diverse internal physiological signals, and how they use that information in combination with sensory experience to organize goal-directed behaviors. Specifically, how are nervous systems organized so that they can make sense of the long list of internal physiological signals that have been identified to date? How do nervous systems organize behavioral outputs so that multiple, sometimes competing, internal needs can be met?

Drosophila melanogaster as a tool to understand mechanisms of homeostatic behavior

The fruit fly *Drosophila melanogaster* is in many ways an ideal tool to address these questions. First, water deprivation specifically motivates *Drosophila* to seek out and consume water, while food deprivation specifically motivates flies to seek and consume sugar (*18*). Thus, fruit flies, like humans and other mammals, exhibit specific appetites for food and water that depend on the internal metabolic need for food and water. Second, despite having a nervous system that differs in organization from that of mammals, *Drosophila* use many of the same peptide molecules and circuit motifs to regulate internal nutrient abundance (*19*). For example, fruit flies use insulin and the insulin receptor to drive nutrient uptake from the hemolymph (insect blood) in fed states, and use an antagonistic peptide, adipokinetic hormone (AKH), to drive nutrient release in starved states, a function that is directly analogous to mammalian glucagon (the similarity is so strong that AKH is sometimes referred to as glucagon even though the two peptides are not strictly homologous (*20*)). Finally, genetic tools available in *Drosophila* make it possible to monitor and manipulate neural activity, as well as to quantify behavior, in a manner not possible in other genetic model organisms.

In the last several years, our lab and others have used these tools to gain insight into molecules and neurons underlying food and water ingestion behavior in *Drosophila*. One theme that has emerged from this research is that, despite the relative simplicity of their nervous systems, *Drosophila*, like mammals, use an incredibly diverse array of peptides, metabolites, and neuromodulators to represent internal nutritional states. These include eight different homologs of the human insulin peptide, the peptides allatostatinA, hugin, adipokinetic hormone (AKH), corazonin, leucokinin, drosulfakinin, diuretic hormone-44 (Dh44), unpaired-2 (Upd-2), short neuropeptide F (sNPF), CCH-amide2 (CCH-a2)**,** the neuromodulators octopamine and dopamine, and the metabolites fructose and glucose (*13*). Many of these peptides are direct or functional homologs of mammalian counter-parts. For example, Dh44 appears to be the homolog of mammalian corticotropin-releasing hormone (CRH), which, like Dh44, has been proposed to play an important role in detecting circulating glucose (*21*), and Upd-2 is a functional homolog of mammalian leptin (*22*).

These peptides act on an equally diverse group of neurons via distinct molecular mechanisms. The various *Drosophila* insulin-like peptides (dILPs) act via insulin receptors on peptidergic neurons in the *Drosophila* higher brain, while AKH, drosulfakinin, leucokinin, corazonin, Dh44, sNPF, and CCH-a2 act via G-protein coupled receptors expressed in

anatomically diverse neurons throughout the *Drosophila* nervous system. Finally, the leptin homolog Upd-2 acts via the JAK-stat receptor, *dome*, in insulin producing neurons in the *Drosophila* higher brain (*22*).

What are the neural circuits that these diverse inputs modulate? In many cases, the answer to this question remains open. However, some insight has been gained by studies examining how internal state influences sensory representations of the external world. As I describe in detail in chapter 4, one conclusion of these studies is that nutrient deprivation appears to potentiate gustatory and olfactory representations of palatable foods, while suppressing representations of unpalatable but potentially nutritious foods.

Despite the progress represented by these findings, many questions about how the *Drosophila* nervous system regulates ingestion remain to be addressed. First, many more neuropeptide signals of nutrient abundance have been discovered than there are neurons sensitive to those signals (*23*), arguing that additional neural sensors of internal state remain to be identified. Second, compared to the long list of peptides and neurons regulating food ingestion in *Drosophila*, relatively few molecules and neurons have been found that directly influence water ingestion. These include the peptides glycoprotein beta -3/5 (GPB-3/5), Leucokinin, and Capability (*capa*), all of which influence water balance in the insect kidney (*24-26*), but whose action on the nervous system is unclear. Finally, a major unresolved question is how the *Drosophila* nervous system integrates such a diversity of signals of internal state. For example, in an animal that is both food and water deprived, how does the nervous system weigh these competing needs to make appropriate behavioral choices?

Concluding Remarks

Homeostasis requires that nervous systems regulate animal behavior in such a way that ingestion of external nutrients is matched to the internal metabolic need for those nutrients. This fact motivates two fundamental questions: how do nervous systems detect diverse internal signals of metabolic need, and how do they use those signals to organize behaviors that meet those needs? This dissertation addresses these questions by identifying molecules and neurons that detect internal signals of sugar and water abundance, and by characterizing how activity of these neurons is propagated to downstream circuits in a manner that influences sugar and water ingestion. Specifically, we identify a novel class of *Drosophila* interoceptive neurons located in the subesophegeal zone (SEZ), the primary relay for taste information in *Drosophila.* We show that these neurons, named ISNs (Interoceptive SEZ Neurons), are sufficient to regulate both sugar and water ingestion: experimentally increasing ISN activity promotes sugar ingestion and suppresses water ingestion, while experimentally silencing them does the opposite. We further show that ISNs sense internal signals of sugar and water abundance, and that this sensitivity arises from co-expression of the adipokinetic hormone receptor (AKHR), a molecular sensor of the hunger peptide adipokinetic hormone (AKH), and Nanchung, an osmosensitive ion channel required for sensitivity to extracellular osmolality. Finally, we identify neurons downstream of ISNs and ask how ISN activity modulates large-scale neural responses to the taste of sugar and water. Taken as a whole, this study identifies novel mechanisms by which the *Drosophila* nervous system senses internal signals of metabolic need, and suggests new principles by which regulators of food and water ingestion interact.

Chapter 2: Coupled sensing of hunger and thirst balances sugar and water consumption

Summary

Hunger and thirst are ancient homeostatic drives for food and water consumption. Although molecular and neural mechanisms underlying these drives are currently being uncovered, less is known about how hunger and thirst interact. Here, we use molecular genetic, behavioral, and anatomical studies in *Drosophila* to identify four neurons that modulate food and water consumption. Activation of these neurons promotes sugar consumption and restricts water consumption, whereas inactivation promotes water consumption and restricts sugar consumption. By calcium imaging studies, we show that these neurons are directly regulated by a hormone signal of nutrient levels and by osmolality. Finally, we identify a hormone receptor and an osmolality-sensitive ion channel that underlie this regulation. Thus, a small population of neurons senses internal signals of nutrient and water availability to balance sugar and water consumption. Our results suggest an elegant mechanism by which interoceptive neurons oppositely regulate homeostatic drives to eat and drink.

This work has been previously published: Jourjine N, Mullaney BC, Mann K, Scott K. 2016. Coupled Sensing of Hunger and Thirst Signals Balances Sugar and Water Consumption. *Cell* 166: 855-66.

Introduction

To achieve homeostasis, animals must regulate consumption of external nutrients based on internal metabolic needs. Remarkably, animals whose nervous systems differ dramatically in organization exhibit some of the same homeostatic consumption behaviors, such as orally consuming food or water in response to starvation or dehydration. While these similarities suggest conserved underlying mechanisms, how nervous systems regulate consumption in a manner that reflects internal state remains an open question.

A key requirement for homeostatic regulation is the ability to sense internal nutrient abundance and either promote consumption in nutrient-deprived states or inhibit consumption in nutrient-replete states. In mammals, a major site of internal nutrient sensing is the hypothalamus, a conserved forebrain region that senses nutrients and coordinates behavioral responses to changes in their abundance (*16*). Neurons in the hypothalamus include direct sensors of circulating sugars like glucose, as well as sensors of metabolic cues like insulin, ghrelin, and glucagon. The hypothalamus also contains neurons whose activity is regulated by extracellular osmolality and are therefore sensitive to internal water abundance (*15, 27*). However, how the nervous system uses information encoded by hypothalamic sensors to regulate consumption of food and water remains unresolved.

Like mammals, the fruit fly *Drosophila melanogaster* regulates consumption of food and water depending on internal metabolic state. Although flies lack a direct homolog of the hypothalamus, neural populations in the *Drosophila* brain function as internal nutrient sensors, including glucose, fructose, and amino acid sensors that regulate feeding decisions (*28-30*). Flies also regulate water consumption based on internal water abundance (*31*), although internal sensors underlying this behavior have not previously been characterized. Thus, mammals and insects both regulate food and water consumption based on internal metabolic state, and in many instances accomplish this regulation by similar mechanisms. However, the neurons and molecules that regulate homeostatic consumption remain incompletely understood. In particular, mechanisms that coordinate the consumption of different essential nutrients, such as sugar or water, have been largely unexplored.

Here we report findings from two behavioral screens for neurons that regulate food or water consumption in *Drosophila*. Surprisingly, these screens independently identified the same four neurons as regulators of both food and water consumption. The neurons are located in the subesophageal zone (SEZ), a key relay for feeding regulation in the fly brain, and we name them Interoceptive SEZ Neurons (ISNs). Using genetic tools, behavioral assays, and calcium imaging, we show that ISNs are sensitive both to an internal signal of nutrient deprivation, the glucagon-like peptide adipokinetic hormone (AKH), and an internal signal of water abundance, extracellular osmolality. We identify the G-protein coupled receptor, adipokinetic hormone receptor (AKHR), and a conserved TRPV channel, Nanchung (Nan), as underlying responses to AKH and osmolality, respectively. Finally, we show that ISNs oppositely regulate sugar and water consumption, suggesting that they function to restore internal homeostasis. The convergence of internal signals of nutrient and water availability onto interoceptive neurons suggests an unexpected principle by which the nervous system might coordinate homeostatic behaviors.

Results

A behavioral screen for neurons that regulate feeding

To identify neurons that regulate feeding, we transiently activated candidate neurons with the heat-activated cation channel, dTRPA1, and determined the effect on feeding in adult flies. Consumption was monitored by scoring the amount of blue dye in the abdomens of flies with access to 200mM sucrose containing blue dye for 30 minutes. Approximately 600 Gal4 lines from the InSite collection (*32*) with expression in the central nervous system were crossed to flies carrying the *UAS-dTRPA1* transgene (*33*), allowing for Gal4-dependent neural activation. Fed flies were tested for sucrose consumption during heat-induced depolarization of Gal4-expressing neurons (Figure 2.1A; Table S1 reports transgenic flies used in this study). Four lines exhibited dramatically increased feeding, with the *954-Gal4* line showing the strongest consumption.

Four neurons in the *954-Gal4* line promote ingestive behaviors to sucrose

To identify neurons causal for increased feeding in the *954-Gal4* line, we began by characterizing its expression pattern. In the central brain, *954-Gal4* drove *UAS-mCD8::GFP* expression in neurons of the *pars intercerebralis*, dorsal lateral protocerebrum, subesophageal zone (SEZ), and ventral nerve cord (VNC) (Figure 2.1B). To identify which neurons contribute to the feeding phenotype of the *954-Gal4* line, we employed an intersectional approach using the Gal4 inhibitor Gal80 to restrict Gal4 expression to smaller neural populations. The *Tshirt-Gal80* transgene (*34*) blocked Gal4 expression in the VNC but did not eliminate increased consumption upon dTRPA1 activation of *954-Gal4* neurons, demonstrating that VNC neurons are not required (Figure 2.S1A). Next, we identified one line, *149-Gal80* (Gordon, M.D., unpublished), that eliminated SEZ GFP expression without affecting *pars intercerebralis* or dorsal lateral protocerebrum expression (Figure 2.S1B). This transgene eliminated the increased feeding phenotype in the *954-Gal4* line, arguing that *954-Gal4* SEZ neurons are necessary for increased consumption.

We screened existing Gal4 collections (*35, 36*) to identify lines that exhibit Gal4 expression in these SEZ neurons and identified two Gal4 lines, *R34G02* and *VT011155*, that labeled neurons that resembled the *954-Gal4* SEZ cluster. The *R34G02* line also drove expression in a pair of VNC neurons and abdominal ganglia projections (Figure 2.1C). Remarkably, the *VT011155* line exclusively labeled the SEZ neurons (Figure 2.1D). Both lines exhibited the feeding phenotype identified in *954-Gal4* (Figure 2.1E-G). In addition, activation of *954-Gal4, R34G02* or *VT011155* neurons with *UAS-dTRPA1* increased rates of proboscis extension to sugar stimuli, a non-ingestive behavior that flies exhibit to an appetitive taste stimulus (Figure 2.S1C). We generated a *R34G02-LexA* line and performed double labeling experiments with the Gal4 lines to test for co-expression and found that *954-Gal4*, *VT011155,* and *R34G02-Gal4* are all co-expressed in the same two SEZ neurons per hemisphere, with *954-Gal4* also showing expression in two additional SEZ neurons per hemisphere (Figure 2.S1D, E). These findings demonstrate that activation of four neurons in the SEZ causes increased feeding and promotes proboscis extension in well-fed animals. We name these interoceptive SEZ neurons (ISNs) and the *VT011155* line which specifically labels them *ISN-Gal4*.

ISNs directly respond to AKH and are indirectly inhibited by insulin

Pre- and post-synaptic sites on ISNs overlap in the dorsal SEZ (Figure 2.S1F). ISNs might therefore be components of feeding sensorimotor circuits, or they may modulate activity in these circuits in response to internal cues. To distinguish between these models, we tested whether ISNs respond to sensory detection of taste compounds. Tastants were applied to the proboscis while monitoring activity in ISNs by GCaMP5G or GCaMP6s calcium imaging in live flies (*37, 38*). Although stimulation with sucrose, water, or the bitter compound denatonium triggered sensory neuron responses, no activation was seen in ISNs (Figure 2.S2), indicating that the ISNs are unlikely to report detection of taste compounds.

An alternative hypothesis is that these neurons encode information about hunger state. As hormones often signal metabolic status, we tested whether existing hormone receptor Gal4 lines marked the ISNs. One line, *adipokinetic hormone receptor (AKHR)-Gal4* (*39*) exhibited strong labeling of ISNs, confirmed by double labeling with *R34G02-LexA*, suggesting these neurons may be regulated by AKH (Figure 2.2A).

AKH is a peptide hormone that is synthesized exclusively by neurosecretory cells in the corpus cardiacum and secreted into the circulating hemolymph, where it acts in a similar manner to mammalian glucagon. AKH secretion is stimulated under low nutrient conditions, which in turn leads to lipolysis, glycogenolysis, and release of sugar and lipid nutrients into the hemolymph from the fat body, the primary site of nutrient storage in *Drosophila* (*40, 41*). The endocrine role of AKH in regulation of insect metabolism is established, and this hormone is well positioned to signal nutrient status to the brain (*39*).

To directly test whether AKH modulates ISNs, calcium levels in these neurons were monitored by GCaMP5G fluorescence upon AKH perfusion in a dissected brain preparation (Figure 2.2B). Brief pulses of AKH produced rapid, robust, and dose-dependent GCaMP5G fluorescence increases with picomolar to nanomolar AKH concentrations, the physiological range of AKH measured in locust hemolymph (*42*). The ISNs of animals lacking AKHR did not respond to AKH, verifying that the AKH-induced responses were a result of activation of AKHR (Figure 2.2C).

In principle, the AKH-induced response might be cell-autonomous (AKH might directly bind to AKHR on ISNs to increase calcium) or non-autonomous (AKH might bind a receptor on other neurons that increase ISN activity via synaptic transmission). To test whether AKH directly modulates ISN activity, we applied the voltage-gated sodium channel blocker tetrodotoxin (TTX) to inhibit action potentials. ISNs responded to AKH even in the presence of TTX (Figure 2.2C), arguing that AKH directly activates ISNs.

AKH plays a role analogous to glucagon in signaling nutrient depletion and promoting release of stored nutrients. Insulin plays an opposing role, signaling nutrient abundance and promoting storage of circulating nutrients. Given the opposing endocrine roles of insulin and AKH, we tested whether insulin might regulate ISNs in a manner opposite to AKH. Insulin application alone did not induce a calcium response in ISNs (not shown). To test whether insulin affects the ability of ISNs to respond to AKH, dissected brains were perfused with two spaced pulses of AKH, separated by a 3-minute perfusion with insulin (Figure 2.2D). Insulin reduced the response of ISNs to AKH in a concentration-dependent manner. To test whether insulin acts cell-autonomously, TTX was applied to eliminate action potentials and non-autonomous effects.

We found that insulin no longer reduced AKH responses in the presence of TTX (Figure 2.2D). This argues that ISNs do not directly sense insulin, but receive synaptic input from other neurons that provide an inhibitory drive onto ISNs. These studies demonstrate that ISNs are capable of receiving and integrating inputs reflecting both low and high nutrient levels, directly responding to AKH and receiving inhibition from an insulin-sensitive pathway.

To directly test whether ISNs report physiological need, we reasoned that the activity in ISNs would likely be different in starved versus fed animals. We monitored ISN activity by cell-attached electrophysiological recordings in the living fly under fed or starved conditions. ISN activity decreased in the fed state and increased in the starved state, and this state-dependent activity of ISNs was absent in the AKHR mutant (Figure 2.2E). These experiments show that the ISNs are modulated in the living animal based on nutritional state and that this requires AKHR.

A behavioral screen for molecules that regulate water consumption

Our studies indicate that ISNs respond to signals of internal energy state and that their activity is sufficient to promote feeding, separating metabolic and neural functions of AKH. In a different behavioral screen to identify molecules that regulate water consumption, we ultimately identified additional molecules that are expressed in ISNs, regulate their activity, and provide unexpected insight into their function.

With the goal of identifying molecules that might signal thirst or water satiety in *Drosophila,* we screened a panel of 94 candidate ion channels and neuropeptide receptors for water consumption defects following RNAi knockdown with the pan-neuronal *nSynaptobrevin-Gal4* (*nSyb-Gal4*) line. Flies were placed in less than 20% relative humidity for 2 hours, which specifically increased water consumption (Lin et al., 2014) (Figure 2.3A). Upon pan-neuronal RNAi expression, the majority of RNAi lines showed behavior similar to GFP RNAi controls (109% control consumption). As expected, RNAi to PPK28, an ion channel expressed in sensory neurons and essential for water taste detection (*43, 44*), reduced water consumption (12% control consumption). In addition, RNAi against a number of genes reproducibly increased or decreased water consumption compared to sibling controls. These included the insulin-like receptor (5% control consumption) and the follicle stimulating hormone receptor (315% control consumption), which have been implicated in water homeostasis in insects (*24, 25, 45*).

Among the candidates with no known role in water consumption behavior was the TRPV family member, Nanchung (Nan) (184% and 197% control consumption, independent RNAi lines). Nan is a non-selective cation channel that participates in *Drosophila* proprioception, hearing, and hygrosensation (*46-49*). Interestingly, TRPV channels function as osmosensors in *C. elegans* and mammals and likely play a role in water consumption regulation in mice (*50-52*). We therefore chose to further investigate the role of Nan in *Drosophila* water consumption.

***nanchung* is required to restrict water consumption**

To examine whether *nan*-expressing neurons regulate water consumption, we tested the behavioral response of *nan* mutants as well as animals expressing *nan* RNAi specifically in *nan-Gal4* neurons, using described lines (*46*). Water consumption time was measured in single flies following two hours of acute desiccation (Figure 2.3B). Both nan^{36a} and nan^{dy5} mutants as well as *nan-Gal4, UAS-nan RNAi* flies consumed significantly more water than controls, demonstrating that *nanchung* is necessary to restrict water consumption.

To examine how activity in *nanchung* neurons influences water consumption, we inducibly activated these neurons with dTRPA1. Flies expressing *UAS-dTRPA1* in *nan-Gal4* neurons reduced water consumption upon dTRPA1 activation. Transient activation of *nan* neurons was also sufficient to rescue elevated water consumption observed in nan^{dy5} heterozygotes (Figure 2.3C), suggesting that *nanchung* neurons function to restrict water consumption.

Nanchung neurons in the SEZ are osmosensitive

The expression pattern of *nanchung* has been described previously using *nan-Gal4* (*46, 47*). These studies found expression in chordotonal organs of the legs and antennae, as well as in a small number of putative interneurons in the higher brain. Because *nan* has been proposed to detect water vapor in antennal neurons, we tested whether antennae were required for *dTRPA1*-mediated activation of *nan* neurons to reduce water consumption in nan^{dy5} heterozygotes and found no role for antennae (not shown). These data argue that Nanchung's function as an antennal sensor of water vapor is independent of its role in water consumption.

An alternative possibility is that Nanchung functions in central brain neurons labeled by *nan-Gal4* to regulate water consumption. Nan belongs to a class of mechanosensitive TRPV channels and is sufficient to confer osmosensitivity to cultured mammalian cells (*46*). Moreover, TRPV channels have been proposed to confer osmosensitivity to central neurons in the mammalian brain (*15, 53*). We therefore tested whether central neurons labeled by the *nan-Gal4* line were directly osmosensitive.

nan-Gal4, UAS-GCaMP6s brains were perfused with artificial hemolymph (AHL) of different osmolalities while GCaMP6s fluorescence was monitored (Chen et al., 2013). Decreasing osmolality caused robust calcium responses from bilaterally symmetric *nan-Gal4* neurons in the ventrolateral SEZ (Figure 2.4A). These responses were dose-dependent and observed following osmolality decreases but not increases (Figure 2.4B, C). To test whether these responses are specific to *nan* SEZ neurons, brains expressing GCaMP6s with the pan-neuronal driver *nSyb-LexA* were perfused with low osmolality solution. Again, strong calcium responses were observed only in the SEZ neurons labeled by *nan-Gal4* (Figure 2.4D; Figure 2.S3). Moreover, Nan is necessary for the osmolality responses, as calcium responses to low osmolality were significantly decreased in a nan^{36a} mutant background and were rescued with a *UAS-nan* transgene (*46*) (Figure 2.4E, F).

These data indicate that *nan* SEZ neurons are uniquely capable of responding to low extracellular osmolality with calcium increases. Because GCaMP6s preferentially reports calcium increases over decreases, we used the genetically encoded voltage sensor ArcLight (*54*) to test whether *nan* SEZ neuron activity is bidirectionally regulated by osmolality changes. Consistent with GCaMP6s imaging, decreasing extracellular osmolality decreased ArcLight fluorescence, indicating depolarization. In addition, we found that increasing extracellular osmolality significantly increased ArcLight fluorescence in these neurons, indicating hyperpolarization (2. 4G, H). Taken together, these data suggest that *nan* SEZ neurons report bidirectional extracellular osmolality changes in the brain.

The ISNs express *nanchung* and *AKHR* and respond to osmolality and AKH

During the course of these studies, we noted that the osmosensitive *nan* SEZ neurons had a similar spatial location and morphology as the ISNs that express *AKHR*, suggesting that they might be the same neurons. We tested this by examining overlap between *nan-Gal4* neurons and the ISNs, marked by *R34G02-LexA*, and indeed found *nan-Gal4* labels the ISNs as well as two additional SEZ neurons per hemisphere (Figure 2.5A). Consistent with this overlap, the ISNs responded to low osmolality and to AKH (Figure 2.5B, C). Responses were detected in neurites and cell bodies (Figure 2.S3C, D). The AKHR-negative, Nan-positive neurons did not respond to osmolality or contribute to consumption behavior (Figure 2.S4), arguing that the ISNs are a unique class of neurons that respond to osmolality and AKH. Thus, two screens for neurons regulating different homeostatic behaviors independently identified the ISNs.

ISNs are responsive to both osmolality and the hormone AKH. To examine how ISNs might integrate these two signals, we first asked whether Nan might be required for ISNs to sense AKH, and whether AKHR might be required for ISNs to sense osmolality. We therefore monitored osmolality responses in *AKHR* mutants and AKH responses in *nan* mutants (Figure 2.5C). By calcium imaging, loss of AKHR did not affect the ability of ISNs to respond to osmolality, nor did loss of Nan affect the AKH response. All imaging experiments were performed under controlled osmolality and AKH conditions, as monitoring GCaMP activity by necessity requires removing cuticle and exposing the brain to artificial hemolymph. Thus, these experiments indicate that each input increases ISNs activity via an independent molecular mechanism, but do not directly monitor interactions between ISN inputs.

We therefore asked whether ISN activity resulting from changes in one input, osmolality, might affect the ability of ISNs to respond to another input, AKH. To test this, we monitored calcium responses to AKH in ISNs of brains perfused with high or low extracellular osmolality. We found that high extracellular osmolality significantly reduced AKH responses by an average of 70% (Figure 2.5D, E). These results argue that ISNs sense extracellular AKH and osmolality via independent molecular mechanisms, AKHR and Nanchung, but that these two inputs regulate a common output, ISN activity.

Starvation reduces *Drosophila* hemolymph osmolality

AKH levels increase with starvation and activate ISNs, consistent with its action as a hunger signal that drives feeding. Low extracellular osmolality also activates ISNs, suggesting that low osmolality might also act as an internal signal of nutrient deprivation. Flies starved for one day have approximately 75% lower hemolymph sugar levels (*55*), and we hypothesized that this reduction in sugar levels might reduce hemolymph osmolality. To test this, we measured the hemolymph osmolality of single fed or starved flies with a temperature gradient osmometer (*56*).

To confirm that we could detect physiological changes in osmolality, we measured hemolymph osmolality of single flies placed in dry (<20% RH) or humid (>80% RH) environments for 6-8 hours. Consistent with previous studies (*57*), desiccation increased hemolymph osmolality by an average of 55 mOsm/kg. In addition, hemolymph osmolality of desiccated flies returned to control levels five minutes after water consumption (Figure 2.6B).

To test the effect of starvation on hemolymph osmolality, hemolymph was collected from single flies that were either fed or starved for 24 hours with access to water. We found that hemolymph osmolality of starved flies was lower than that of well-fed animals by ~30 mOsm/kg

(Figure 2.6C). Importantly, physiological changes in osmolality of the magnitude observed following starvation were sufficient to elicit responses from ISNs in imaging preparations (Figure 2.6D, E). Thus, both low extracellular osmolality and increased AKH abundance may be starvation signals that increase ISN activity and promote feeding.

ISNs oppositely regulate sugar and water consumption

Taken together, our data suggest a model in which ISNs are sensitive to internal signals for both water and sugar abundance, and are sufficient to modulate both water and sugar consumption. To directly ask how ISN activity impacts sugar and water consumption, we drove *dTRPA1* expression with *ISN-Gal4*, which exclusively labels ISNs. Consistent with our previous observations, *ISN-Gal4, UAS-dTRPA1* flies avidly consumed sucrose upon TRP activation at 32°C, but not at 23°C. In contrast, these flies exhibited markedly reduced water consumption at 32°C but not at 23°C (Figure 2.7A).

To test the effect of inhibiting ISN activity on water and sugar consumption, we used *ISN-Gal4* to selectively drive expression of RNAi against *nSynaptobrevin (nSyb),* which is required for synaptic transmission. Flies expressing *nSyb* RNAi in ISNs increased water consumption relative to controls by almost twofold. In contrast, expression of *nSyb* RNAi in ISNs decreased sucrose intake by an average of 44% (Figure 2.7B). Thus, neural activity in ISNs oppositely regulates sugar and water consumption behaviors: increased ISN activity both promotes sugar and restricts water consumption, whereas decreased activity promotes water and restricts sugar consumption.

To ask whether *nanchung* and *AKHR* are important for the ability of ISNs to regulate food and water intake, we expressed *nan* RNAi or *AKHR* RNAi selectively in ISNs and examined the effect on water and sucrose consumption. Flies expressing either of two independent *nan* RNAi constructs in ISNs increased water consumption and decreased sucrose consumption relative to controls, consistent with phenotypes observed when silencing ISNs (Figure 2.7C, S5A-C). Flies expressing *nan* RNAi under the control of *nSyb-Gal4* and *nan-Gal4* drivers produced the same reciprocal effects on water and sucrose consumption (Figure 2.S5D, E). Like flies expressing *nan* RNAi, flies expressing *AKHR* RNAi in ISNs also increased water intake and decreased sucrose intake relative to controls (Figure 2.7D). The *nan* and *AKHR* RNAi data is consistent with the notion that both AKHR and osmolality contribute to the activation of ISNs. The loss of either signal decreased activity in ISNs, leading to loss-of-function phenotypes similar to those observed when silencing ISNs with nSyb RNAi.

The finding that the ISNs sense signals of hunger and thirst, AKH and osmolality, and oppositely regulate sugar and water consumption, suggests that hunger and thirst may be competing drives under some conditions. To test this, we examined whether there were consumption differences in flies with competing needs. Under conditions when flies were not thirsty, there was no drive to consume water and this was not affected by starvation state (Figure 2.7E). However, under conditions when flies were mildly starved (2 hours), we found that sucrose consumption was reduced in thirsty flies compared to water-sated flies (Figure 2.7E). These data argue that under conditions of competing needs, there is a balance between water and sucrose consumption. As the relative weight of these needs changes, the balance would be predicted to change as well.

Discussion

In this study, we uncover a neural mechanism that coordinates two essential homeostatic behaviors: sugar and water consumption. This coordination is achieved by two neurons per SEZ hemisphere of the *Drosophila* brain, the ISNs, which are sensitive to internal signals for both hunger and thirst and whose activity oppositely regulates sugar and water consumption (Figure 2.7F). The antagonistic manner in which ISNs couple these behaviors suggests a regulatory principle by which animal nervous systems might promote internal osmotic and metabolic homeostasis.

Four neurons oppositely regulate sugar and water consumption in *Drosophila*

Low internal osmolality and high AKH are signals of water satiety and hunger, respectively. ISN activity increases both in the presence of low extracellular osmolality and AKH. We find that increasing ISN activity promotes sugar consumption and reduces water consumption. Conversely, high internal osmolality and low AKH are signals of thirst and food satiety. ISN activity decreases and AKH responses are reduced in the presence of high extracellular osmolality or insulin. Decreasing ISN activity increases water consumption and reduces sugar consumption.

How do ISNs achieve opposite regulation of a single behavior, consumption, in a manner that depends on the substance being consumed? One possibility is that the downstream targets of ISNs include interneurons involved in the behavioral response to water and sugar taste. This model predicts that increased ISN activity promotes the ability of sugar taste interneurons to drive consumption while inhibiting the ability of water taste interneurons to do so. It may be possible to test hypotheses about the neural circuits in which ISNs participate through the use of large scale calcium imaging.

Molecules for sensing internal hunger and thirst cues

ISNs regulate sugar and water consumption in a manner that appropriately reflects internal hunger and thirst states. Here, we show that two genes, *AKHR* and *nanchung*, are expressed in ISNs and function to confer sensitivity to these states.

AKHR is a G-protein coupled receptor expressed in the fat body and the brain that has been well characterized in the context of insect metabolic regulation (*39, 42*). The ligand for this receptor, AKH, is secreted into the hemolymph by specialized neurosecretory cells in the corpus cardiacum (*41*), where it acts under conditions of food deprivation. Here, we identify a role for AKH in regulating the activity of four interneurons in the SEZ, the ISNs, and show that this activity promotes sugar consumption. AKH abundance in the hemolymph therefore promotes feeding via the ISNs. Manipulating AKHR exclusively in the ISNs provided a means to separate the metabolic and neural effects of AKH, uncovering a role for AKH in the nervous system.

Sensors for internal hemolymph osmolality have not previously been described. Here, we find that the non-selective cation channel Nanchung is expressed in ISNs and is required for their responses to low osmolality. Although we do not know if Nan is the direct osmosensor in ISNs, previous studies found that Nan confers low osmolality responses when expressed in

heterologous cells (*46*), consistent with this notion. Nan family members of the TRPV4 family have been shown to participate in osmosensation in *C. elegans* and mammals (*50-52*), suggesting an ancient and conserved function. Nanchung participates in sensory detection of mechanical stimuli in *Drosophila*, including proprioception, audition, and low humidity sensing (*46-49*). It is interesting that the same molecule that is involved in external sensory detection of mechanical stimuli also participates in internal detection of osmolality, a mechanical stimulus. Similar molecular re-tooling has recently been described for the GR43a gustatory receptor, which acts as a sensory receptor to monitor fructose in the environment and as an internal sensor monitoring circulating fructose levels in brain hemolymph (*28*).

In the mammalian brain, osmosensitive neurons are generally found in areas which lack a blood-brain barrier. The blood-brain barrier of Drosophila expresses multiple aquaporins and may potentially regulate hemolymph osmolality (*58*). Whether changes in hemolymph osmolality are regulated by the blood-brain barrier to impact ISN activity is an interesting question for future study.

Coupling of sugar and water consumption behaviors as a mechanism for homeostasis

ISNs oppositely regulate the behavioral responses to hunger and thirst states. How might this type of coordination be adaptive? One possibility is suggested by the fact that sugar and water consumption perturb internal osmotic homeostasis in opposite directions. In *Drosophila* and mammals, sugar consumption leads to increased blood-sugar levels and increased blood osmolality. Conversely, water consumption leads to lowered blood osmolality. Our studies show that ISNs are sensitive to extracellular osmolality, and that they oppositely regulate sugar and water consumption. Under high osmotic conditions, decreased ISN activity promotes water consumption, reducing internal osmolality. Under low osmotic conditions, increased ISN activity promotes sucrose consumption, increasing internal osmolality. Thus, ISNs may monitor internal osmolality to reciprocally regulate sugar and water consumption to restore homeostasis.

Reciprocal regulation of food and water consumption has been reported in both classical and recent rodent studies. For example, increasing blood osmolality promotes water consumption and inhibits food consumption in rats, whereas decreasing osmolality has the opposite effect (*59*). In addition, ghrelin, a key internal signal for hunger in mammals, is sufficient not only to promote feeding but also to inhibit water consumption in rats (*60*). Thus, vertebrates and invertebrates may share mechanisms for coupling water and sugar consumption in a manner that promotes homeostasis. In *Drosophila*, the convergence of internal signals onto the ISNs provides a mechanism to weigh homeostatic deviations and drive consumption to restore balance.

Other neurons in the *Drosophila* brain process homeostatic needs for water and sugar separately. For example, water reward and sugar reward are processed by different subsets of mushroom body input neurons, likely independent of gustatory sensory activation (*18, 61-63*). Neuropeptide F, small Neuropeptide F, and dopamine are all signals of nutrient deprivation that promote nutrient intake (*40, 64-67*). Circulating glucose and fructose in the hemolymph also report the nutritional state and alter feeding behavior by direct activation of a few central neurons (*21, 28*). The ISNs are unique in that they detect multiple internal state signals and use this information to weigh competing needs. In addition to parallel, independent pathways for eating and drinking, this study demonstrates the existence of a pathway that couples these drives.

Experimental Procedures

Additional details are available in Extended Experimental Procedures.

Blue Dye Consumption experiments

Flies (15-20/vial) were transferred from food to filter paper soaked in 200mM sucrose and blue dye. After feeding animals were scored a 0 (no dye in abdomen), 1 (less than half of the abdomen was blue), or 2 (half or more of the abdomen contained dye). The scores of all flies in one vial were averaged and considered one trial.

Proboscis Extension Response Assays

PER was performed as described (*67*), except that each animal was considered a data point, and was categorized as responding 0, 1, 2, or 3 times.

Temporal Consumption Assays

Assays were performed as described (Pool et al., 2014). Animals were presented with a taste stimulus ten times and total consumption time was monitored. To generate thirsty flies, flies were placed in a sealed chamber with ~250g $CaSO_4$ (Drierite, stock# 23001) for 2 hours, unless otherwise noted.

Immunohistochemistry

Immunohistochemistry was performed as described (Marella et al., 2012).

Calcium and voltage imaging

GCaMP5G or GCaMP6s imaging of taste responses was performed as described (*37*). Stacks of 14-20 Z-slices were collected at approximately 0.3 Hz. For GCaMP5G or GCaMP6s imaging of AKH or osmolality responses, the brain was removed in ice-cold calcium and magnesium-free artificial hemolymph-like solution (AHL), transferred to a perfusion chamber with room temperature AHL, and immobilized with tungsten wire. Image analysis was performed in ImageJ.

Hemolymph osmolality measurements

An osmometer was assembled and used as described (*56*), with minor modifications detailed in Extended Experimental Procedures.

Electrophysiology

Extracellular recordings were performed in live animals as described (Pool et al., 2014).

Statistical Analyses

Student's t-test, with Sidak correction for multiple comparisons, was used to compare two groups. ANOVA followed by Tukey's post hoc test was used to compare three or more groups. ANOVA followed by Dunnet's post hoc test was used to compare multiple responses of varying stimuli.

Author Contributions

N.J. performed the RNAi screen and characterized the role of Nanchung. B.M. performed the neural activation screen and characterized the role of AKHR. N.J. and B.M performed calcium imaging, behavioral, and osmolality measurement studies. K.M. performed electrophysiology. N.J., B.M., and K.S. wrote the manuscript and K.S. supervised the study.

Figures

Figure 2.1

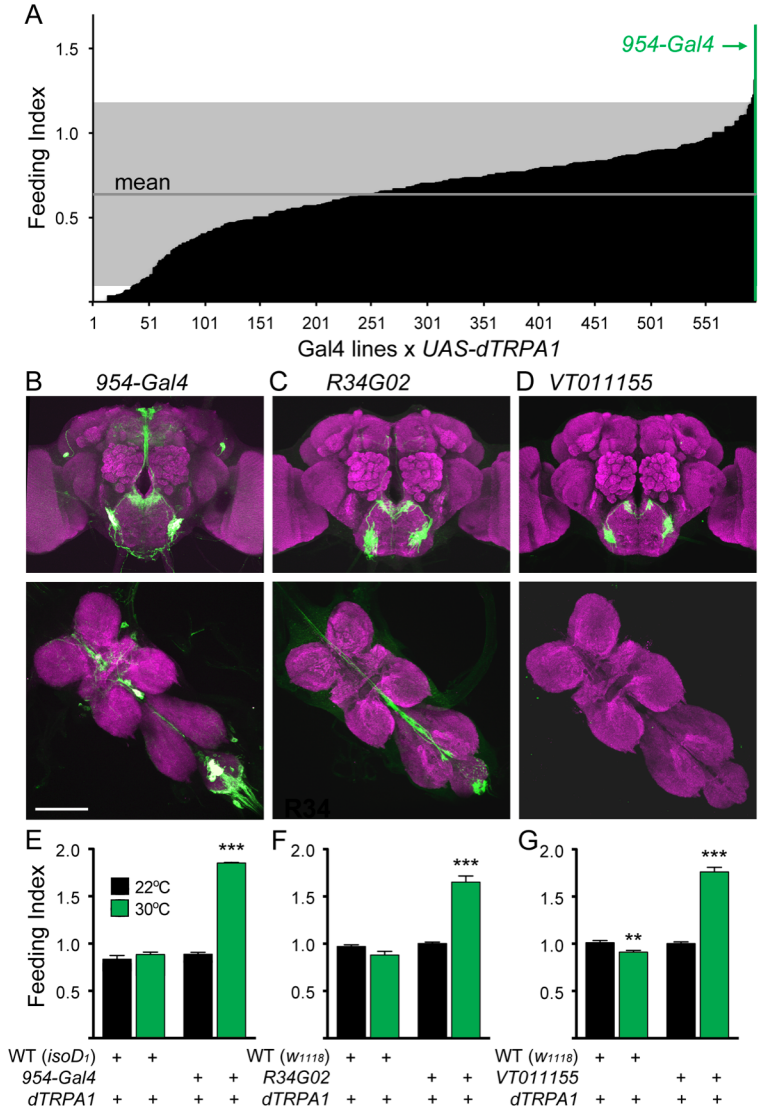

Figure 2.1 Identification of neurons that promote sucrose consumption

A. Behavioral screen for flies that overconsume sucrose. Gal4 lines were crossed to *UAS-dTRPA1* for heat-inducible neural activation and tested for sucrose consumption at 30°C under non-deprived conditions (n=5-30 flies/line). Gray marks 2 standard deviations from the mean.

B-D. (B) Expression of *954-Gal4, UAS-mCD8::GFP* (green) in brain (top) and ventral nerve cord (middle), (C) *R34G02* expression, (D) *VT011155* expression. Scale 100 µm.

E-G. (E) Sucrose consumption of *isoD*^{1} (WT), *UAS-dTRPA1* flies or *954-Gal4, UAS-dTRPA1* flies at 30°C (upon neural activation) and 22°C (control). (F) *R34G02* sucrose consumption phenotype, (WT = *w*^{1118}), (G) *VT011155* sucrose consumption phenotype, (WT = *w*^{1118}). n=5-8 vials, 15-20 flies/vial, mean ± SEM, **p<0.01, ***p<0.001, t-tests (23˚C vs 32˚C) with Holm-Sidak correction**.**

See Figure 2.S1 for additional experiments to identify the neurons that promote sucrose consumption. See Table S1 for fly genotypes for all experiments.

Figure 2.2

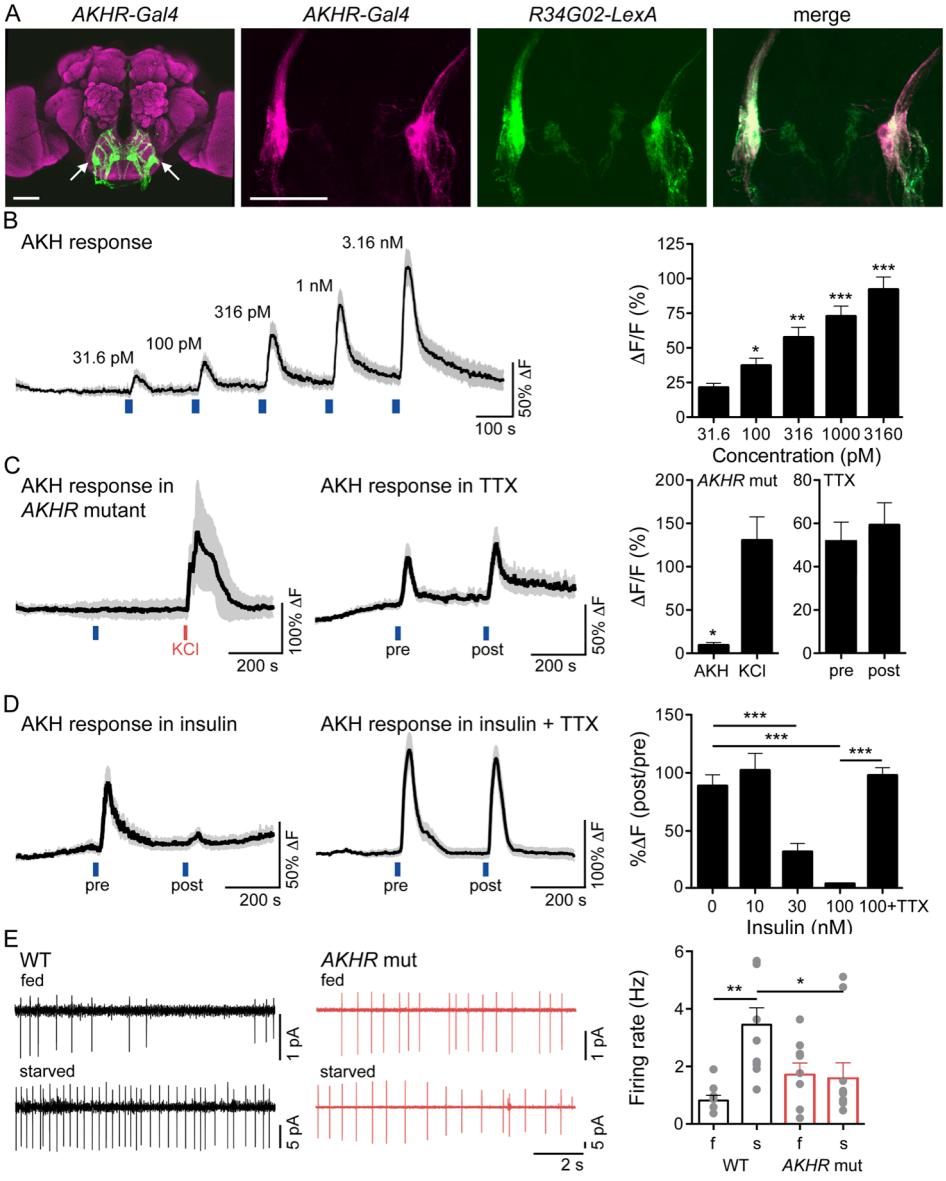
A
AKHR-Gal4
AKHR-Gal4
R34G02-LexA
merge
B
AKH response
3.16 nM
1 nM
316 pM
100 pM
31.6 pM
50% ΔF
100 s
ΔF/F (%)
31.6 100 316 1000 3160
Concentration (pM)
C
AKH response in AKHR mutant
AKH response in TTX
KCl
100% ΔF
200 s
pre
post
50% ΔF
AKHR mut
TTX
AKH KCl
pre post
D
AKH response in insulin
AKH response in insulin + TTX
%ΔF (post/pre)
0 10 30 100 100+TTX
Insulin (nM)
E
WT
fed
starved
AKHR mut
1 pA
5 pA
2 s
Firing rate (Hz)
f s f s
WT
AKHR mut

Figure 2.2 ISNs respond to AKH and are inhibited by insulin

A. (left) Expression of *AKHR-Gal4, UAS-mCD8::GFP* in brain. (second) *AKHR-Gal4, UAS-mCD8::RFP* in SEZ, (third) *R34G02-LexA, lexAop-mCD8::GFP* in SEZ, (right) overlay. Scale 50 μm.

B. (left) GCaMP5G increase in ISNs in response to AKH (31.6 pM, 100 pM, 316 pM, 1 nM, 3.16 nM) applied at the blue lines. n=7, mean (black line) ± SEM (grey). (right) Maximum GCaMP5G increase (%ΔF/F) to AKH, mean ± SEM, same data as trace. Repeated-measures one way ANOVA followed by holm-sidak post hoc test, comparing to 31.6 pM response. *p<0.05, **p<0.01, ***p<0.001.

C. (left) GCaMP5G increase in ISNs to 1 nM AKH (blue line) or 30 mM KCl (red line) in the *AKHR* mutant. n=5, mean ± SEM. (middle) GCaMP5G increase in ISNs to 316 pM AKH (blue line) pre- or post-TTX (100 nM) application. n=8, mean ± SEM. (right) GCaMP5G increase (%ΔF/F) to AKH in the *AKHR* mutant (t-test, *p<0.05) or pre- or post-TTX application (t-test, ns). Mean ± SEM, same data as traces.

D. (left) GCaMP5G increase in ISNs to 316 pM AKH (blue line) pre- or post-insulin (100 nM) application. n=11, mean ± SEM. (middle) GCaMP5G increase in ISNs to 316 pM AKH (blue line) pre- or post-insulin (100 nM) and TTX (100 nM) application. n=10, mean ± SEM. (right) GCaMP5G change (%ΔF). Mean ± SEM, insulin concentrations in the absence of TTX: One-way ANOVA with Dunnet's post hoc test comparing to 0 nM Insulin, ***p<0.001. Effect of TTX: t-test (100nM Insulin vs. 100nM insulin + TTX), ***p<0.001, same data as traces plus additional insulin concentrations.

E. (left) Example cell-attached recordings from $AKHR^{+}$ SEZ neurons in *AKHR* mutant or wild type flies, fed (f) or starved (s) 24H, and (right) summary graph. n = 6-11, mean +/- SEM, one-way ANOVA, Tukey Post Hoc, **p<0.01, *p<0.05. See Figure 2.S2, showing that ISNs are not taste-responsive.

Figure 2.3

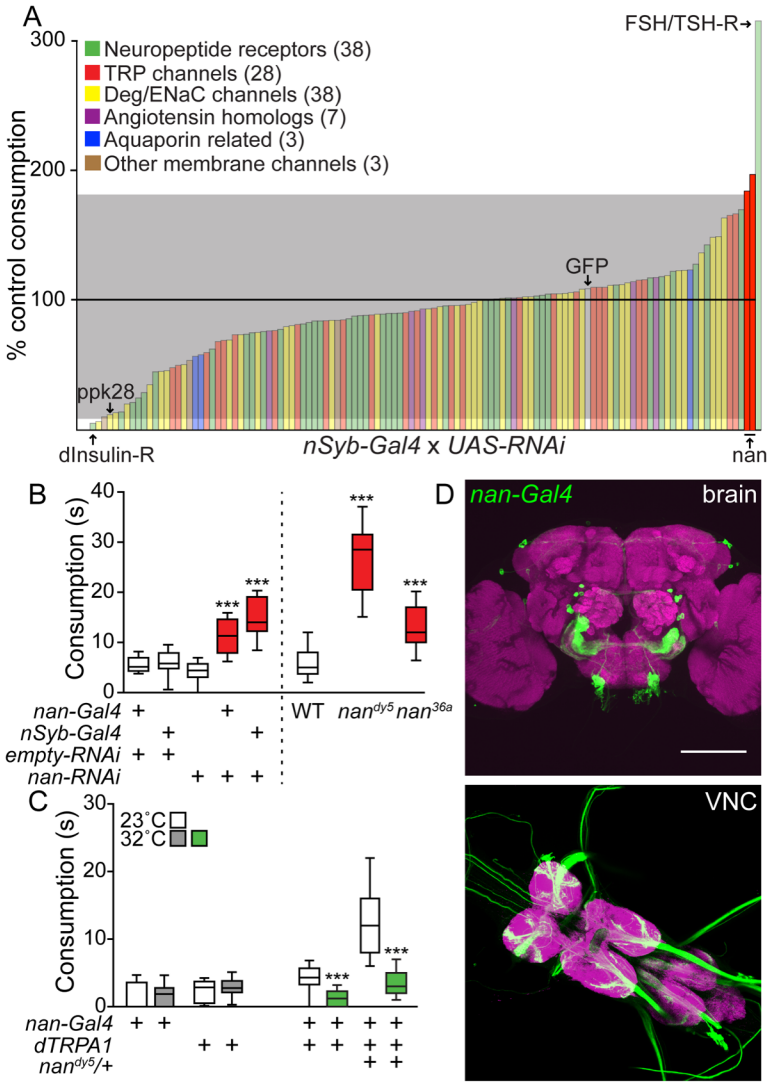
A
FSH/TSH-R
300
200
100
% control consumption
Neuropeptide receptors (38)
TRP channels (28)
Deg/ENaC channels (38)
Angiotensin homologs (7)
Aquaporin related (3)
Other membrane channels (3)
GFP
ppk28
dInsulin-R
nSyb-Gal4 x UAS-RNAi
nan
B
Consumption (s)
40
30
20
10
0
***
nan-Gal4
nSyb-Gal4
empty-RNAi
nan-RNAi
WT
nan^dy5 nan^36a
C
Consumption (s)
30
20
10
0
23˚C
32˚C
nan-Gal4
dTRPA1
nan^dy5/+
D
nan-Gal4
brain
VNC

Figure 2.3 Identification of *nanchung* and its role in water consumption

A. Behavioral screen for genes regulating water consumption. *UAS-RNAi* lines were crossed to *nSyb-Gal4*. 10 RNAi and 10 sibling control flies were assayed/RNAi line. Average water consumption time in RNAi group versus sibling control was used to calculate % control consumption. Gray marks 2 standard deviations from mean. Two *nan* RNAi lines (BSC# 31674 and 31925) are highlighted in red. Behavioral data for *nan* RNAi BSC# 31925 are shown unless noted.

B. Water consumption in *nan* RNAi and *nan* mutant backgrounds. For all box plots, whiskers = 10^{th} to 90^{th} percentile, box = 25^{th} to 75^{th} percentile, and line in box = median. n=28-60 flies, one-way ANOVA, Tukey Post Hoc: for RNAi experiments (***$p<0.001$), and for mutant experiments (***$p<0.001$).

C. Activating *nan-Gal4* neurons affects water consumption. n=20-63 flies, t-test, Holm-Sidak correction, (23˚C vs 32˚C per genotype), ***$p<0.001$.

D. *nan-Gal4, UAS-mCD8::GFP* expression in the brain (top) and VNC (bottom). Scale 100 μm.

Figure 2.4

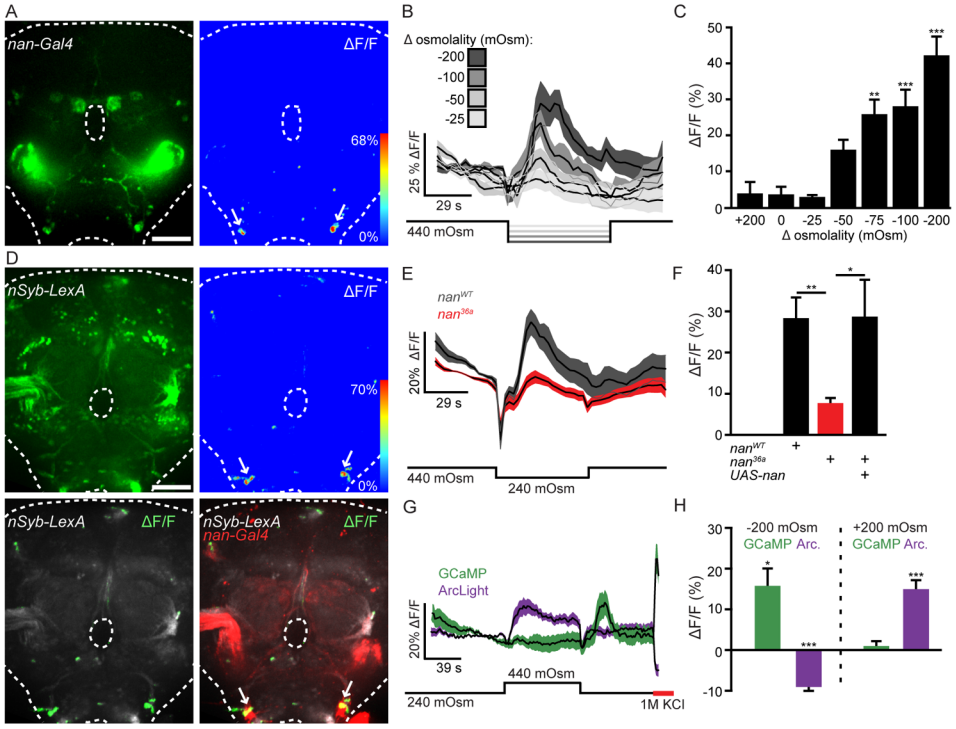

Figure 2.4 Nanchung SEZ neurons respond to osmolality

A. *nan-Gal4, UAS-GCaMP6s* expression in brain (left) and example ΔF/F heat-map of the same brain (right) upon an extracellular osmolality decrease of 200mOsm/kg. Scale 50 µm.

B. ΔF/F traces (mean ± SEM) for osmolality decreases of 25, 50, 100, and 200 mOsm/Kg (n=9-12 brains/condition).

C. Maximum ΔF/F responses (mean ± SEM) for osmolality changes. n=7-12 brains/condition, one-way ANOVA, Dunnet's Post Hoc to mock (0 mOsm change) **p<0.01, ***p<0.001, data from B plus additional osmolalities.

D. (top left) *nSyb-LexA, lexAop-GCaMP6s* expression in brain. (top right) ΔF/F heat-map to an osmolality decrease of 200mOsm/kg in the same brain. (bottom left) ΔF/F response (green) overlaid on *nSyb-LexA, lexAop-GCaMP6s* expression (grey). (bottom right) ΔF/F response (green) overplayed on *nSyb-LexA, lexAop-GCaMP6s* (grey) and *nan-Gal4* expression (red) in same brain. Scale 50 µm.

E. ΔF/F traces upon osmolality decreases of 200 mOsm/Kg in nan^{36a} mutant or wild type (WT) flies. n=28-33. E-H: data are mean ± SEM.

F. ΔF/F graphs for WT, mutant, and rescue flies (*UAS-nan;* nan^{36a}). n=33, 28, and 12. one-way ANOVA, Tukey Post Hoc, *p<0.05, **p<0.01, data from E plus rescue.

G. ΔF/F traces to 200 mOsm/Kg osmolality decreases in flies expressing *UAS-GCaMP6s* (green, n=9 brains) or *UAS-ArcLight* (magenta, n=11 brains) in ISNs.

H. ΔF/F graphs for GCaMP6s and ArcLight from F. One sample t-tests for difference from theoretical mean of 0.0, *p<0.05, ***p<0.001.

See also Figure 2.S3, showing quantification of whole brain responses.

Figure 2.5

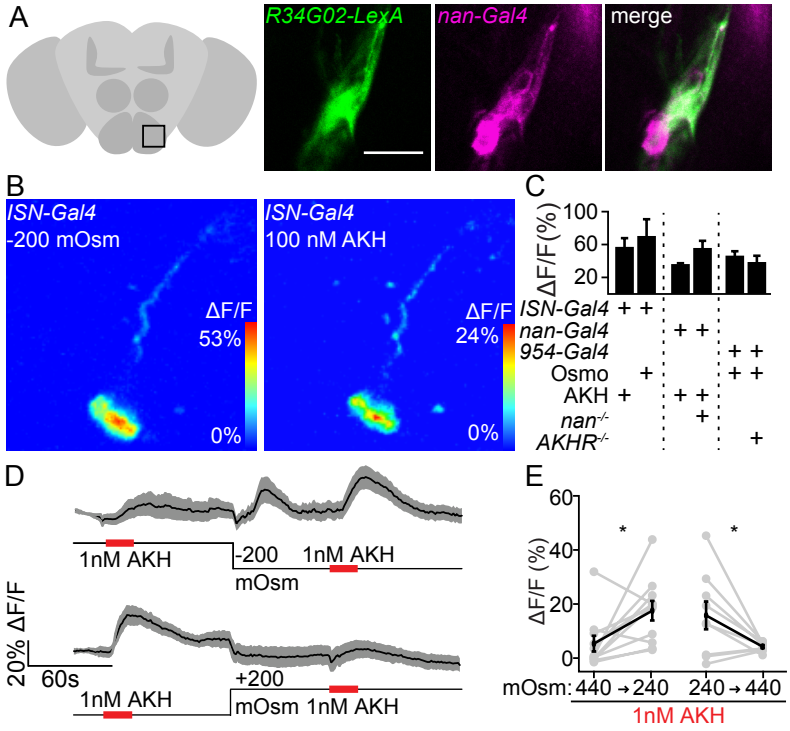

Figure 2.5 Nanchung SEZ neurons are ISNs

A. Co-expression of *R34G02-LexA* and *nan-Gal4* in ISNs. Zoom shows one *nan-Gal4* cluster. Scale 20 μm.

B. (left) Low osmolality response and (right) AKH response in the same cell.

C. maximum ΔF/F graphs (mean ± SEM) to 200 mOsm/kg osmolality decreases (Osmo) or 1 nM AKH in control or mutant backgrounds. n=5-10 brains, t-test Holm-Sidak correction, ns.

D. ΔF/F traces (mean ± SEM) to 1 nM AKH in 440 mOsm/kg (high) or 240 mOsm/Kg (low) extracellular osmolality and graph of ΔF/F responses. Top: n=9 brains. Bottom: n = 11 brains.

E. Quantification of ΔF/F graphs from D, mean ± SEM. brains, paired t-test, *p<0.05.

See also Figure 2.S4, showing that the AKHR-, Nan+ neurons do not respond to osmolality.

Figure 2.6

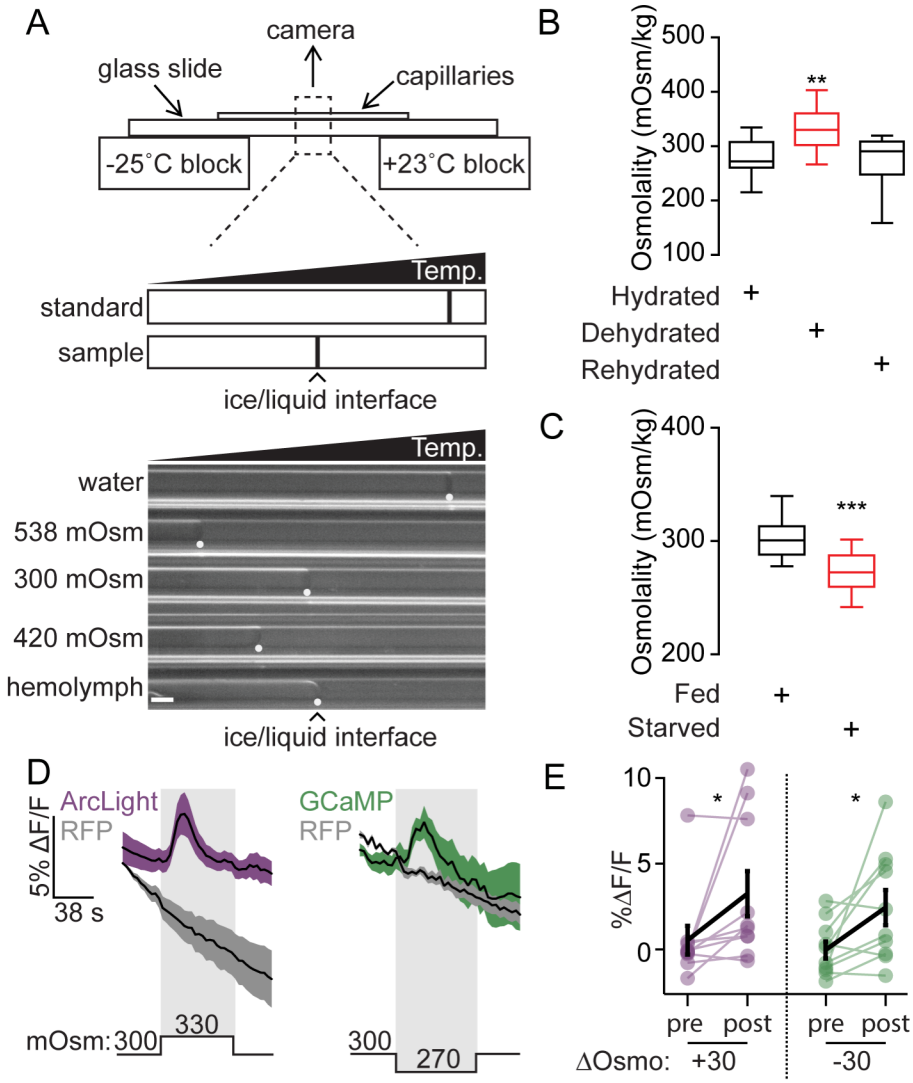

Figure 2.6 *Drosophila* hemolymph osmolality decreases during starvation

A. Top: Temperature (Temp.) gradient osmometer. Distance between sample and standard ice/liquid interfaces was used to calculate sample osmolality. Bottom: Freezing interfaces (white dots) from standards and single fly hemolymph. Scale 0.05 mm.

B. Desiccation affects hemolymph osmolality. n=14-17, one way ANOVA, Tukey's Post Hoc, **p<0.01. Dehydrated: 6 hours at <20% RH. Hydrated: 6 hours in a humid box. Rehydrated: water was administered as described in methods.

C. Starvation affects hemolymph osmolality. n=14, t-test, ***p<0.001.

D. ΔF/F traces (mean ± SEM) to 30 mOsm/Kg osmolality decreases or increases in flies expressing *UAS-GCaMP6s* (green, n=10 brains) or *UAS-ArcLight* (magenta, n=10 brains) in ISNs.

E. ΔF/F graphs (mean ± SEM) for GCaMP6s and ArcLight from D. Wilcoxon matched-pairs signed rank test, *p<0.05.

Figure 2.7

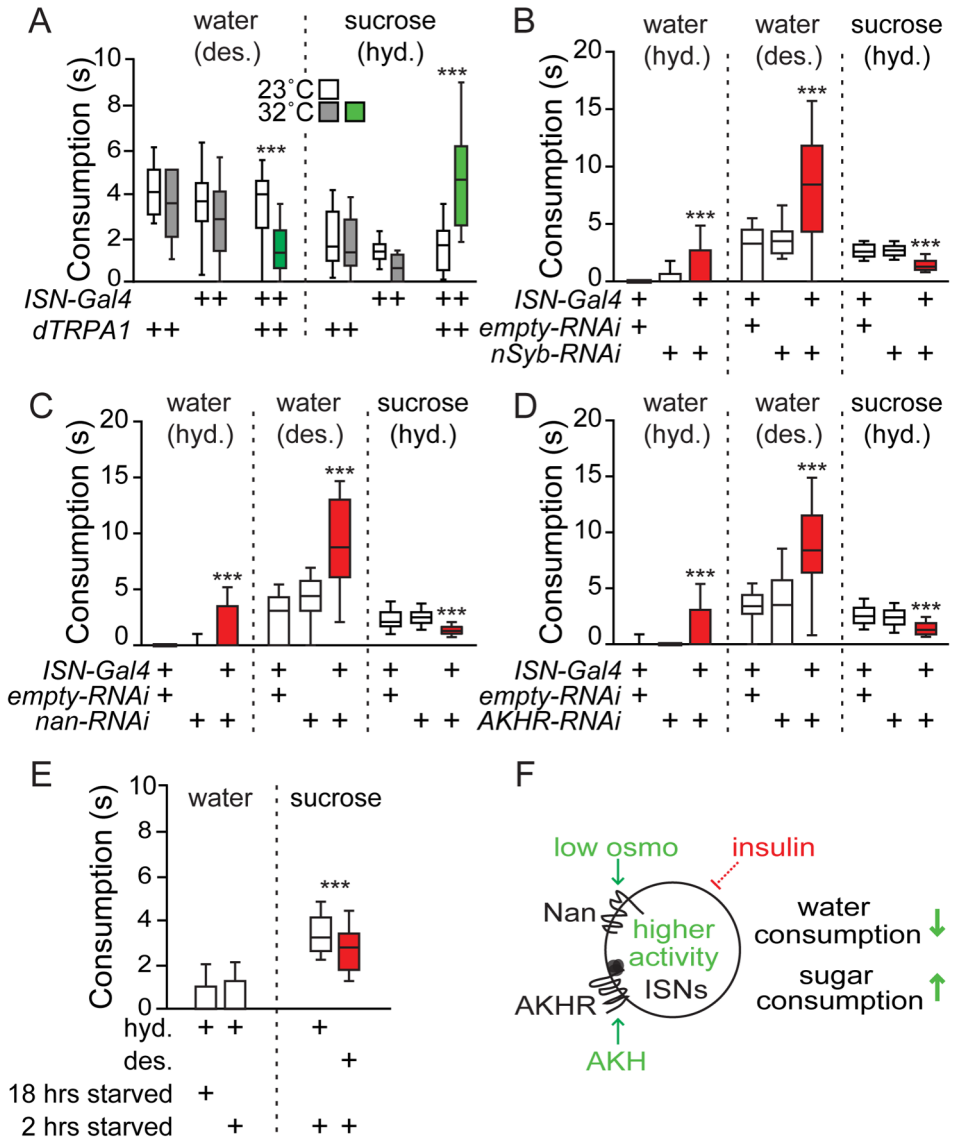
A
water (des.)
sucrose (hyd.)
Consumption (s)
23˚C
32˚C
***
ISN-Gal4 ++ ++ ++ ++ ++
dTRPA1 ++ ++ ++ ++
B
water (hyd.)
water (des.)
sucrose (hyd.)
ISN-Gal4 + + + + +
empty-RNAi + + +
nSyb-RNAi + + + + +
C
ISN-Gal4 + + + + + +
empty-RNAi + + +
nan-RNAi + + + + + +
D
ISN-Gal4 + + + + + +
empty-RNAi + + +
AKHR-RNAi + + + + + +
E
water
sucrose
hyd. + + +
des. +
18 hrs starved +
2 hrs starved + + +
F
low osmo
insulin
Nan
higher activity
ISNs
AKHR
AKH
water consumption
sugar consumption

Figure 2.7 ISNs promote sucrose consumption and inhibit water consumption

A. ISN activation with dTRPA1 alters water and 1M sucrose consumption. Desiccated (des.), hydrated (hyd.). n=30-76 flies. Water consumption: ***p<0.001, t-tests (23˚C vs 32˚C) with Holm-Sidak correction.

B. ISN silencing with *nSyb* RNAi affects water and sugar consumption. n=38-57 flies. B-D: one-way ANOVA, Tukey's Post Hoc, ***p<0.001.

C. ISN-specific *nan* RNAi affects water and sugar consumption. n=37-67 flies.

D. ISN-specific *AKHR* RNAi affects water and sugar consumption. n=22-70 flies.

E. Desiccation affects sugar consumption in wild type flies. n = 84-101, ***p<.001, t-test (hyd. vs. des.).

F. Low osmolality (osmo) and high AKH increase ISN activity, which promotes sugar consumption and inhibits water consumption. Insulin indirectly inhibits ISNs. High osmo and low AKH reduce ISN activity to promote water consumption and inhibit sugar consumption. See Figure 2.S5 for additional behavioral experiments.

Supplemental Figure Legends

Figure 2.S1

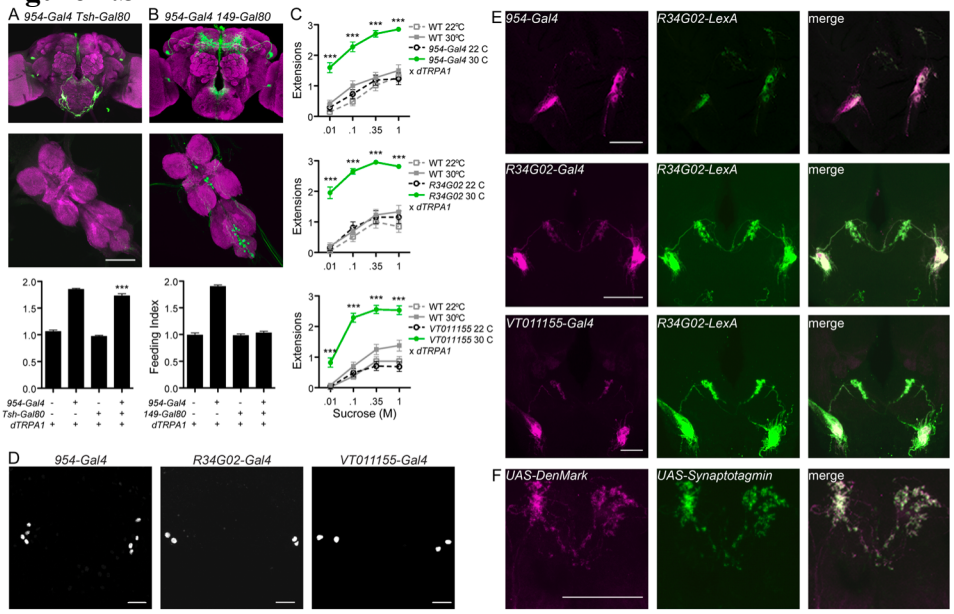

Figure 2.S1 Neurons that promote sucrose consumption, related to Figure 2.1.

A. *Tshirt-Gal80* (*Tsh-Gal80*) eliminated Gal4 expression in the ventral nerve cord but did not eliminate increased sucrose consumption upon dTRPA1 activation of *954-Gal4* neurons. n=5-6 vials, 12-20 flies/vial, mean ± SEM, one-way ANOVA, Tukey's Post Hoc, ***p<0.001.

B. *149-Gal80* eliminated Gal4 expression in SEZ neurons and eliminated increased sucrose consumption upon dTRPA1 activation of *954-Gal4* neurons. n=5-6 vials, 12-20 flies/vial, mean ± SEM, one-way ANOVA, Tukey's Post Hoc, ***p<0.001.

C. Activation of *954-Gal4*, *R34G02*, or *VT011155* neurons upon dTRPA1-mediated depolarization at 30°C increased proboscis extension to sucrose concentrations. n=39-48, mean ± SEM, ***p<0.001 t-test (22 vs. 30°C), Holm-Sidak correction. WT = $isoD^1$ (top), w^{1118} (others).

D. *954-Gal4, AKHR-Gal4,* and *VT011155-Gal4* nuclear expression in the SEZ. There are four neurons in each *954-Gal4* cluster, two neurons in each *AKHR-Gal4* cluster, and two neurons in each *VT011155-Gal4* cluster.

E. (top) *954-Gal4, UAS-mCD8::RFP* and *R34G02-LexA*, *lexAop-mCD8::GFP* flies showed co-expression of reporters in ISNs. (middle) *R34G02-Gal4, UAS-mCD8::tdTomato* and *R34G02-LexA*, *lexAop-mCD2::GFP* showed co-expression of reporters in ISNs. (bottom) *VT011155, UAS-mCD8::tdTomato* and *R34G02-LexA*, *lexAop-mCD2::GFP* flies showed co-expression of reporters in ISNs. Scale 50 m.

F. DenMark and Synaptotagmin expression in ISN neurites, showing overlapping pre- and post-synaptic sites in the dorsal SEZ. Scale 20 μm.

Figure 2.S2

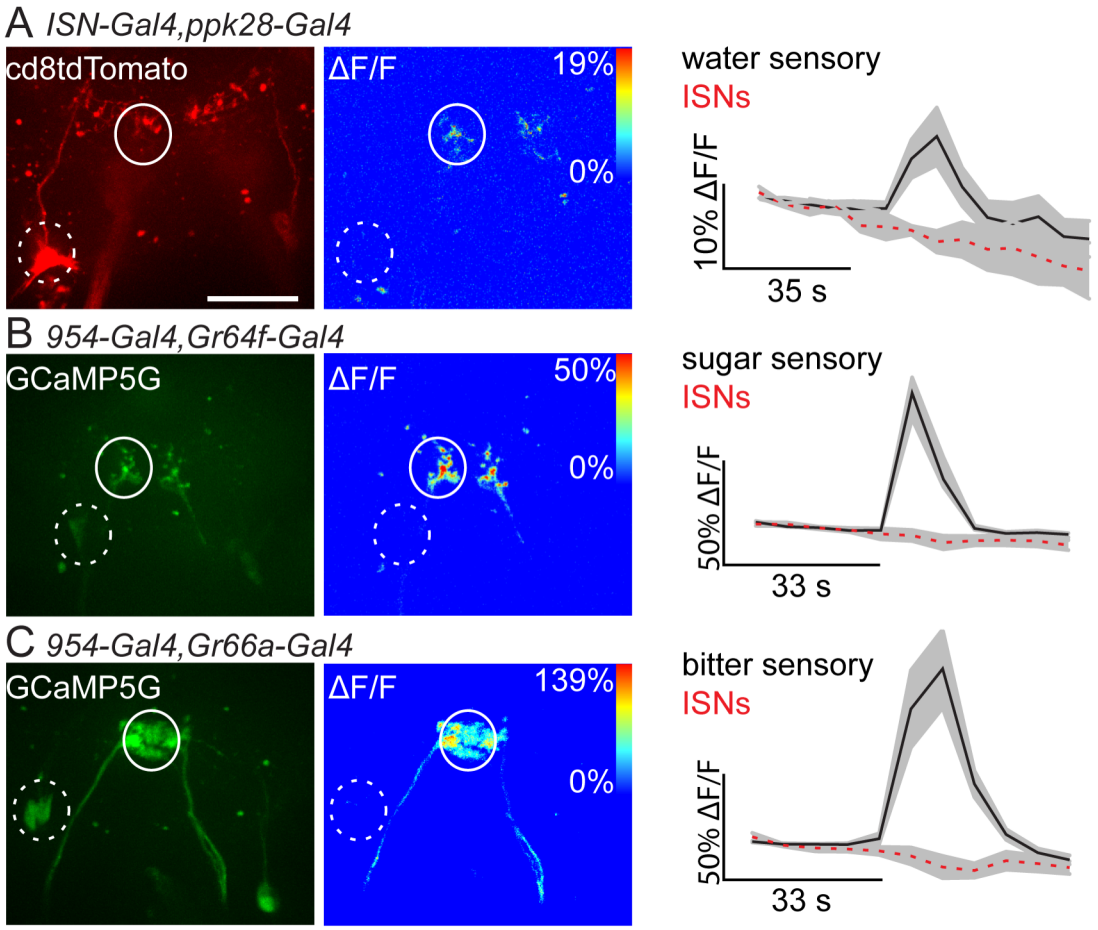

Figure 2.S2 ISNs are not taste responsive, related to Figure 2.2.

A. (left) Expression of mCD8::tdTomato in ISNs and *ppk28* positive water-taste projections that also express GCaMP6s. (middle) Example ΔF/F heat-map of GCaMP6s increase in brain from left panel upon stimulation of the proboscis with water. Solid ROI: water taste projections. Dashed ROI: ISN cell bodies. (right) ΔF/F traces (mean ± SEM) for water taste stimuli for water taste projections (solid line) or ISN cell bodies (dashed line). n=6 brains. Scale 50 µm. One sample t-tests for difference from theoretical mean of 0.0, water sensory **p<0.01, ISNs ns.

B. (left) Expression of GCaMP5G in ISNs and *Gr64f* positive sugar-taste projections. (middle) Example ΔF/F heat-map of fluorescence increase in brain from left panel upon stimulation of the proboscis with 1M sucrose. Solid ROI: sugar taste projections. Dashed ROI: ISN cell bodies. (right) ΔF/F traces (mean ± SEM) for sugar taste stimuli for sugar taste projections (solid line) or ISN cell bodies (dashed line). n=6 brains. One sample t-tests for difference from theoretical mean of 0.0, sugar sensory ***p<0.001, ISNs ns.

C. (left) Expression of GCaMP5G in ISNs and *Gr66a* positive bitter-taste projections. (middle) Example ΔF/F heat-map of fluorescence increase in brain from left panel upon stimulation of the proboscis with 10 mM denatonium. Solid ROI: bitter taste projections. Dashed ROI: ISN cell bodies. (right) ΔF/F traces (mean ± SEM) for bitter taste stimuli for bitter taste projections (solid line) or ISN cell bodies (dashed line). n=6 brains. One sample t-tests for difference from theoretical mean of 0.0, bitter sensory **p<0.01, ISNs ns.

Figure 2.S3

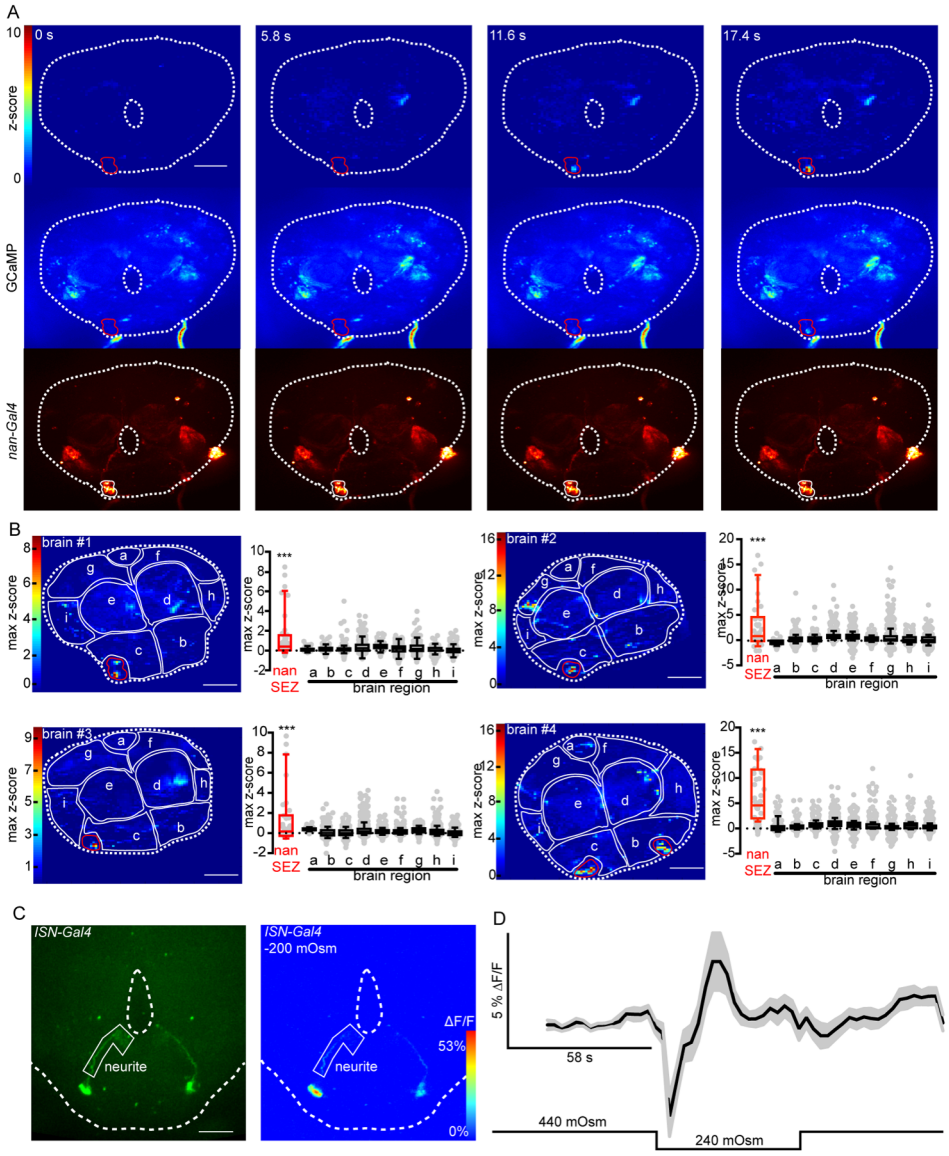
A
0 s
5.8 s
11.6 s
17.4 s
z-score
GCaMP
nan-Gal4
B
brain #1
brain #2
brain #3
brain #4
max z-score
nan
SEZ
a b c d e f g h i
brain region
C
ISN-Gal4
neurite
ISN-Gal4
-200 mOsm
ΔF/F
53%
0%
D
5 % ΔF/F
58 s
440 mOsm
240 mOsm

Figure 2.S3 Behavioral phenotypes with *nan* RNAi, related to Figure 2.4.

A. Example response to 200 mOsm/kg decrease in *nSyb-LexA, lexAop-GCaMP6s; nan-Gal4, UAS-cd8tdTomato*

Brain. (Top) brain tiled with 7, 225 ROIs color coded by the number of standard deviations each ROI's ΔF/F value is from the mean of all ΔF/F values (z-score). (Middle) Raw GCaMP fluorescence at each time point. (Bottom) Raw cd8tdTomato fluorescence at each time point, showing only the left nan^+ SEZ cluster is present in this brain. One or both ISN clusters are often lost during dissection because ISN cell bodies sit in a nerve that needs to be cut to separate the brain from the cuticle. Perfusion channels were switched at t = 0. In these experiments, 6 s were required to replace high osmolality with low osmolality solution inside the imaging chamber. Cd8tdTomato expression was used to trace nan^+ SEZ cluster outline (solid line), which includes two ISNs and two additional cells (see figure 2.S5). Scale 100 μm.

B. Maximum z-scores for each of 7,225 ROIs in four replicate brains. Cd8tdTomato expression was used to trace ISN outline (indicated by red outline). Brain regions were traced using gross neuropil morphology. Brain regions correspond to the *pars intercerebralis* (a), right SEZ (b), left SEZ (c), right antennal lobe (d), left antennal lobe (e), and higher brain (f-i). One way ANOVAs, tukey's post hoc, ***$p < 0.0001$. Brain #1 is the brain in A, above. Brain #4 is the brain in Figure 2.4D.

C. (Left) *GCaMP6s* expression in ISNs, with ROI drawn around left neurite. (Middle) Example ΔF/F heat-map of GCaMP6s increase in cell body and neurite of ISNs in response to 200 mOsm/kg decrease. Figure 2.5B is a zoomed-in image of the left ISN in this image.

D. ΔF/F trace (mean ± SEM) for neurite responses to 200 mOsm/kg decrease (n = 14 brains).

Figure 2.S4

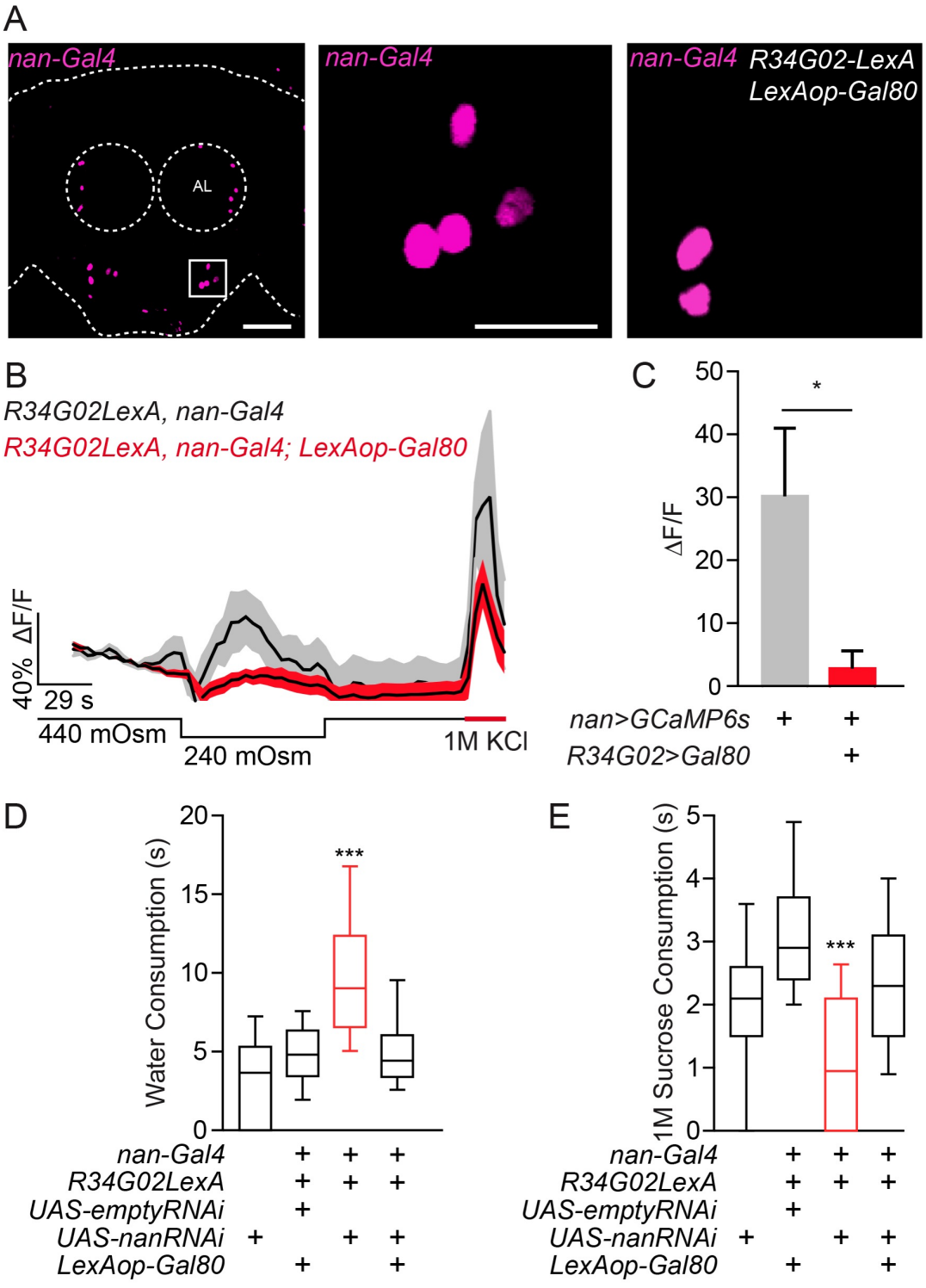
A
nan-Gal4
AL
nan-Gal4
nan-Gal4 R34G02-LexA
LexAop-Gal80
B
R34G02LexA, nan-Gal4
R34G02LexA, nan-Gal4; LexAop-Gal80
40% ΔF/F
29 s
440 mOsm
240 mOsm
1M KCl
C
ΔF/F
50
40
30
20
10
0
*
nan>GCaMP6s + +
R34G02>Gal80 +
D
Water Consumption (s)
20
15
10
5
0
***
nan-Gal4 + + +
R34G02LexA + + +
UAS-emptyRNAi +
UAS-nanRNAi + + +
LexAop-Gal80 + +
E
1M Sucrose Consumption (s)
5
4
3
2
1
0
***
nan-Gal4 + + +
R34G02LexA + + +
UAS-emptyRNAi +
UAS-nanRNAi + + +
LexAop-Gal80 + +

Figure 2.S4 Non-ISN, nan^{+} neurons do not respond to osmolality or affect consumption behavior, related to figure 2.5.

A. Left: nuclear expression of *nan-Gal4*. Scale 50 um. Middle: Zoom of left panel showing four *nan-Gal4* nuclei in a single SEZ cluster. Scale 20 um. Right: *Gal80* excludes expression of *nan-Gal4* in ISNs.

B. ΔF/F traces (mean ± SEM) to 200 mOsm/Kg osmolality decreases in flies expressing *UAS-GCaMP6s* in *nan* positive SEZ neurons in the presence (*R34G02LexA, nan-Gal4*) or absence (*R34G02LexA, nan-Gal4*; *LexAop-Gal80*) of ISNs.

C. Maximum ΔF/F (mean ± SEM) responses of traces in panel C. n=7 for each condition. one-way ANOVA, t-test *p<0.05.

D. ISNs are required for water consumption phenotype of *nan-Gal4>UAS-nanRNAi* flies. one-way ANOVA, Tukey's Post Hoc, ***p<0.001.

E. ISNs are required for sugar consumption phenotype of *nan-Gal4>UAS-nanRNAi* flies. one-way ANOVA,
Tukey's Post Hoc, ***p<0.001.

Figure 2.S5

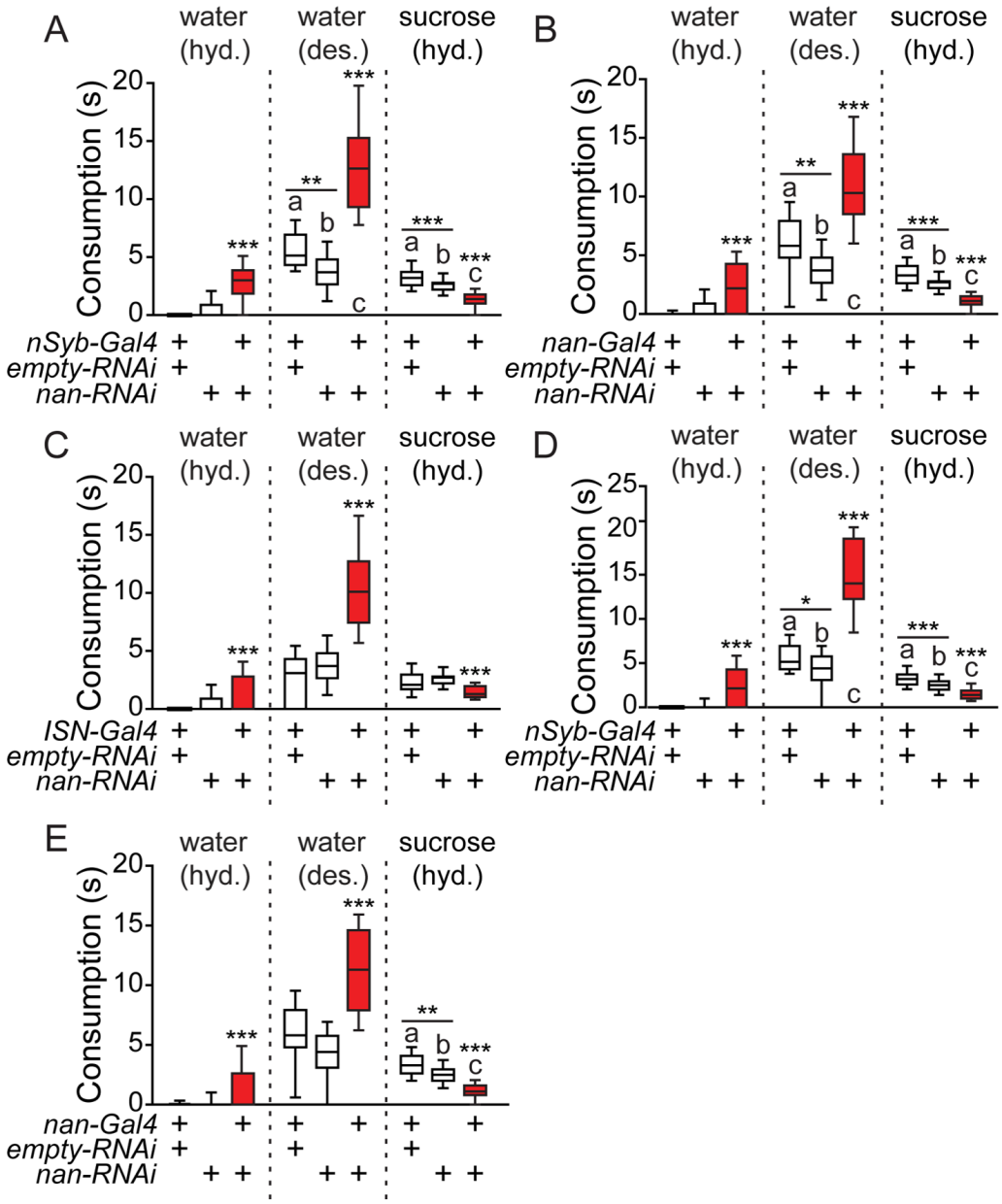

Figure 2.S5 Behavioral phenotypes with *nan* RNAi, related to Figure 2.7.

A. *nan-RNAi* (BSC# 31674) phenotypes with *nSyb-Gal4* driver. Desiccated (des.), hydrated (hyd.). n=46-65 flies, one-way ANOVA, Tukey's Post Hoc, **p<0.01, ***p<0.001.

B. *nan-RNAi* (BSC# 31674) phenotypes with *nan-Gal4* driver. n=46-65 flies, one-way ANOVA, Tukey's Post Hoc, **p<0.01, ***p<0.001.

C. *nan-RNAi* (BSC# 31674) phenotypes with *ISN-Gal4* driver (*ISN-Gal4*). n=37-73 flies, one-way ANOVA, Tukey's Post Hoc, ***p<0.001.

D. *nan-RNAi* (BSC# 31925) phenotypes with *nSyb-Gal4* driver. n=48-67 flies, one-way ANOVA, Tukey's Post Hoc, *p<0.05, **p<0.01, ***p<0.001.

E. *nan-RNAi* (BSC# 31925) phenotypes with *nan-Gal4* driver. n=48-73 flies, one-way ANOVA, Tukey's Post Hoc, **p<0.01, ***p<0.001.

Extended Experimental Procedures

Blue Dye Consumption experiments

15-20 female flies were transferred to vials with 2.5cm filter paper (Whatman) soaked with 300 l of 200mM sucrose with 0.25mg/mL blue dye (Erioglaucine, Sigma). The cotton flug was soaked with water. In the initial screen, flies were allowed to feed for 30 min, and the sucrose soaked filter paper was at the vial bottom. For subsequent experiments, flies were allowed to feed for 2 hrs in inverted vials with the sucrose paper at the vial top. For 30°C experiments, vials were pre-warmed 20 min at 30°C.

Temporal Consumption Assays

Flies were mounted on glass slides with nail polish, then placed in a humidified chamber for 2 hrs. Each animal was presented a tastant 10 times on the proboscis and forelegs, and consumption time was recorded. Consumption time correlates with consumption volume.

RNAi crosses used for temporal consumption assays were maintained at 25˚C, 65% relative humidity (RH). Flies were aged 2-7 days (initial RNAi screen) or 4-7 days (other assays). Prior to testing, flies were provided water and allowed to drink to satiety, unless the experimental tastant was water. However, in tests for a reduction in sucrose consumption, flies were not provided water prior to testing to exclude interactions between sucrose consumption and water consumption.

For temporal consumption assays using thirsty flies, flies were mounted as described above and placed in a sealed chamber with ~250g $CaSO_4$ (Drierite, stock# 23001) for 2 hours, unless otherwise noted. Each animal was provided distilled water 10 times and cumulative drinking time was recorded.

For dTRPA1 experiments, crosses to *UAS-dTRPA1; UAS-dTRPA1/TM2* flies were raised at 20˚C, 60% RH. Flies with two copies of *UAS-dTRPA1* were aged 2-4 or 4-7 days. Flies were heated on a Peltier device for five min before testing.

Behavioral experiments using RNAi

For *nan* RNAi experiments, RNAi-only controls were performed subsequent to Gal4-only controls and experimental genotypes. Data from the same +/*nan RNAi* (BSC# 31925) controls is shown in Figure 2.3B, 7C, and S7D-E. Data from the same +/*nan RNAi* (BSC# 31674) control is shown in Figure 2.S7A-C.

Immunohistochemistry

The primary antibodies were rabbit anti-GFP (Invitrogen, 1:1000), mouse anti-GFP (Sigma 1:1000), rabbit anti-RFP (Biovision, 1:500), mouse anti-Bruchpilot (nc82) (Developmental Studies Hybridoma Bank, 1:500). For double labeling experiments, *R34G02-LexA* (BSC#54138) and *R34G02-LexA* (made for this study) were used. *R34G02-LexA* (BSC#54138) was used in Figure 2.5A, 2.S1C (VT011155 double label), 2.S5A, and 2.S5B. The *R34G02-LexA* made for this study was used for in Figure 2.2A and the *954-Gal4* double label in Figure 2.S1C.

Calcium and voltage imaging

For experiments involving AKH, AHL with hormone or KCl was applied as indicated. For serial applications, the protocol was 0-300 sec AHL, 300-320 sec 316pM AKH in AHL, 320-620 sec drug treatment (TTX, insulin, or insulin + TTX), 620-640 sec 316pM AKH in AHL, 640-900 sec AHL. Single-plane imaging was performed with a 20x water immersion objective on a Zeiss PASCAL confocal microscope, with an open pinhole. Images were collected at 1 Hz.

For GCaMP6s imaging of osmolality responses, brains were dissected, pinned, and perfused as above. Brains were imaged on a 3i spinning disc confocal microscope with a 20x water immersion objective at ~0.3 Hz. For ArcLight experiments, imaging rate was ~0.8 Hz, analysis was performed on max-z projections of 10 sections per time point, 0.8-1.4 m sections. For GCaMP6s imaging, analysis was done on max-z projections of 17 imaging sections, 0.8-1.4 m sections. $\%\Delta F/F = 100\%*((F_t-F_0)/F_0)$, where F_0 is the mean fluorescence of 5-15 time points prior to stimulus onset and F_t is the fluorescence at each time point. Max $\Delta F/F = F_{max} - F_0$, where F_{max} is the maximum $\Delta F/F$ observed during the stimulus. For ArcLight responses following osmolality decreases that occur subsequent to a prior increase (figure 2.4G, H), minimum $\Delta F/F$ was calculated as $F_{min} - F_0$, where F_{min} is the minimum $\Delta F/F$ observed in a window beginning 6 s following osmolality decrease and ending 38 s thereafter.

Hemolymph osmolality measurements

The osmometer was placed in a glass-lidded box with desiccant (Drierite) to prevent condensation. Coolant was ethanol chilled to -60°C. Standards and samples were loaded into square capillaries (0.05mm x 0.05 mm, Vitro Dynamics). For each measurement, 4 standards were included: distilled water, 150mM, 210mM, and 269mM NaCl, as well as hemolymph from four individual flies. Osmolality measurements from three standards (water, 150mM NaCl and 269mM NaCl) were used to fit a second-order polynomial curve, to calculate osmolality of experimental samples. The difference between known and measured osmolality of the fourth standard (210mM NaCl) was used to estimate error. An Olympus SZX16 microscope with a mounted camera (Point Grey Firefly MV) captured images of the ice-liquid interface. The distance from the water standard to each NaCl standard and experimental sample was measured using Adobe Photoshop.

To collect hemolymph of single flies, non-anesthetized flies were loaded into a pipette tip and positive pressure was applied, such that the head protruded. Removing head cuticle including the antenna caused hemolymph to protrude; this was collected in a capillary.

Flies were desiccated or hydrated in the same manner as in temporal consumption assays, except that treatment time was 6 hours instead of 2 hours. Also, flies desiccated or hydrated for hemolymph collection were allowed to walk freely in an empty vial capped with mesh cloth. Flies were starved in vials with wet flugs containing kimwipes soaked in water. In Figure 2.6C, flies were rehydrated by presentation of a water droplet in the same manner as in temporal consumption assays.

Generation of *R34G02-LexA*

A 1,066-bp genomic DNA fragment, containing the R34G02 tile from the FlyLight collection (Pfeiffer et al., 2012), was amplified using GAGGCTCTTTATGATCCCGTGGACG and CGACGACACTCGCCACAACCCAAAG primers, and recombined into the pBPLexA::p65Uw plasmid (Pfeiffer et al., 2010).

Table S1: Transgenic flies used in this study, related to Figure 2.1

Figure	Genotypes Used
2.1A	*Clandinin-Gal4 x UAS-dTRPA1, UAS-dTRPA1*
2.1B	*954-Gal4/+; UAS-mCD8::GFP/+; +/+*
2.1C	*+/UAS-mCD8::GFP; R34G02/+*
2.1D	*+/UAS-mCD8::GFP; VT011155/+*
2.1E	*954-Gal4/+; UAS-dTRPA1/+; UAS-dTRPA1/+* (*isoD*^{1} background) *UAS-dTRPA1/+; UAS-dTRPA1/+* (*isoD*^{1} background)
2.1F	*+/UAS-dTRPA1; R34G02/UAS-dTRPA1* (w^{1118} background) *UAS-dTRPA1/+; UAS-dTRPA1/+* (w^{1118} background)
2.1G	*+/UAS-dTRPA1; VT011155/UAS-dTRPA1* (w^{1118} background) *UAS-dTRPA1/+; UAS-dTRPA1/+* (w^{1118} background)
2.2A (left panel)	*+/UAS-mCD8::GFP; +/AKHR-Gal4*
2.2A (other panels)	*+/lexAop-mCD8::GFP, UAS-mCD8::RFP; R34G02-LexA/+; AKHR-Gal4/+*
2.2B	*954-Gal4;+/+; UAS-GCaMP5G*
2.2C	AKH response in AKHR mutant: *954-Gal4; AKHR*^{null}*/AKHR*^{null}*; UAS-GCaMP5G* Other panels: *954-Gal4;+/+; UAS-GCaMP5G*
2.2D	*954-Gal4;+/+; UAS-GCaMP5G*
2.2E	*954-Gal4/+; UAS-mCD8::GFP/+*
2.3A	*nSyb-Gal4/+; UAS-RNAi/UAS-dcr* (experimental for each RNAi candidate) *+/+; UAS-RNAi/UAS-dcr* (control for each RNAi candidate)
2.3B	WT: w^{1118} Otherwise as shown in figure
2.3C	As shown in figure
2.3D	*nan-Gal4/UAS-mCD8::GFP; +/+*
2.4A-C	*nan-Gal4; UAS-GCaMP6s/+*
2.4D	*nan-Gal4, UAS-mCD8::tdTomato/+, nSyb-LexA, lexAop-GCaMP6s/+*
2.4E	*nan*^{WT}: *nan-Gal4, UAS-GCaMP6s/+; +/+* *nan*^{36a}: *nan-Gal4, UAS-GCaMP6s/+; nan*^{36a}
2.4F	*nan*^{WT}: *nan-Gal4, UAS-GCaMP6s/+;* *nan*^{36a}: *nan-Gal4, UAS-GCaMP6s/+; nan*^{36a} *UAS-nan*: *nan-Gal4, UAS-GCaMP6s/UAS-nan; nan*^{36a}
2.4G-H	GCaMP: *+/+; VT011155, UAS-GCaMP6s/+* Arc.: *UAS-ArcLight/+; VT011155/+*
2.5A	*nan-Gal4, UAS-mCD8::tdTomato/R34G02-LexA (BSC#54138); lexAop-mCD2::GFP/+*
2.5B	*+/+; VT011155, UAS-GCaMP6s/+*
2.5C	Left: *+/+; VT011155, UAS-GCaMP6s/+* Middle: *nan-Gal4, UAS-GCaMP6s/+; +/+* *nan-Gal4, UAS-GCaMP6s/+; nan*^{36a}

	Right: *954-Gal4; +/+; UAS-GCaMP5G* *954-Gal4; AKHR^{null}; UAS-GCaMP5G*
2.5D-E	*+/+; VT011155, UAS-GCaMP6s/+*
2.6A-C	*CantonS*
2.6D, E	*UAS-cd8tdTomato/+; VT011155, UAS-ArcLight/+* *UAS-cd8tdTomato/+; VT011155, UAS-GCaMP6s/+*
2.7A-D	As shown in figure
2.7E	*CantonS*
2.S1A (top two panels)	*954-Gal4/+*; *UAS-dTRPA1*/*Tsh-Gal80*; *UAS-dTRPA1/ UAS-mCD8::GFP*
2.S1A (bottom panel, left to right)	*UAS-dTRPA1/+; UAS-dTRPA1/UAS-mCD8::GFP* (*isoD^{1}* background) *954-Gal4/+; UAS-dTRPA1/+; UAS-dTRPA1/+* (*isoD^{1}* background) *Tsh-Gal80/UAS-dTRPA1; UAS-mCD8::GFP/UAS-dTRPA1* *954-Gal4/+*; *UAS-dTRPA1*/*Tsh-Gal80*; *UAS-dTRPA1/UAS-mCD8::GFP*
2.S1B (top two panels)	*954-Gal4/+; UAS-mCD8::GFP/+; 149-Gal80/+*
2.S1B (bottom panel, left to right)	*UAS-dTRPA1*/+; *UAS-dTRPA1*/+ (*isoD^{1}* background) *954-Gal4/+; UAS-dTRPA1/+; UAS-dTRPA1/+* (*isoD^{1}* background) *UAS-dTRPA1/+; UAS-dTRPA1/149-Gal80* *954-Gal4/+; UAS-dTRPA1/+; UAS-dTRPA1/149-Gal80*
2.S1C (top panel)	WT x *dTRPA1*: *UAS-dTRPA1*/+; *UAS-dTRPA1*/+ (*isoD^{1}* background) *954-Gal4* x *dTRPA1*: *954-Gal4; UAS-dTRPA1/+; UAS-dTRPA1/+* (*isoD^{1}* background)
2.S1C (middle panel)	WT x *dTRPA1*: *UAS-dTRPA1*/+; *UAS-dTRPA1*/+ (*w^{1118}* background) *R34G02* x *dTRPA1*: *UAS-dTRPA1/+; UAS-dTRPA1/R34G02* (*w^{1118}* background)
2.S1C (bottom panel)	WT x *dTRPA1*: *UAS-dTRPA1*/+; *UAS-dTRPA1*/+ (*w^{1118}* background) *VT011155* x *dTRPA1*: *UAS-dTRPA1/+; UAS-dTRPA1/VT011155* (*w^{1118}* background)
2.S1D (left to right)	*954-Gal4/+; +/+; UAS-redStinger/+* *R34G02-Gal4/+; UAS-redStinger/+* *+/+; VT011155-Gal4/UAS-redStinger*
2.S1E	Top three panels: *954-Gal4/lexAop-mCD8::GFP, UAS-mCD8::RFP; R34G02-LexA/+; +/+* Middle three panels: *+/lexAop-mCD8::GFP, UAS-mCD8::RFP; R34G02-LexA/R34G02-Gal4; +/+* Bottom three panels: *UAS-mCD8::tdTomato/R34G02-LexA (BSC#54138); VT011155/lexAop-mCD2::GFP*
2.S1F	+/*UAS-DenMark, UAS-eGFP::synaptotagmin*; *VT011155/ UAS-DenMark, UAS-eGFP::synaptotagmin*
2.S2A	*UAS-GCaMP6s, UAS-mCD8::tdTomato/+; ppk28-Gal4/VT011155*

2.S2B	*954-Gal4/+; Gr64f-Gal4/+; UAS-GCaMP5G/+*
2.S2C	*954-Gal4/+; Gr66a-Gal4/+; UAS-GCaMP5G/+*
2.S3A, B	*nan-Gal4, UAS-mCD8::tdTomato/+, nSyb-LexA, lexAop-GCaMP6s/+*
2.S3C, D	+/+; *VT011155, UAS-GCaMP6s*
2.S4A	*nan-Gal4, R34G02-LexA(BSC#54138)/+; +/UAS-RedStinger* *nan-Gal4, R34G02-LexA(BSC#54138)/+; LexAop-Gal80/UAS-RedStinger*
2.S4B, C	*nan-Gal4, R34G02-LexA(BSC#54138)/+; +/UAS-GCaMP6s* *nan-Gal4, R34G02-LexA(BSC#54138)/+; LexAop-Gal80/UAS-GCaMP6s*
2.S4D, E	As shown in figure.
2.S5	As shown in figure.

Chapter 3: Characterization of neural circuits regulating food and water ingestion

Summary

Food and water ingestion are goal directed behaviors essential for animal survival. To regulate these behaviors, animal nervous systems must weigh multiple, sometimes competing metabolic needs. Understanding how neural circuits accomplish this task is a major question in neuroscience. Recently, we identified a population of four neurons, the ISNs (Interoceptive SEZ Neurons), that integrate internal signals of hunger and thirst, and are sufficient to modulate both food and water ingestion. Interestingly, ISN activity has opposing effects on sugar and water ingestion, concurrently promoting the former and suppressing the latter. Here, we use genetic tools and calcium imaging studies to search for neural circuits downstream of ISNs that mediate this regulation. We identify the neurotransmitter most likely employed by ISNs, determine the anatomy of neurons post-synaptic to ISNs, and characterize how ISN activity influences neural responses to the taste of sugar and water. These studies contribute to our understanding of how neural circuits integrate internal signals of metabolic need to coordinate essential but mutually exclusive homeostatic behaviors.

Introduction

Nutrient homeostasis is a basic requirement for life. In animals, nutrient homeostasis depends on neural circuits that integrate multiple internal signals of metabolic need to orchestrate coherent, goal-direct behaviors. While components of circuits underlying homeostatic behaviors have been identified, none have been anatomically traced from input to output, and the components that have been identified are in almost all cases internal sensors of specific metabolic needs. For example, neural populations in the arcuate nucleus of the mammalian hypothalamus have been identified that are specifically sensitive to circulating leptin, a signal of food satiety, and ghrelin, and signal of hunger, among other signals (*69, 70*). Similarly, neurons in the sub-fornical organ, a mammalian brain region on the anterior wall of the third ventricle, have been identified that directly sense the osmolality of the cerebrospinal fluid (*27*).

Understanding how the nervous system processes information encoded by these interoceptive neurons has been challenging for two major reasons. First, most studies of homeostatic behavior have been carried out in mammals, where even simple nervous systems contain billions of neurons. Second, the tools for mapping and understanding complex neural circuits have so far failed to combine a high level of anatomical resolution with information about neural activity.

Among these tools, electron microscopy (EM) is the gold standard for determining circuit connectivity at synaptic resolution. While this approach has led to key insights (*71, 72*), the complexity of EM data sets has also made them challenging to interpret (*73*). More recently, rabies-based viral tracers have been successfully used as a circuit tracing strategy that sacrifices the resolution of EM tracing while improving speed and reducing cost (*74*). These tracers rely on injection of modified rabies virus into a brain region of interest, from which the rabies virus spreads in an anterograde fashion (i.e., from post to pre-synaptic neurons), taking with it a marker (typically fluorescence) to determine neural anatomy. These tracers have been used to map neurons post-synaptic to internal sensors of blood osmolality (*75*) and metabolic need (*76*). However, like most circuits in the mammalian brain, neurons downstream of these sensors exhibit a high degree of interconnectivity and redundancy, and project to a large number of brain areas. This complexity has made it challenging to learn general principles of neural circuit design.

A complementary approach to understand neural circuit function is to characterize functional, rather than anatomical connectivity. This approach requires monitoring activity in large neural populations in living animals, ideally those in which internal physiological variables can be experimentally manipulated. The technical challenge posed by this requirement has impeded the use of functional imaging as a tool to study neural circuits for homeostatic behaviors until relatively recently. For example, Knight, Sternson, Andermann, and colleagues have recently used head-mounted endoscopes, optrodes, and fiber photometry to monitor large scale neural activity in the arcuate nucleus of the hypothalamus (*17, 76, 77*). These studies have shown that sensors of metabolic need can be rapidly modulated by sensory experience, and, in combination with retrograde tracing strategies, this sensory modulation has been traced to inhibitory neurons projecting from another compartment of the hypothalamus (*78*). However, tools for mapping and imaging neural circuits are still restricted to relatively small regions of the brain, such as the arcuate nucleus. New approaches will therefore be required to gain deeper insight into neural circuits regulating homeostatic behaviors.

One approach is to study these neural circuits in an organism that performs homeostatic behaviors, but has a smaller and simpler nervous system than those of mammals. *Drosophila melanogaster* is such an organism. *Drosophila* exhibits behaviors, such as the oral ingestion of sugar and water, that strongly resemble homeostatic behaviors observed in mammals, but use a nervous system that contains about 10^4 fewer neurons. Moreover, an EM volume of the entire *Drosophila* brain has recently been generated (*79*). Studying *Drosophila* nervous system therefore provides an approach to understand homeostatic behavior in a way that has thus far been challenging in mammals.

Here, I use a combination of behavioral genetics, large-scale calcium imaging, and circuit tracing to begin characterizing how a population of *Drosophila* interoceptive neurons influences food and water ingestion. These neurons, the ISNs, are unique in that they sense internal physiological signals of both sugar and water abundance, and integrate those signals to oppositely regulate food and water ingestion. The results presented here provide insight into how they achieve this opposite regulation, with implications for understanding how homeostatic circuits coordinate essential survival behaviors.

Results

Drosophila insulin-like peptide 3 (dILP-3) is likely the ISN neurotransmitter

ISN-specific RNAi knockdown of *n-synaptobrevin* causes flies to increase water ingestion approximately two-fold over controls (*80*). Because *n-synaptobrevin* is directly required for the release of neurotransmitters and a handful of neuropeptides, knockdown of enzymes required for the biosynthesis of the ISN neurotransmitter(s) should cause a similar increase in water ingestion behavior. I therefore carried out a behavioral screen for neurotransmitter biosynthesis enzymes that, when knocked down in ISNs by RNAi, caused flies to increase water ingestion over controls.

Specifically, I used *ISN-Gal4* to drive expression of *UAS-RNAi* constructs targeting enzymes responsible for synthesis of the major neurotransmitters utilized by the *Drosophila* nervous system, as well as some neuropeptides. I then measured water ingestion time following ten presentations of a water droplet to the proboscis and tarsi of single flies. *ISN-Gal4* drives expression in ISNs and in no other neurons in the *Drosophila* nervous system. This assay therefore allowed me to measure the effect of neurotransmitter loss specifically in ISNs.

Surprisingly, RNAi knockdown of enzymes required for the biosynthesis of canonical excitatory and inhibitory neurotransmitters failed to influence water ingestion (Figure 3.1A). In contrast, ISN-specific RNAi knockdown of *Drosophila insulin-like peptide 3* (*dILP-3*) caused flies to ingest about twice as much water as controls, an effect indistinguishable from that observed following knockdown of *n-synaptobrevin* (t-test, $p = 0.16$). The *Drosophila* genome encodes eight insulin-like peptides, seven of which (dILPs 1-7) may function in adult animals (*81*). I therefore tested the effect of RNAi knockdown of dILPs1-7 on water ingestion behavior. Out of these, only dILP-3 was required in ISNs for appropriate water ingestion behavior (Figure 3.1A).

A key feature of ISNs is their opposing influence on water and sugar ingestion: ISN silencing by *n-synaptobrevin* RNAi is sufficient to concurrently promote water ingestion and suppress sugar ingestion. If dILP-3 is the ISN neurotransmitter, then *ISN-specific* expression of *dILP-3* RNAi should both increase water ingestion and suppress sugar ingestion. This was the case. Flies expressing *dILP-3* RNAi under the control of *ISN-Gal4* ingested more water than

controls in both hydrated and dehydrated states, consistent with the screen results described above. Following two hours of food deprivation, they also ingested significantly less sugar than controls (Figure 3.1B, top). Thus, loss of dILP-3 in ISNs causes a behavioral phenotype qualitatively indistinguishable from complete silencing of ISN neurotransmission (Figure 3.1B, bottom).

Taken together, these results argue that ISNs are peptidergic neurons that release dILP-3. This claim is consistent with the fact that ISNs have relatively large cell bodies, a property shared by other peptidergic neurons in the *Drosophila* nervous system (*81, 82*). Demonstrating that ISNs release dILP-3 however, requires directly observing this peptide in ISN cell bodies or processes. Quantifying peptide abundances in *Drosophila* neurons is currently challenging, as antibody staining often fails to detect weakly expressed peptides, and Gal-4 lines driven by enhancer elements of peptide genes may not recapitulate endogenous expression. I found that a dILP3-Gal4 line drives expression in SEZ neurons that resemble ISNs (Figure 3.1C), and antibody staining using an anti-dILP-3 antibody revealed weak staining in ISN cell bodies (Figure 3.1D). Nonetheless, I cannot exclude the possibility that dILP-3 Gal4 expression does not reflect endogenous dILP-3 expression, nor can I exclude the possibility dILP-3 antibody signal in ISN cell bodies reflects non-specific background staining. Thus, direct evidence of dILP-3 in ISNs will likely require a more direct, but also time intensive, approach such as creating of a dILP-3::GFP knock-in fly or performing ISN single cell RNAi sequencing.

A behavioral screen for neurons functioning downstream of ISN activity

The pre and post-synaptic terminals of ISNs are distant from gustatory neurons, and ISNs are not activated by gustatory input (*80*). ISNs nonetheless exert a powerful, taste-dependent effect on ingestion, promoting ingestion in the case of sugar taste and suppressing it in the case of water taste. Neural circuits down-stream of ISNs must therefore exist that mediate these taste dependent effects on behavior. I carried out a behavioral screen to identify the neurons that comprise these circuits.

To do this, I identified candidate Gal4 lines that satisfied three criteria. First, they labeled relatively sparse subsets of the *Drosophila* nervous system. Second, they contained neurons with processes in close proximity to ISN pre-synaptic terminals. Finally, because ISNs likely release dILP-3 as a neurotransmitter, I chose Gal4 lines that were driven by enhancer elements of the *Drosophila insulin receptor* gene. Candidates were identified on the basis of alignments of Gal4 expression patterns to a standard reference brain. This approach produced 14 candidates (Figure 3.2A, Table 3.S1). If any of these Gal4 line contained neurons post-synaptic to ISNs, then silencing them should lead to ingestion phenotypes reminiscent of those observed following ISN silencing. I therefore tested these lines by monitoring water ingestion in flies in which candidate Gal4s drove expression of *n-synaptobrevin* RNAi. Only two candidates, *R45B08-Gal4* (candidate 1) and *VT063185-Gal4* (candidate 2), caused strong water ingestion phenotypes following *n-synaptobrevin*-based RNAi silencing.

Each of the candidates tested label >50 neurons in the *Drosophila* central brain (Figure 2.2B). However, of these, only a small number appeared to contact ISNs in whole brain alignments of expression patterns. The neurons in *VT063185-Gal4* that were proximal to ISNs appeared to be a novel class of SEZ neurons, which we named “bridle”. The neurons in *R45B08-Gal4* that made contact with ISNs resembled a previously described neural class, aSG7, which has already been described in the context of *Drosophila* feeding regulation (*83*).

To directly test the role of these neurons in regulating sugar and water ingestion, we designed a set of transgenic split Gal4 lines that exclusively labeled bridle or aSG7 (Figure 3.2B). Split Gal4 lines produce sparse expression by using enhancer elements from one Gal4 to drive the expression of a fusion of the Gal4 DNA binding domain (Gal4-DBD) and a leucine zipper domain, while using the enhancer elements of another Gal4 to drive expression of a fusion of the Gal4 activation domain (AD) and a leucine zipper domain. In neurons where the expression patterns of these two Gal4 lines overlap, Gal4-DBD and Gal4-AD are both expressed, and Gal4 is reconstituted via interaction between the two leucine zippers.

I used bridle and aSG7 split Gal4 lines to drive expression of csChrimson, a light sensitive cation channel that causes neural activity when exposed to red light (*84*). While activating aSG7 mildly suppressed water ingestion, it had no effect on sugar ingestion (Figure 2C-D). Moreover, activating bridle neurons failed to affect either sugar or water ingestion behavior (Figure 3.2C-D). While weak driver strength may explain these negative results, it is possible that aSG7 and bridle do not function downstream of ISNs. I therefore took an alternative approach to identify neurons post-synaptic to ISNs.

Anatomical characterization of neurons post-synaptic to ISNs

To determine the anatomy of neurons post-synaptic to ISNs, I used a recently developed genetic tool, *transTANGO,* to perform anterograde neural tracing from ISNs (*85*). *transTANGO* takes advantage of a synthetic signaling pathway to drive post-synaptic fluorophore expression in a manner that is strictly dependent on Gal4 expression in a neuron of interest (Figure 3.3A). Specifically, Gal4 expression drives expression of a synaptically targeted, membrane tethered fusion of human glucagon. At the synapse, glucagon binds an engineered, post-synaptic glucagon receptor delivered to all neurons by the *transTANGO* transgene. Binding of glucagon to its receptor triggers a synthetic signaling cascade that results in RFP expression exclusively in neurons post-synaptic to those expressing Gal4. As ISN-Gal4 is expressed in ISNs and in no other neurons, *transTANGO* is an ideal tool to identify the ISN post-synaptic partners. To do this, I generated flies that expressed the *transTANGO* system under the control of ISN-Gal4. I then fixed and stained the brains and ventral nerve cords (VNCs) of 5-10 day old female flies to detect RFP expressed in ISN post-synaptic neurons.

ISN-Gal4/UAS-transTANGO brains exhibited RFP expression in ~20 neurons in the central brain (Figure 3.3B, left, Figure 3.3C). The cell bodies of these neurons were located exclusively in the SEZ and the medial *pars intercerebralis* (PI), a higher brain region with important roles in regulating nutrient homeostasis. There are 3-5 post-synaptic neurons per hemisphere in the dorsal SEZ (Figure 3.3D, left), 3-5 neurons in the PI (Figure 3.3D, middle), and 2-4 neurons per hemisphere in ventromedial SEZ (Figure 3.3D, right). No clear cell bodies could be detected in the VNC, although there was diffuse RFP signal, suggesting that some of the neurons in the central brain might have descending projections (Figure 3.3B, right). These neurons sent clear projections to only two regions in the *Drosophila* nervous system: the dorsal SEZ, where the pre-synaptic terminals of the ISNs reside, and the PI. This anatomy is compelling because the PI plays a critical role in nutrient homeostasis, and is the location of multiple peptidergic neurons with diverse effects on sugar and water balance (*81*). Importantly, neither bridle nor aSG7 appeared to be labeled by RFP in *ISN-Gal4*/*transTANGO* flies, consistent with the failure to detect strong effects of bridle and aSG7 activity on water and sugar ingestion. These results argue that a relatively small number of neurons are directly post-synaptic to ISNs, and that they may influence nutrient homeostasis via interactions with the PI.

Adipokinetic hormone potentiates sugar, but not water, taste responses in a starvation dependent manner

The results presented above argue that ISNs use dILP-3 to influence sugar and water ingestion via downstream circuits innervating the PI. However, it remains unclear how ISN activity shapes neural responses to the taste of sugar and water. To address this question, I used large-scale neural imaging approaches developed in our lab (*37*) to characterize taste responses in the SEZ in the presence or absence of AKH, the hunger peptide that increases ISN activity.

Previous work in our lab has shown that there are approximately 36 sugar taste-responsive neurons (*37*). To ask how AKH modulates these neural representations of sugar taste, I used nuclear localized GCaMP6s to monitor sugar taste responses in the presence or absence of 10 nM AKH, a concentration known to elicit responses from ISNs (*80*). Specifically, I performed whole SEZ imaging of responses to 1M sucrose applied to the proboscis of a live fly. I then perfused 10 nM AKH onto the exposed brain, waited 15 minutes, then repeated the 1M sucrose application. I then compared GCaMP6s responses pre- and post-AKH application for each nucleus.

I found that AKH application increased the magnitude of GCaMP6s responses to sugar taste (Figure 3.4A-C). There was no difference in GCaMP6s responses pre- and post-mock perfusion of artificial hemolymph (AHL) lacking AKH (Figure 3.4D-F). If AKH potentiates sugar taste responsive circuits, one might expect that starvation, an internal state that causes AKH release, might also potentiate these responses. Specifically, starvation might prevent the application of additional, exogenous AKH from further increasing sugar taste responses. To test this hypothesis, I monitored whole SEZ responses to sugar taste before or after application of 10 nM AKH in flies that had been starved for 24 hours. Starvation abolished the effect of AKH on sugar taste responses (Figure 3.4G-I). This result is consistent with the possibility that endogenous AKH released during starvation potentiates sugar taste responses, thus rendering exogenous AKH unable to further potentiate those responses.

One challenge of whole brain imaging is that the identities of neurons exhibiting taste responses is largely unknown. I therefore repeated the experimental approach described above with Gal4 lines that exhibited restricted expression in neural populations with known identity. The neurons that appeared to be most sensitive to AKH application have large cell bodies in the dorso-medial SEZ. Because this is the location of the motor neurons responsible for causing proboscis pumping (and thus ingestion), I hypothesized motor neuron responses to sugar taste might be potentiated by AKH. I therefore performed live calcium imaging with flies expressing *GCaMP6s* exclusively in these motor neurons and monitored responses to 1M sucrose applied to the proboscis before and after 15 minutes of exposure to 10 nM AKH. Consistent with the whole brain data described above, I observed that AKH significantly increased calcium responses in pumping motor neurons to the taste of 1M sucrose (Figure 3.4J, K).

These results suggest that starvation might potentiate sugar taste responses via AKH acting through ISNs. Although ISNs are the only neurons described to date that are AKH sensitive, there may be others. In particular, the AKHR-Gal4 line labels *Gr64f* sugar taste projections, raising the possibility that AKH may act directly on sensory neurons. To test this possibility, I performed live calcium imaging experiments in flies expressing *GCamP6s* exclusively in *Gr64f* projections, and asked if exogenous AKH potentiated responses in these projections following proboscis application of 1M sucrose. It did. Fifteen minutes of exposure to 10 nM AKH increased calcium responses to 1M sucrose in sugar taste projections by ~6%

(Figure 3.4L). Perfusion of mock AKH (AHL only) had no effect on responses (Figure 3.4L). Thus, AKH may act directly on sugar taste projections in addition to its effect on ISN activity.

The results above suggest that ISNs may modulate sugar taste responses following starvation. Do they also modulate water taste responses? To address this question, I performed live calcium imaging experiments with flies expressing GCaMP6s in *ppk-28* water taste projections, which transmit information about water taste from the proboscis to the SEZ. In contrast to the effect of AKH on sugar taste projections, I did not observe any effect of AKH on *ppk-28* sensory neuron responses to water taste (Figure 3.4M). Increasing ISN activity suppresses water ingestion, suggesting that AKH (and, by extension, ISN activity) may suppress water taste responses in ppk-28 sensory neurons. However, because *GCaMP6s* preferentially reports increases in activity, and because water taste responses are already relatively weak compared to responses to other taste modalities (*37*), the assay described here may not be sensitive enough to detect this suppression. I also tested the effect of AKH on whole SEZ responses to water taste. However, I was not able to detect responses to water taste even prior to AKH application (data not shown), likely because water alone produces very weak SEZ responses (*37*). As a result, AKH may modulate whole SEZ responses to water taste, but detecting these effects will require stronger activation of water gustatory neurons, perhaps by transgenic expression of light or ATP sensitive cation channels.

Taken together, these data suggest that ISN activity potentiates SEZ responses to sugar taste but not water taste. However, AKH also potentiates responses in sugar gustatory neurons themselves. An important next step will be understanding the extent to which potentiation of sensory neurons or potentiation of ISN activity contributes to the SEZ-wide increase in sugar taste sensitivity following AKH exposure.

Discussion

In this study, I describe mechanisms by which a type of *Drosophila* interoceptive neuron, the ISNs, influences downstream neural circuits to homeostatically regulate sugar and water ingestion. These mechanisms involve dILP-3, a *Drosophila* insulin-like peptide, which ISNs likely release, and ISN post-synaptic neurons that heavily innervate the *pars intercerebralis*, a region in *Drosophila* higher brain with essential roles in nutrient homeostasis. This work provides a starting point for understanding how one group of interoceptive neurons, the ISNs, influence large scale neural circuits to achieve nutritional homeostasis.

The ISNs as dILP-3 producing peptidergic neurons

A key finding of this work is that ISNs require *Drosophila* insulin-like peptide 3 (dILP-3) to regulate food and water ingestion. Animals in which dILP-3 has been specifically removed from ISNs inappropriately consume too much water and too little food compared to controls, the same phenotype that results from complete silencing of ISNs. ISNs therefore likely utilize dILP-3 as a neurotransmitter to communicate with downstream circuits. Neuropeptides in *Drosophila* and mammals can be co-released with canonical neurotransmitters such as GABA and glutamate (*86, 87*). While we cannot exclude the possibility that weak expression of RNAi against neurotransmitter biosynthesis enzymes resulted in false negatives, the fact that the effect of ISN-specific loss of dILP-3 is indistinguishable from the effect of ISN-specific loss of *n-synaptobrevin* argues that dILP-3 is the only neurotransmitter released by ISNs.

The *Drosophila* genome encodes eight insulin-like peptides and one broadly expressed insulin receptor (*81*). dILP-6, -7, and -8 are expressed in *Drosophila* adipose tissue, gut, and larval imaginal discs, respectively, and appear to play roles in growth control. dILP-1 and d-ILP4 are the least understood of the *Drosophila* insulin-like peptides. dILP-1 may be expressed during pupation, and dILP-4 is expressed in the embryo mesoderm. Their biological functions are unknown.

dILP-3 belongs to a group of insulin-like peptides, including dILP-2 and d-ILP-5, that are produced and released from medial neurosecretory cells, a population of peptidergic neurons located in *pars intercerebralis (81)*. The expression of these dILPs appears to be tightly coordinated, as loss of *dilp-2* results in increased expression of *dilp-3* and *dilp-5*, and *dilp-3* is required for the expression of *dilp-2* and *dilp-5*. These peptides also appear to play distinct roles in nutritional homeostasis. In larvae, for example, circulating amino acids selectively promote the secretion of dILP-2 and circulating sugars selectively promote the secretion of dILP-3. Interestingly, this dILP-3 secretion is dependent on AKH, the same peptide that activates ISNs in adult *Drosophila (88)*.

Thus, dILP-3 plays important roles in sugar homeostasis, and may interact with other dILPs (in particular, dILP-2) to regulate overall nutritional homeostasis. Its key role in sugar homeostasis is consistent with the function of ISNs as interoceptive neurons of internal sugar abundance. Identifying the targets of dILP-3 released by ISNs, and their effect on dILP-2 and dILP-5 release from the PI, will be an exciting avenue for future research. In addition, it will be important to determine whether dILP-3 released by ISNs enters the hemolymph, where it may function in a manner similar to that released by neurons in the PI, or whether its targets are restricted to ISN post-synaptic neurons.

The role of the *pars intercerebralis* in mediating ISN function

Neurons directly post-synaptic to ISNs densely innervate the *pars intercerebralis* (PI). The PI has been studied extensively in *Drosophila* in the context of both sugar and water homeostasis (*81, 82*). As described above, neurons in the PI release dILPs-2,3, and 5, important regulators of nutrient homeostasis. The PI also plays a role in regulating water balance via another class of Leucokinin-expressing peptidergic neurons (*89*). The PI is thus poised to influence internal signals relevant for both food and water ingestion. The fact that neurons post-synaptic to ISNs innervate this region suggests that ISNs influence these behaviors via modulation of PI function. How might this modulation be achieved?

One possibility is that ISN activity, via its postsynaptic partners, increases or decreases the release of peptides from the PI that affect the drive to ingest sugar and water. One way to test this possibility would be to use mass spectrometry to determine peptide abundance in *Drosophila* hemolymph before and after experimental activation of ISNs. While this approach is challenging, it could provide important insights into how ISNs engage with established peptide systems regulating nutritional homeostasis. In particular, it will be interesting to determine whether ISN activation influences the release of leucokinin and capability, peptides known to regulate water balance in the insect kidney (*90, 91*). These peptides were also uncovered in an RNAi screen for regulators of water ingestion, arguing that changes in their abundance are sufficient to influence water ingestion behavior (see chapter 2).

Another, non-mutually exclusive possibility is that reciprocal interactions coordinate neural activity in ISNs and PI neurons. The circuit-tracing data above suggest that ISNs may influence PI activity. However, the ability of ISNs to respond to AKH is also strongly suppressed

by insulin in a cell autonomous manner. As the primary sources of secreted insulin in the *Drosophila* nervous system, neurons in the PI are good candidates for mediating this suppression. Functional imaging studies in which the ISNs are activated while monitoring activity in PI neurons (and vice versa) will be an important approach for testing the existence of feedback between ISNs and the PI.

Finally, an important question for future research will be whether any of the neurons directly post-synaptic to ISNs are taste sensitive. Our lab has found that bitter taste causes strong responses in PI neurons, but sugar taste does not (*37*). However, these experiments were performed in starved flies and the role of ISN activity was not tested. Testing whether ISN activity can influence taste responsiveness in the PI, and the extent to which this depends on ISN post-synaptic neurons, should provide insight into how ISN activity gives rise to different behavioral responses to the taste of sugar and water.

The effect of ISN activity on whole-brain responses to taste input

AKH, a peptide that increases activity in ISNs, specifically potentiates large scale neural responses to the taste of sugar. This potentiation was observed in the inputs to neural circuits that process sugar taste (*Gr64f* projections), the outputs of those circuits (pumping motor neurons), as well as interneurons. There was no effect of AKH on gustatory representation of water taste (*ppk-28* projections). Thus, ISNs may oppositely regulate sugar and water ingestion by specifically potentiating or de-potentiating the neural representations of sugar or water taste. An important next step will be to test whether the modulation of interneuron and motor neuron responses observed here result from ISN activity, potentiation of gustatory neurons, or some combination of the two.

To date, several interoceptive neurons have been identified that respond to various internal signals of nutrient abundance, including fructose (*28*), amino acids (*92*), and glucose (*21*). Among these, the ISNs are unique in that they are sensitive to multiple signals of physiological need (AKH and osmolality), and use those signals to influence multiple behaviors (sugar and water ingestion). The *Drosophila* nervous system likely uses information from all of these sensors, as well as more that remain to be discovered, to organize coherent, goal directed behaviors that result in the ingestion of sugar and water. How information from these various internal sensors is integrated by the *Drosophila* nervous system remains an unanswered question. However, the work presented here contributes to answering this question by identifying molecules and neurons through which the ISNs influence a key mediator of nutritional homeostasis in *Drosophila*, the *pars intercerebralis*. Further studies that establish the relationship between the ISNs, the PI, and other neural sensors of physiological need will be an important step towards understanding how nervous systems integrate information about metabolic state to regulate behavior and maintain homeostasis.

Experimental Procedures

Temporal Consumption Assays

Flies were mounted on glass slides with nail polish, then placed in a humidified chamber for 2 hrs. Each animal was presented a tastant 10 times on the proboscis and forelegs, and consumption time was recorded. Consumption time correlates with consumption volume.

RNAi crosses used for temporal consumption assays were maintained at 25˚C, 65% relative humidity (RH). Flies were aged 4-7 days. In tests for sucrose consumption, flies were not provided water prior to testing to exclude interactions between sucrose consumption and water consumption.

For temporal consumption assays using thirsty flies, flies were mounted as described above and placed in a sealed chamber with ~250g $CaSO_4$ (Drierite, stock# 23001) for 2 hours, unless otherwise noted. Each animal was provided distilled water 10 times and cumulative drinking time was recorded.

Immunohistochemistry

The primary antibodies were rabbit anti-GFP (Invitrogen, 1:1000), mouse anti-GFP (Sigma 1:1000), rabbit anti-RFP (Biovision, 1:500), mouse anti-Bruchpilot (nc82) (Developmental Studies Hybridoma Bank, 1:500). The rabbit anti-dILP-3 antibody used in this study was a gift from Jan Veenstra and used at a final concentration of 1:500.

Calcium imaging

Flies were dissected and presented with tastant (1M sucrose or water) as described (*37*). For "pre AKH" tastant applications, AHL was perfused over the brain from ~1 minute prior to imaging. Perfusion of 10 nM AKH (in AHL) was initiated ~1 minute following the "pre AKH" tastant presentation, and continued for ~ 2 minutes. Perfusion was then stopped, and brains were allowed to rest in 10 nM AKH for a subsequent 13 minutes, at which time "post AKH" tastant application imaging was initiated.

Brains were imaged on a 3i spinning disc confocal microscope with a 20x water immersion objective at ~0.3 Hz. Analysis was done on max-z projections of 17 imaging sections, 0.8-1.4 um sections. $\%\Delta F/F = 100\%*((F_t-F_0)/F_0)$, where F_0 is the mean fluorescence of 5-10 time points prior to stimulus onset and F_t is the fluorescence at each time point. Max $\Delta F/F = F_{max} - F_0$, where F_{max} is the maximum $\Delta F/F$ observed during the stimulus. Prior to analysis, each imaging file was registered to its first frame to minimize movement. "Post AKH" imaging files were then registered to the first frame of the corresponding "Pre AKH" imaging file to minimize the effect of drift during the 15 minutes of AKH exposure. Registration was performed in MATLAB as described (*93*). ROIs were drawn by hand in imageJ.

Statistical Analyses

Student's t-tests (paired or unpaired) were used to compare two groups. One way ANOVA followed by Sidak or Dunnet post hoc tests were used to compare two or more groups. Sidak's post hoc test was used to compare pairs of data (e.g. +/- RNAi) and Dunnet's post hoc test was used to compare each treatment to a control (e.g. w^{1118}). Analyses were performed in Prism.

Author Contributions

N.J. performed the experiments and wrote the manuscript. Gabriella Sterne generated the split Gal4 lines. The images in Figure 2B were generated by the Janelia and Vienna Tiles *Gal-4* collections, respectively. K.S. supervised the study.

Figures
Figure 3.1

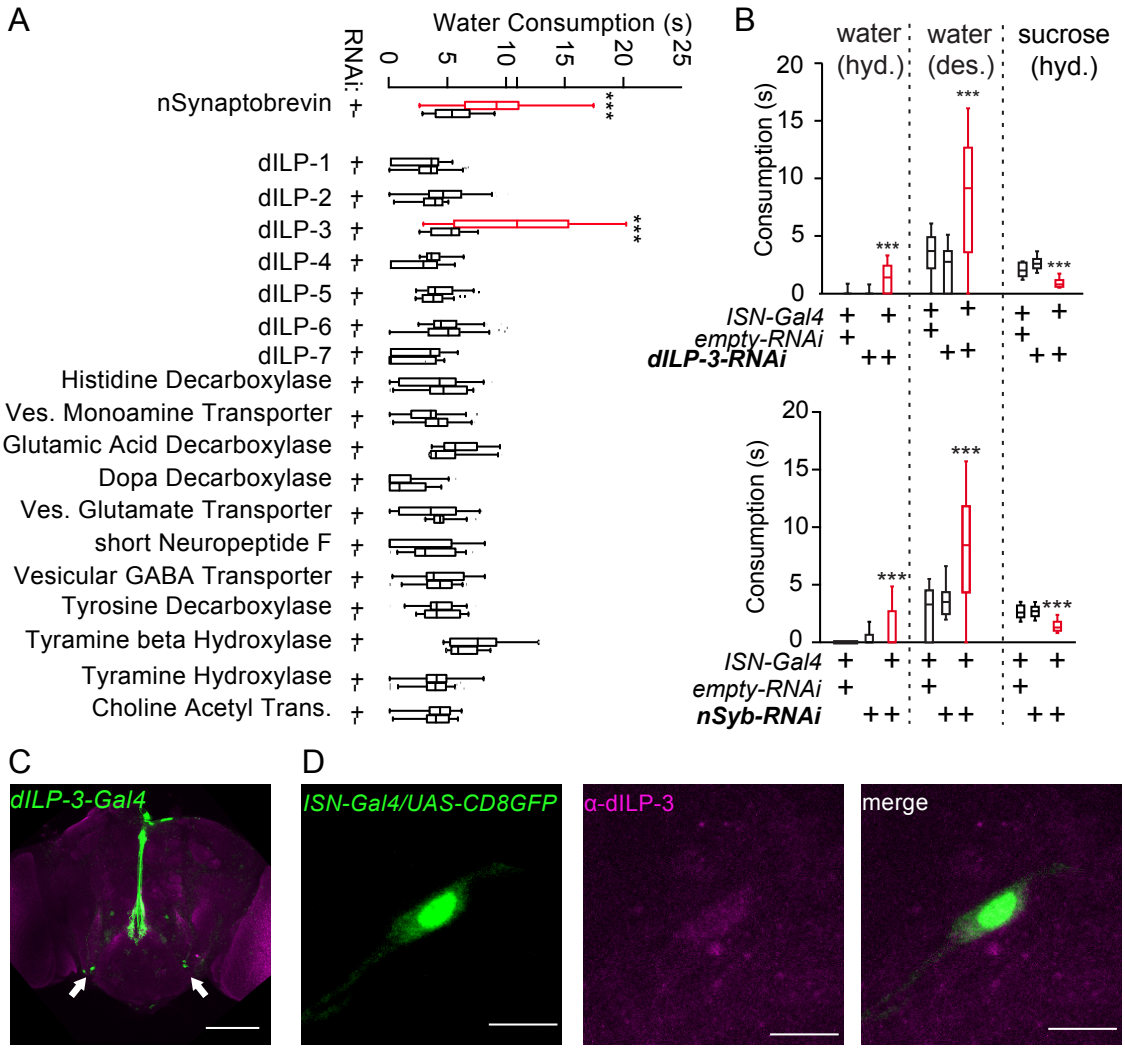

Figure 3.1 dILP-3 is an ISN neurotransmitter
A. RNAi screen for neuropeptides and neurotransmitters required by ISNs. n = 8-72, one-way ANOVA, Sidak's multiple comparison test, ***p<0.001. Ves. = Vesicular.
B. Water and sucrose consumption in flies expressing dILP-3 RNAi in ISNs. hyd.=hydrated, des. = desiccated. nSyb RNAi data from chapter 2 are reprinted here for comparison.
C. *dILP-3-Gal4, UAS-mCD8::GFP* expression in the brain. Arrows indicate neurons that resemble ISNs. Scale = 100μm**.**
D. ISN cluster from an *ISN-Gal4/UAS-GCaMP6s* brain. Top: GCaMP6s expression in one ISN cluster. Middle: anti-dILP-3 antibody signal. Bottom: overlay of top and middle panels. Scale = 10μm.

Figure 3.2

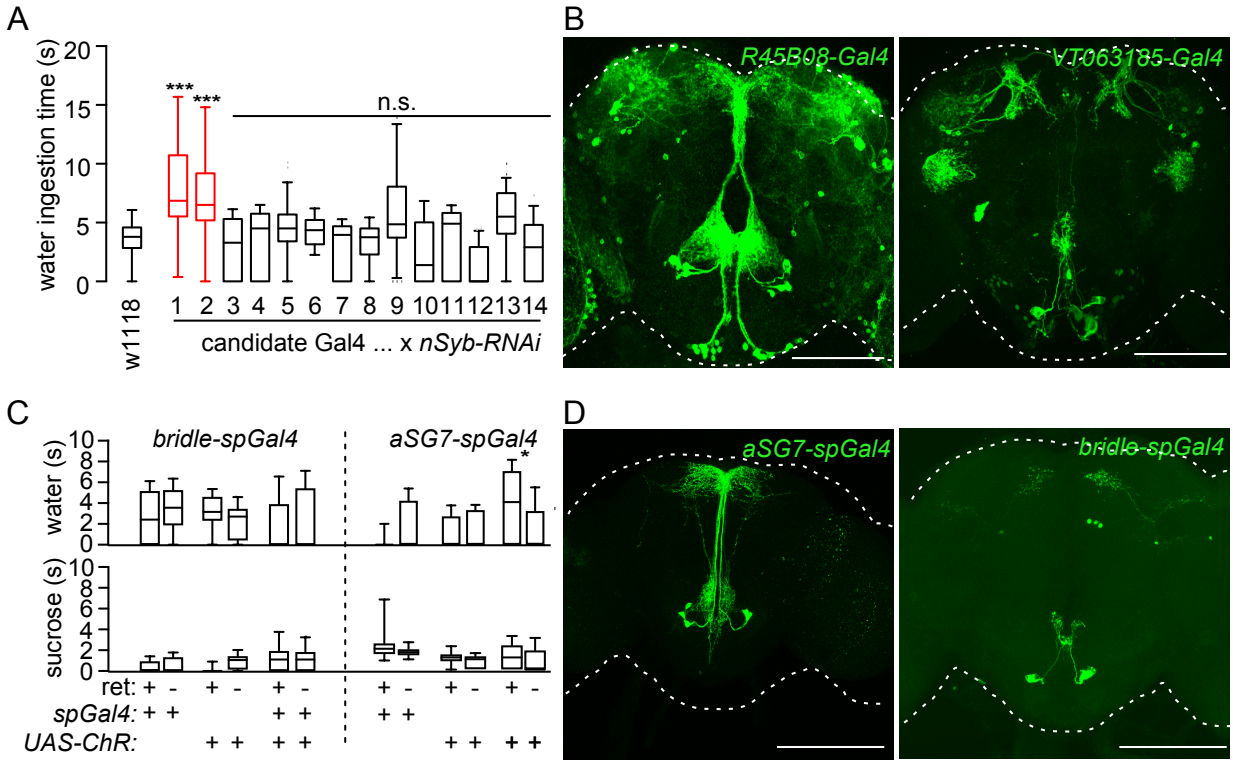
A
water ingestion time (s)
20
15
10
5
0
***
***
n.s.
w1118
1 2 3 4 5 6 7 8 9 10 11 12 13 14
candidate Gal4 ... x nSyb-RNAi
B
R45B08-Gal4
VT063185-Gal4
C
bridle-spGal4
aSG7-spGal4
water (s)
sucrose (s)
10
8
6
4
2
0
*
ret: + - + - + - + - + - + -
spGal4: + + + + + + + +
UAS-ChR: + + + + + + + +
D
aSG7-spGal4
bridle-spGal4

Figure 3.2 Candidate neurons post-synaptic to ISNs
A. A screen of Gal4 lines identified as candidate ISN post-synaptic neurons. Candidate 1 is *R45B08-Gal4* and candidate 2 is *VT063185-Gal4*. Remaining candidates are listed in table 1. n = 8-38. One-way ANOVA, Dunnet's multiple comparison test, ***p<0.001.
B. Brain expression of *R45B08-Gal4* (left, Janelia FlyLight Collection) and *VT063185-Gal4* (right, Dickson Lab, Vienna Tiles collection). Scale = 100 μm.
C. Effect of *bridle-spGal4* and *aSG7-spGal4* activation on sugar and water ingestion. Ret.=retinal. ChR=csChrimson. n = 16-32. *p<0.05, one way ANOVA, Sidak's multiple comparison test.
D. Expression of aSG7 and bridle split Gal4's in the brain. *aSG7-spGal4* is made from *R45B08-Gal4* enhancers driving expression of the Gal4 activation domain and *R61H08-Gal4* enhancers driving expression of the Gal4 DNA binding domain. *bridle-spGal4* is made from *R71G01-Gal4* enhancers driving the Gal4 activation domain and *VT026953-Gal4* enhancers driving the Gal4 DNA binding domain. Scale = 100 μm.

Figure 3.3

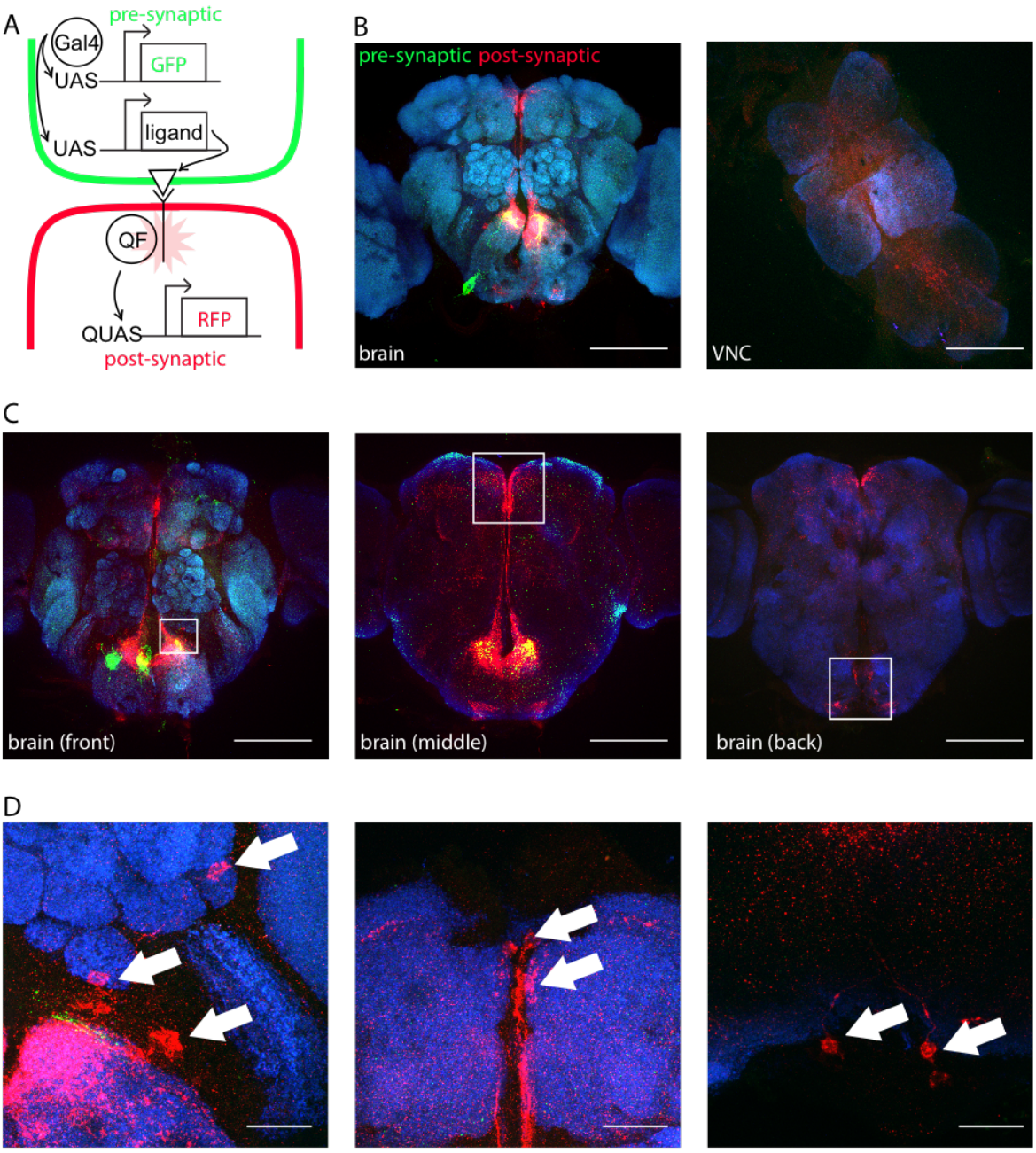
A
pre-synaptic
Gal4
UAS
GFP
UAS
ligand
QF
QUAS
RFP
post-synaptic
B
pre-synaptic post-synaptic
brain
VNC
C
brain (front)
brain (middle)
brain (back)
D

Figure 3.3 Anatomical characterization of ISN post-synaptic neurons
A. Illustration of trans-TANGO strategy to label neurons post-synaptic to a neuron of interest.
B. Expression pattern of pre- and post-synaptic neurons in *ISN-Gal4/UAS-transTANGO* brain and VNC of trans-TANGO driven by expression of *ISN-Gal4*. Green: ISNs. Red: post-synaptic neurons. Blue: neuropil. Scale = 100μm.
C. Front, back, and middle thirds of a confocal Z-stack of an *ISN-Gal4/UAS-transTANGO* brain. Scale = 100μm. White boxes correspond to brain regions covered by high magnification zooms in D.
D. Zooms of ISN post-synaptic neurons showing cell bodies (white arrows) in dorsal SEZ (D'), *pars intercerebralis* (D''), and ventral SEZ (D''') Scale = 100μm.

Figure 3.4

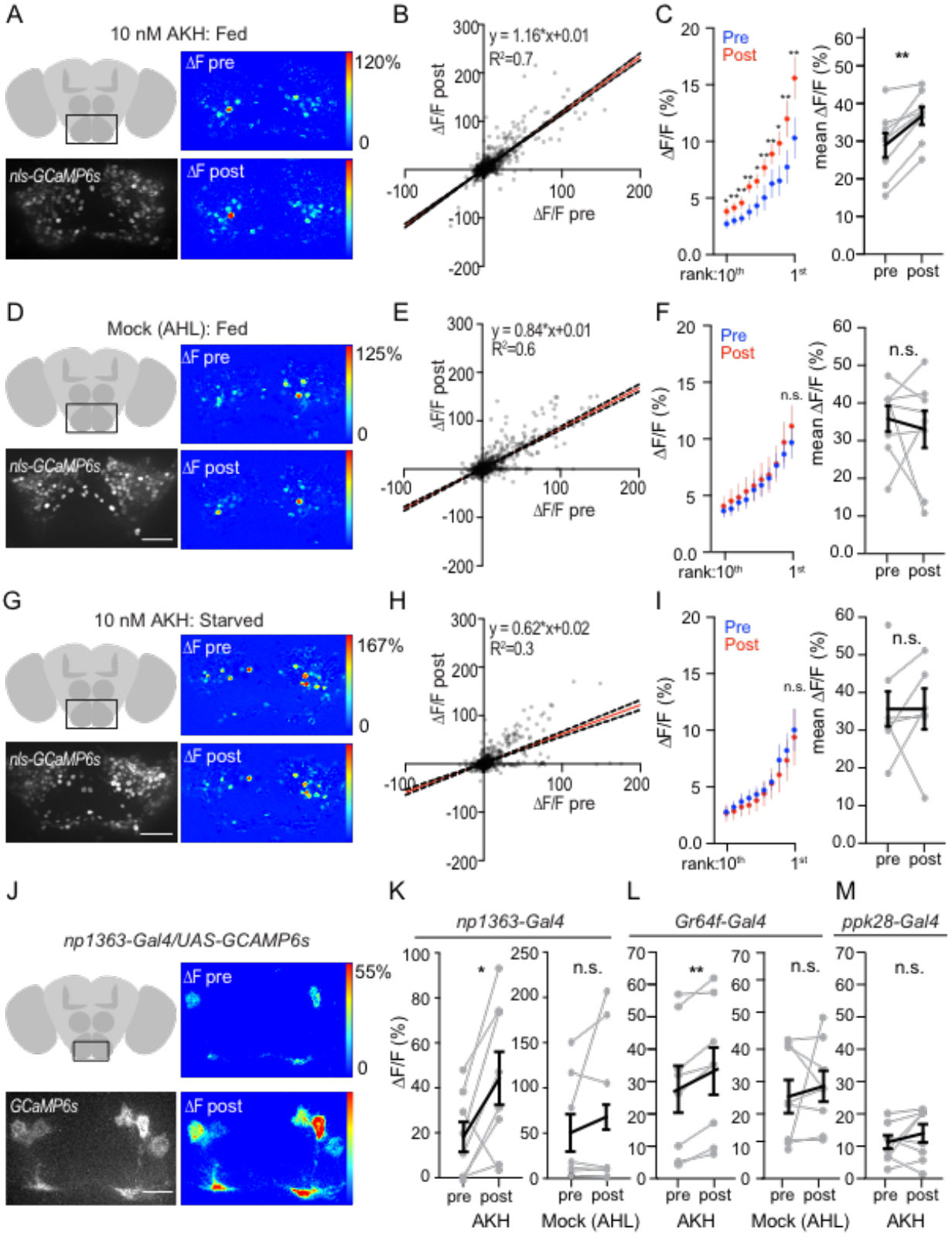
A
10 nM AKH: Fed
ΔF pre
120%
0
nls-GCaMP6s
ΔF post
B
y = 1.16*x+0.01
R²=0.7
ΔF/F post
ΔF/F pre
C
Pre
Post
ΔF/F (%)
rank:10th
1st
mean ΔF/F (%)
pre post
D
Mock (AHL): Fed
125%
E
y = 0.84*x+0.01
R²=0.6
F
n.s.
G
10 nM AKH: Starved
167%
H
y = 0.62*x+0.02
R²=0.3
I
J
np1363-Gal4/UAS-GCAMP6s
55%
GCaMP6s
K
np1363-Gal4
L
Gr64f-Gal4
M
ppk28-Gal4
AKH
Mock (AHL)

Figure 3.4 AKH modulates taste responses in the SEZ

A. Whole SEZ *nls-GCaMP6s* responses to proboscis application of 1M sucrose before and 15 minutes after exposure to 10 nM AKH. Scale = 50μm.

B. Response (ΔF/F) pre-AKH vs. response post-15 minutes exposure to 10nM AKH. Red line: best fit line +/- 95% confidence interval.

C. (left)Average responses of 10 highest responding neurons, +/- S.E. pre- and post-15 minutes exposure to 10 nM AKH. n = 8 brains per treatment, paired t-tests, *p<0.05, **p<0.01. (right) Average response of all responding neurons ((ΔF/F > 10%) +/- S.E, pre- and post-15 minutes exposure to 10 nM AKH. n = 8, paired t-test, **p<0.01.

D. Whole SEZ *nls-GCaMP6s* responses to proboscis application of 1M sucrose before and 15 minutes after exposure to AHL. Scale = 50μm.

E. Response (ΔF/F) pre-AKH vs. response post-15 minutes exposure to AHL. Red line: best fit line +/- 95% confidence interval.

F. (left) Average responses of 10 highest responding neurons, +/- S.E. pre- and post-15 minutes exposure to AHL. n = 8 brains per treatment, paired t-tests, n.s. (right) Average response of all responding neurons ((ΔF/F > 10%) +/- S.E, pre- and post-15 minutes exposure to AHL. n = 8, paired t-test, n.s.

G. Whole SEZ *nls-GCaMP6s* responses to proboscis application of 1M sucrose before and 15 minutes after exposure to 10 nM AKH following 24 hours of starvation. Scale = 50μm.

H. Response (ΔF/F) pre-AKH vs. response post-15 minutes exposure to 10nM AKH following 24 hours of starvation. Red line: best fit line +/- 95% confidence interval.

I. (left) Average responses of 10 highest responding neurons, +/- S.E. pre- and post-15 minutes exposure to 10 nM AKH. n = 7 brains per treatment, paired t-tests, n.s. (right) Average response of all responding neurons (ΔF/F > 10%) +/- S.E, pre and post 15 minutes exposure to 10 nM AKH. n = 7, paired t-test, n.s.

J. Pumping motor neuron responses to proboscis application of 1M sucrose before and 15 minutes after exposure to 10 nM AKH. Scale = 50μm.

K. Pumping motor neuron responses before and 15 minutes after exposure to 10 nM AKH or AHL. n = 8, paired t-test, *p<0.05.

L. Gr64f sugar taste projection responses before and 15 minutes after exposure to 10 nM AKH or AHL. n = 8, paired t-test, **p<0.01.

M. *ppk-28* water taste projection responses before and 15 minutes after exposure to 10 nM AKH. n = 8, paired t-test, n.s.

Table 1: List of *Drosophila strains* used

Figure	Genotype
1A	*UAS-dcr/+;VT011155-Gal4/UAS-RNAi*
1B	*UAS-dcr/+;VT011155-Gal4/UAS-dILP-3-RNAi(BSC#33681)* *UAS-dcr/+;VT011155-Gal4/UAS-nSyb-RNAi(BSC#31983)/+* *UAS-dcr/+;VT011155-Gal4/UAS-empty-RNAi(BSC#36303)* *+/+; +/ UAS-dILP-3-RNAi(BSC#33681)* *+/+; +/UAS-empty-RNAi(BSC#36303)* *+/+; +/UAS-nSyb-RNAi(BSC#31983)/+* w^{1118}
1C	*dILP-3-Gal4/+; UAS-mCD8::GFP/+*
1D	*UAS-CD8::GFP/+; VT011155-Gal4/+*
2A	w^{1118} *UAS-nSyb-RNAi(BSC#31983)* Candidate 1: *R45B08-Gal4* Candidate 2: *VT063185-Gal4* Candidate 3: *R29A03-Gal4* Candidate 4: *VT025786-Gal4* Candidate 5: *R28D03-Gal4* Candidate 6: *R28E09-Gal4* Candidate 7: *R28E02-Gal4* Candidate 8: *VT012719-Gal4* Candidate 9: *VT035031-Gal4* Candidate 10: *R28A11-Gal4* Candidate 11: *VT025786-Gal4* Candidate 12: *R28G01-Gal4* Candidate 13: *R28G04-Gal4* Candidate 14: *R37B05-Gal4*
2B	*R45B08-AD/+; R61H08-DBD/UAS-mCD8::GFP* *R71G01-AD/+; VT026953-DBD/UAS-GCaMP6s*
2C	spGal4 only: *R45B08-AD/+; R61H08-DBD/+* *R71G01-AD/+; VT026953-DBD/+* UAS-ChR only: *+/+;+/UAS-csChrimson* spGal4/UAS-ChR: *R45B08-AD/+; R61H08-DBD/ UAS-csChrimson* *R71G01-AD/+; VT026953-DBD/ UAS-csChrimson*
3	*+/+; VT01155-Gal4/UAS-transTANGO*
4A-I	*+/+; nSyb-Gal4/UAS-nls-GCaMP6s*
4J-K	*np1363-Gal4/+; UAS-GCaMP6s/+*
4L	*Gr64f-Gal4/+; UAS-GCaMP6s/+*
4M	*UAS-GCaMP6s, UAS-tdTomato/+; ppk28-Gal4/+*

Chapter 4: Discussion

Summary

In animals, nervous systems regulate the ingestion of food and water in a manner that reflects internal metabolic need. While the coordination of these two ingestive behaviors is essential for homeostasis, it has been unclear how internal signals of hunger and thirst interact to effectively coordinate food and water ingestion. In the last year, work in insects and mammals has begun to elucidate some of these interactions. As reviewed here, these studies have identified novel molecular and neural mechanisms through which regulation of food and water ingestion is coupled. These mechanisms include peptide signals that modulate neural circuits for both thirst and hunger, neurons that regulate both food and water ingestion, and neurons that integrate sensory information about both food and water in the external world. These studies argue that a deeper understanding of hunger and thirst will require closer examination of how these two biological drives interact.

This work has been previously published: Jourjine N., 2017. Hunger and thirst interact to regulate ingestive behavior in flies and mammals. *Bioessays* 39(5).

Introduction

"The desires of the body are few: relief from cold, hunger, and thirst."
– Roger Bacon, *Opus Majus*

Animal behavior is constrained by the metabolic needs of cells, and few needs are more fundamental than those of food and water. While some exceptional animals can survive for extended periods without either of these, most must ingest both on a daily basis. Remarkably, animal nervous systems regulate ingestion in a manner that precisely reflects internal metabolic need. This regulation is observed in animals with diverse nervous system organizations and evolutionary histories, suggesting shared principles of nervous system function. Nonetheless, how animal nervous systems regulate ingestion in a manner that reflects internal need remains an open and fundamental question.

Two key links between ingestion and metabolic need are the subjective experiences of hunger and thirst. As the medieval scientist Roger Bacon makes clear in the quote above, these experiences are among the most basic facts of life. Nonetheless, the biological mechanisms underlying hunger and thirst remain largely mysterious. For example, which aspects of nervous system function give rise to these experiences? What explains the powerful influence they have on our behavior? Entire fields of behavioral neuroscience and psychology have been devoted to addressing these questions, and they have made key conceptual contributions to our understanding of hunger and thirst (*94*). One such contribution is the notion that hunger and thirst are, like sexual arousal, aggression, and fear, biological "drives", internal motivational states that cause behaviors oriented toward a specific goal. A long history of theoretical models has elaborated on the concept of drive to explain how hunger and thirst control behavior. For example, some have proposed that a key property of drives is to gradually increase in intensity until an animal performs specific actions (*95*), while others have posited various positive or negative interactions among drives (*96*).

Despite the conceptual contributions that these models have made, experimental tools to directly test whether and how neural circuits utilize them have been lacking. As a result, fundamental questions remain about the relationship between internal metabolic need, biological drives, and behavior. Historically these questions have been addressed by studying specific food or water ingestion behaviors in isolation, with the assumption that mechanisms underlying these behaviors are analogous but ultimately separable. While this approach has led to fundamental insights, it has generally not addressed how neural circuits for food and water ingestion might interact. In the last year, however, work in insects and mammals has identified novel intersection points between mechanisms regulating hunger and thirst, and these studies have provided insight into the problem of how nervous systems coordinate distinct behaviors to satisfy multiple internal needs. Here, I review recent progress toward understanding the neural regulation of hunger and thirst by focusing on three key questions: which aspects of internal physiology signal food and water deprivation to the nervous system? What are the identities of the neurons that detect these signals to generate the "drive" associated with hunger and thirst? And finally, how does activity in these neurons regulate behavior? As I argue below, the answers to these questions suggest that a deeper understanding of hunger and thirst will require examining how these biological drives interact to regulate ingestive behavior.

What are the internal signals of food and water deprivation?

Internal Signals of food deprivation

A key way animals measure metabolic need is by detecting molecules that participate directly in metabolism. In animals, glucose is the starting point for cellular metabolism, and an essential function of food ingestion is to supply this sugar to cells for use in the biochemical pathways that produce ATP. In addition, blood glucose levels correlate with the sensation of hunger in humans (*97*). These observations led to the hypothesis that nervous systems directly measure glucose abundance as a signal of metabolic need and hunger (*97*). This hypothesis has been supported by the observation that a small number of neurons in both mammalian and insect brains are sensitive to circulating glucose (*21, 97, 98*), although how these neurons regulate behavior remains unclear. In addition, neurons in the *Drosophila* brain sense fructose, another sugar that can be used in cellular metabolism, and this appears to be important both for promoting feeding in starved flies and suppressing feeding in satiated flies (*28*). Insects and mammals have also been proposed to directly sense another important building block of cellular metabolism: amino acids. Interestingly, the same protein kinase – GCN2 – has been implicated in amino acid sensing in mammals and insects, although its role in mammals has been debated (*92, 99-101*). Thus, mammals and insects sense internal metabolic need by detecting multiple molecules that directly participate in cellular metabolism.

Internal nutrient sensing is an elegant way to directly link feeding with the metabolic need for food. It is perhaps surprising, then, that most of the signals proposed to regulate feeding are in fact peptides that don't participate directly in metabolic processes. The first of these to be discovered was cholecystokinin (CCK), a 58-amino acid peptide secreted by the gut. Exogenous CCK is sufficient to restrict meal size in rats, arguing that CCK is a satiety factor (*102*). Since this discovery, many other peptide hormones have been proposed to regulate feeding in insects and mammals [Table 4.1]. The sheer number of these peptides is daunting. However, this diversity is partly explained by the observation that different intensities of hunger, and different components of feeding behavior (e.g., initiation and termination), are often regulated by different peptide systems (*103-105*). For example, two key peptide regulators of feeding, ghrelin and leptin, function by exerting opposing effects on hunger: ghrelin promotes it while leptin suppresses it (*69, 70*).

Thus, insects and mammals use multiple direct signals (molecules that participate in metabolism) and indirect signals (peptide hormones) to sense the internal need for food. Understanding how these diverse, time varying signals are integrated by the nervous system to produce appropriate ingestive behaviors is an important avenue for future research.

Internal signals of water deprivation

Water is a fundamental requirement for all biological processes, and, as a result, most land animals cannot survive for more than a few days without it. Powerful regulatory mechanisms must therefore exist to ensure that water ingestion occurs on a regular basis. Although the details of these mechanisms differ from those described above in the context of hunger, a conserved theme is that the nervous system integrates multiple direct and indirect signals to measure the internal need for water.

The most direct signals of internal water abundance are properties of blood, in particular its osmolarity and volume. Increasing blood osmolarity and decreasing volume are both potent stimulators of thirst in humans and water ingestion in other mammals. Conversely, decreasing blood osmolarity or increasing volume suppress thirst and water ingestion. In water deprived animals, these direct signals act on the nervous system and kidneys to initiate the renin-angiotensin system (*106*), a cascade of secondary peptides that regulate the kidneys and circulatory system to minimize water loss. This cascade also causes the secretion of the neuropeptide vasopressin (also known as anti-diuretic hormone). Like the other peptides in the renin-angiotensin system, vasopressin regulates water reabsorption in the kidneys. However, vasopressin is also sufficient to evoke intense water ingestion behavior, suggesting that it acts as a peptide signal of thirst (*107, 108*). Interestingly, vasopressin release has also been shown to be induced by CCK, the gut peptide discussed above that has critical functions in regulating food ingestion (*14*). While the behavioral relevance of this finding remains unclear, it suggests the possibility of complex interactions between neuropeptide systems underlying hunger and thirst.

Relative to mammals, insects have large surface area to volume ratios and are therefore at constant risk of losing internal water through evaporation (*109, 110*). For many insects, the only way to recover this lost water is to ingest it. Nonetheless, relatively little is known about the regulation of water ingestion behavior in invertebrates. Like mammals, it appears that hemolymph (insect blood) osmolarity and volume are important signals of water deprivation (*110*). In addition, a handful of neuropeptides – such as leucokinin, insulin, capability (capa), and glycoprotein beta 3/5 (GPB-3/5) – have been shown to regulate water balance in the insect kidney (*26, 45, 62*). Interestingly, insulin and leucokinin are also regulators of feeding behavior in *Drosophila* (*62*), suggesting cross-talk between peptide systems for food and water ingestion. How these peptides act on the nervous system to influence water ingestion behavior, and how their release is related to dehydration, remain important questions to be addressed.

Thirst in insects appears to exhibit some key similarities with thirst in mammals: it is caused by changes in blood (hemolymph) volume and osmolarity, it is likely heavily regulated by neuropeptides, and some of those peptides interact with peptide systems for food ingestion. However, there are also differences. For example, due to their flexible exoskeleton, dehydration in insects can be accompanied by a large reduction in blood volume. In addition, while loss of blood volume is a potent stimulator of thirst in mammals, most recent studies have specifically manipulated blood osmolarity (*75, 111, 112*). An interesting question for future research will be to ask how thirst induced by changes in blood volume differs from thirst induced by changes in blood osmolarity. A second potential difference between insect and mammalian thirst systems is the well-documented distinction between need-based and need-free water ingestion in mammals. Specifically, water ingestion in mammals can be induced by changes in internal blood osmolarity and volume (need-based), or it can be independent of internal need (need-free). A recent example of such need-free ingestion is the observation that mice increase drinking prior to sleep to offset overnight water loss (*108*). It will be interesting to see whether the distinction between need-free and need-based water ingestion also holds in insects.

Which neurons detect internal signals of food and water deprivation?

Neurons for sensing food deprivation

The nervous system orchestrates complex feeding behaviors in response to multiple signals of metabolic need. Which neurons detect these signals and by which mechanisms? An early approach to address this question was to lesion or electrically stimulate specific brain regions and ask what effect these manipulations had on food and water ingestion (*16, 113-115*). While these experiments were difficult to interpret because lesions lacked cell-type specificity, many studies found that removing or stimulating neurons in the hypothalamus, a conserved mammalian forebrain region, could evoke intense, specific ingestive behaviors.

More recently, genetically defined neural populations have been identified in the hypothalamus whose activity influences feeding behavior (*116-119*). Among these, neurons that express agouti related peptide (AgRP neurons) or pro-opiomelanocortin (POMC neurons) were found to exert potent and opposing effects on food ingestion: AgRP neurons promote ingestion and are required for feeding, while POMC neurons inhibit feeding. Importantly, these neurons express receptors that make them directly sensitive to some of the internal signals of metabolic need discussed above. These include ghrelin, which promotes activity in AgRP neurons and causes feeding (*70*), and leptin, which promotes activity in POMC neurons to suppress feeding (*69*). AgRP and POMC neurons therefore provide an important link between signals of internal metabolic state and neural circuits underlying ingestive behaviors. Understanding how they integrate these signals to regulate behavior is an important open question.

While insects lack a brain structure directly analogous to the hypothalamus, they do have regions that play functionally similar roles. One of these areas is the *pars intercerebralis* (PI), a dorsal brain region containing multiple neuroendocrine cells. PI neurons are the major site of insulin release in *Drosophila*, and neurons in and near the PI are directly sensitive to circulating glucose and fructose (*21, 28, 98*). In addition, another group of PI neurons is indirectly sensitive to the *Drosophila* ortholog of leptin, *upd-2*, which is released from adipose tissue and causes insulin release from the PI (*22*). Mammalian leptin can rescue *upd-2* mutant phenotypes in *Drosophila*, suggesting homology, although the effects of *upd-2* on feeding behavior in *Drosophila* are unclear (*22*). Other neurons in the *Drosophila* brain have been identified that are sensitive to amino acid imbalances, insulin, and several neuropeptides (e.g., sNPF, AKH, and allatostatin A) (*62, 64, 80, 92, 120*). However, many more *Drosophila* neuropeptides have been discovered than neurons sensitive to those peptides (*23*), arguing that neural sensors of metabolic need remain to be identified.

Neurons for sensing water deprivation

In the mammalian brain, neurons in the anterior wall of the third ventricle are directly sensitive to blood osmolarity, a key internal signal of thirst and hydration (*15*). Recently, genetic approaches have made it possible to control the activity of neurons in this region in a cell type specific manner (*121*). These approaches have identified two populations of neurons in the subfornical organ (SFO) that have opposing effects on water ingestion [Figure 4.1]. One of these populations is marked by expression of the enzyme neuronal nitric oxide synthase (nNOS) and is sufficient to promote water ingestion. The other, marked by the vesicular GABA transporter (VGAT), inhibits water ingestion. nNOS+ SFO neurons are also sensitive to the key internal

signal of hydration state, blood osmolarity. Moreover, nNOS+ neurons increase activity in thirsty animals, thereby linking water ingestion behavior to a measure of internal water abundance (*75*).

nNOS+ and VGAT+ SFO neurons are thus functionally analogous to AgRP and POMC neurons in the hypothalamus, which exert opposing effects on food ingestion. The discovery of these neural populations reveals an intriguing parallel between circuits regulating hunger and thirst: both utilize paired pathways in which each member of the pair exerts an opposing effect on behavior [Figure 4.1]. Whether this similarity is superficial, or if it reflects an adaptive circuit motif, will be an interesting area for future investigation.

Studies of thirst in insects have generally lagged behind those in mammals, due in part to the difficulty of lesioning and electrode stimulation in small brains. Early studies in blowflies and *Drosophila* showed that the nervous systems of these insects regulate both foraging for and ingestion of water (*110, 122*), although neurons that regulated these behaviors were not identified at the time. More recently, our lab has shown that the *Drosophila* gustatory system contains dedicated water-taste neurons, and identified the molecular basis of water sensing in these neurons as the osmolarity-sensitive ion channel *ppk-28* (*43*). We have also identified four neurons in the central brain that sense internal water abundance via a different osmolarity-sensitive ion channel, *nanchung*, and that regulate water ingestion. Interestingly, *nanchung* belongs to the TRPV family, and members of this family have also been proposed to function as sensors of blood osmolarity in mammals (*15, 53*). As I describe below, osmosensitive *nanchung* neurons also sense a key internal signal of food deprivation, making them an important intersection point for the regulation of food and water ingestion in *Drosophila* (*80*).

How do sensors of food and water deprivation regulate behavior?

Interoceptive neurons in insects and mammals detect multiple signals of metabolic need. As described above, these neurons are in many cases sufficient to rapidly regulate complex ingestive behaviors. What are the neural circuits through which they achieve this regulation?

One way to address this question is to ask which brain regions contain axonal projections of interoceptive neurons. Neural tracing strategies have, for example, been used to demonstrate connectivity between hunger promoting AgRP neurons and multiple brain regions. These include the paraventricular hypothalamus (PVH) and lateral hypothalamus (LH), among others (*76*)[Figure 4.2]. Thirst promoting nNOS+ SFO neurons also send axonal projections to the PVH (*75*). It will be interesting to test whether brain regions such as the PVH, which receive input from both hunger and thirst centers, function in integrating internal signals of food and water deprivation.

Understanding the anatomy of neural circuits is necessary for understanding how they regulate behavior, but it is not sufficient: knowledge of neural activity in those circuits is also required. Simultaneously monitoring neural activity in all brain regions that regulate food and water ingestion remains technically out of reach, but important insights have recently come from monitoring activity in interoceptive neurons that directly sense internal signals of food and water deprivation.

In mice, monitoring activity in AgRP neurons revealed that their activity gradually increases during starvation, consistent with the notion that they are sensing internal signals of food deprivation whose abundance correlates with starvation (*17*). Surprisingly, however, when starved mice were presented with food, activity in AgRP neurons was reduced within seconds to levels observed in satiated mice, and this occurred prior to ingestion. This reduction appears to

be caused by leptin receptor expressing inhibitory neurons in another region of the hypothalamus (*78*). Rapid sensitivity to sensory information was also observed in thirst promoting nNOS+ SFO neurons (*75*). As is the case with AgRP neurons, nNOS+ neurons gradually increased their activity level during water deprivation, consistent with their being sensitive to internal signals of water abundance. As a further similarity to AgRP neurons, this activity was rapidly reduced the moment mice taste water and before ingested water could have modified their internal state. nNos+ neurons differ from AgRP neurons in that only tasting water, and not seeing or expecting it, is sufficient to alter activity. Nonetheless these findings argue that neurons that sense internal signals of food and water deprivation are also highly sensitive to sensory information about the presence of food and water in the external world.

Work in *Drosophila* has uncovered a second theme: modulation of sensory systems by internal signals of deprivation. In the taste system, Anderson and colleagues have shown that multiple neuromodulators that signal hunger also alter activity in gustatory neurons. For example, they have shown that starvation increases dopamine release onto sugar gustatory neurons, and this increases the sensitivity of these neurons to sugar taste, thereby making ingestion more likely (*65*). Conversely, neuropeptides released in starved flies reduce the magnitude of bitter responses in bitter sensing gustatory neurons, thus reducing the threshold for ingesting unpalatable – but potentially nutritious – foods (*66*). Interestingly, Gordon and colleagues have recently identified an independent mechanism for achieving the same effect (*123*). This involves a novel class of central neurons, OA-VL, that release the neuromodulator octopamine onto bitter sensory neurons, potentiating their sensitivity to bitter substances. OA-VL neurons are inhibited during starvation, resulting in a decrease in sensitivity of bitter gustatory neurons and a reduction of the threshold for ingesting food. Modulation of sensory systems by internal state has also been observed in mammals: in mice, starvation-dependent increases in a class of neuromodulators, the endocannabinoids, potentiate olfactory sensitivity to food odors, and this potentiation is sufficient to increase feeding (*124*).

Thus, interoceptive neurons that detect internal signals of nutrient deprivation can modulate activity in sensory systems that detect signals of nutrients in the external world. Conversely, these sensory systems can also rapidly modulate activity in interoceptive neurons. Rapid feedback between sensors of an animal's internal state and the external world might therefore be an important feature of neural circuits regulating ingestion. However, the larger question of how nervous systems use information from internal sensors of food and water deprivation to produce appropriate ingestive behaviors remains largely unanswered. To address this question, it will be important to monitor activity in the large-scale neural circuits connecting interoceptive neurons to sensory and motor systems.

Coordinated regulation of food and water ingestion

Most studies have examined food or water ingestion independently. In many ways, this approach is justified: eating and drinking are qualitatively different behaviors, and hunger and thirst are distinct internal experiences. However, it is also clear that regulatory mechanisms underlying these behaviors interact in humans and other animals (*125-127*). For example, recent studies in mice have shown that ghrelin, a key internal signal of hunger, is capable of modulating water ingestion behavior (*60*), and that the subfornical organ, a key regulator of thirst, contains neurons that are sensitive to multiple signals of hunger (*128-130*)**.**

While these findings are intriguing, the nature of cross talk between systems regulating food and water ingestion has remained elusive. However, three studies within the last several months (*75, 80, 112*) have shed light on this cross-talk by identifying novel mechanisms coupling the regulation of food and water ingestion. These studies argue that understanding these behaviors will require a deeper examination of how the regulatory systems underlying them interact.

Coordination of food and water ingestion in Drosophila

Two behavioral screens were recently carried out in our lab with the goal of identifying neurons that regulate sugar and water ingestion behavior, respectively. Surprisingly, the same four neurons were identified in both of these screens (*80*). These neurons reside in the subesophegeal zone (SEZ) of the fly brain, a key region for taste information processing and feeding regulation, and for this reason we named them ISNs (Interoceptive SEZ Neurons). ISN activity has a striking effect on ingestive behavior: experimentally increasing activity not only promotes food ingestion, but also restricts water ingestion. Silencing neural activity in ISNs has the opposite effect.

ISNs are not directly regulated by the taste of sugar or water. Instead, ISN activity is regulated by two signals of internal physiology: insect glucagon (adipokinetic hormone, AKH), a peptide signal of food deprivation, and hemolymph osmolarity, a signal of water deprivation. Underlying this sensitivity is the fact that ISNs co-express a G protein coupled receptor that binds AKH, and the TRPV family member *nanchung*, which is sensitive to extracellular osmolarity (*46*). Thus, by expressing molecular sensors of both AKH and osmolarity, ISNs integrate internal signals of both hunger and thirst.

Why might this integration be adaptive? In the wild, animals often experience internal signals of both food and water deprivation and must balance these needs to make appropriate decisions about which to ingest. To address how ISN activity responded to concurrent signals of food and water deprivation, we applied AKH to ISNs in extracellular solutions designed to resemble the hemolymph osmolarity of either a thirsty fly (high osmolarity) or a water satiated fly (low osmolarity). We found that in high osmolarity solutions reflecting thirst, responses to the hunger signal AKH were strongly diminished. This result suggests that signals of water deprivation can gate ISN responses to signals of food deprivation. Consistent with this hypothesis, we found that thirst suppresses feeding in wild type flies. Thus, coupling hunger and thirst signals via ISNs may allow flies to prioritize ingestion of water, which is more essential for survival, over ingestion of food.

Coordination of food and water ingestion in mammals

Three recent studies have identified a similar pattern of regulation in mice. First, Knight and colleagues have directly observed neural activity in thirst promoting nNOS+ SFO neurons (*75*). As described above, they found that activity in these neurons increased both in thirsty mice and in mice whose blood osmolarity was experimentally raised, consistent with the function of these neurons in promoting water ingestion. Surprisingly, however, they also observed that activity in these thirst promoting neurons increased immediately upon the initiation of food ingestion. Similar findings have been described by Andermann and colleagues in vasopressin secreting neurons of the posterior pituitary. Vasopressin neurons regulate blood osmolarity by

releasing vasopressin in high osmolarity states. Vasopressin then acts on the kidneys and brain to conserve water and stimulate thirst. Andermann *et al.* observed that in high osmolarity states, neural activity in vasopressin secreting neurons rapidly decreases upon presentation of water or water-predicting cues. Conversely, neural activity rapidly increases upon initiation of food ingestion (but not cues predicting food) (*111*). Thus, thirst regulatory neurons in two distinct brain regions are acutely sensitive to sensory information about both food and water.

Why should neurons that regulate water ingestion be sensitive to food? One answer comes from the observation that water and food both alter a key internal signal for thirst – blood osmolarity – and they do this in an opposing manner: water ingestion causes blood osmolarity to decrease; food ingestion causes it to increase. Thus, sensory modulation of thirst neurons by food reflects the fact that internal signals of food and water deprivation do not vary independently. Specifically, ingestion of food alters internal signals of both thirst and hunger.

As a further demonstration of the interconnectedness of thirst and hunger, Knight and colleagues tested the effect of silencing nNOS+ SFO neurons on water and food ingestion. As expected for a thirst promoting neuron, silencing restricted water consumption. However, silencing also caused mice to increase food ingestion. This increase appears to occur because silencing nNOS+ SFO neurons inhibits dehydration induced anorexia, a behavior that limits feeding in thirsty mice. Thus, neurons that sense internal signals of water deprivation are sensitive not only to the taste of water, but also the taste of food, and are sufficient to oppositely regulate ingestion of water and food.

Manipulating activity in a population of neurons originally identified in the context of thirst affects both water and food ingestion. Does manipulating a population of neurons originally identified in the context of hunger do the same? Recent work by Krashes and colleagues (*112*) addressed this question by optogenetically activating hunger promoting AgRP neurons and asking what effect this had on a panel of behaviors. As observed in several previous studies, activation of AgRP neurons was sufficient to promote feeding. However, it also greatly reduced water ingestion, suggesting competition between the two biological drives – hunger and thirst – underlying these behaviors. Taken together, these studies argue that, in flies and mammals, interoceptive neurons detecting internal signals of food and water deprivation also regulate ingestion of food and water in a reciprocal manner: neurons that promote the ingestion of food suppress the ingestion of water and vice versa [Figure 4.3].

Krashes and colleagues also observed that AgRP activation suppressed behaviors related to anxiety, innate fear, and social interactions. This raises a fundamental question: does inhibition of thirst by hunger (or vice versa) reflect a mechanism by which all behaviors other than feeding are non-specifically suppressed during hunger states, or does it reflect a mechanism by which neural circuits for hunger and thirst specifically interact with one another? Non-specific suppression of behaviors that an animal is not currently engaged in is a well-documented and important principle by which nervous systems select behavioral outputs (*131*). It is also consistent with the observation that AgRP induced hunger inhibits not just water ingestion (and, presumably, thirst), but also behaviors associated with anxiety and fear. However, these two possibilities are not mutually exclusive. The evidence reviewed above from flies and mice also suggests specific mechanisms by which hunger and thirst interact: in mammals, neurons regulating water ingestion are sensitive to the presence of both food and water in the external world, and in *Drosophila* the same neurons sense internal signals of both hunger and thirst. Thus, there exists evidence that hunger and thirst may interact by both specific

and non-specific mechanisms. Understanding the neural circuits underlying these interactions, and how they regulate behavior, will be an exciting avenue for future research.

A potentially informative example of such interactions between biological drives comes from recent studies of aggression and sexual arousal. These drives underlie fighting and mating behaviors, respectively, and the choice between them is a fundamental decision animals must make when encountering another member of the same species. Surprisingly, the neural circuits that regulate fighting and mating have recently been shown to share key populations of neurons in *Drosophila* and mammals (*12*). These neurons are sufficient to influence both aggression and sexual arousal, arguing that aggression and arousal are directly coupled by activity of a single population of neurons. This regulatory logic is reminiscent of ISNs, whose activity couples thirst and hunger in *Drosophila*. These observations suggest the hypothesis that nervous systems might coordinate pairs of opposing biological drives by coupling their regulation to common neural populations. How activity in a single population of neurons can concurrently regulate mutually exclusive behaviors, and to what extent this principle can be generalized to other behaviors, are exciting questions for future research.

Conserved mechanisms or superficial similarities?

Hunger and thirst systems in flies and mammals share many features, such as internal signals that promote eating and drinking, the essential role of neuropeptides, and the antagonistic interactions between hunger and thirst drives outlined above. However, there are also important differences in ingestive behavior between these animal lineages. One crucial difference is that flies, while capable of eating solid food (*18*), usually consume sugars that have been dissolved in water. An important question is whether the different ingestion strategies of flies and mammals have driven the evolution of different circuits for thirst and hunger, or whether some circuit mechanisms have been conserved. In particular, it remains to be seen whether the convergence of hunger and thirst signals onto the same neural population (the ISNs) is unique to flies, or whether this convergence is also an important regulator of mammalian thirst and hunger. In support of the latter possibility, some mammalian neurons appear to integrate hunger and thirst signals in a manner similar to ISNs. For example, a subset of SFO neurons have been shown to be sensitive to circulating glucose and ghrelin, hunger signals, as well as extracellular osmolarity, a thirst signal (*128, 129, 132*). However, it is also clear that other functionally distinct neural populations, such as AgRP/POMC neurons in the arcuate nucleus, and nNOS/VGAT neurons in the SFO, detect signals of thirst and hunger separately.

The extent to which neural circuits for hunger and thirst are conserved between mice and flies is currently an open question. Nonetheless, the need for food and water is an ancient physiological constraint that has shaped the evolution of neural circuits in both of these lineages. Continued investigation into hunger and thirst in these animal models should therefore provide insights into how different nervous systems solve the basic problem of providing food and water to internal metabolic processes.

Conclusions and outlook

One of the most remarkable properties of animal nervous systems is their ability to satisfy diverse internal metabolic needs by coordinating multiple ingestive behaviors. Two important

insights have emerged from recent studies of this fundamental ability. First, neurons that sense internal signals of food and water deprivation are rapidly modulated by sensory information about food and water in the external world. Thus, information about internal metabolic need and information about food and water in the external world are integrated directly by neurons that sense internal signals of food and water deprivation. Second, neural mechanisms exist in both mammals and insects that drive antagonistic interactions between hunger and thirst: in mammals, neurons that are sufficient to promote food ingestion also suppress water ingestion and *vice versa.* In *Drosophila*, a single class of neurons, the ISNs, is sensitive to internal signals of both food and water deprivation, and is sufficient to oppositely regulate ingestion of both sugar and water. Understanding the logic of neural circuits that mediate this antagonism is an exciting area for future research.

A central question in neuroscience is how nervous systems integrate information about internal state with sensory information about the external world to select appropriate behaviors. By identifying neural circuits that are sensitive to both internal state and the external world, studies of hunger and thirst are in a position to begin addressing this question in unprecedented depth. Future studies in insects and mammals should provide exciting insights into how nervous systems coordinate diverse behaviors to satisfy diverse metabolic needs.

Figures
Figure 3.1

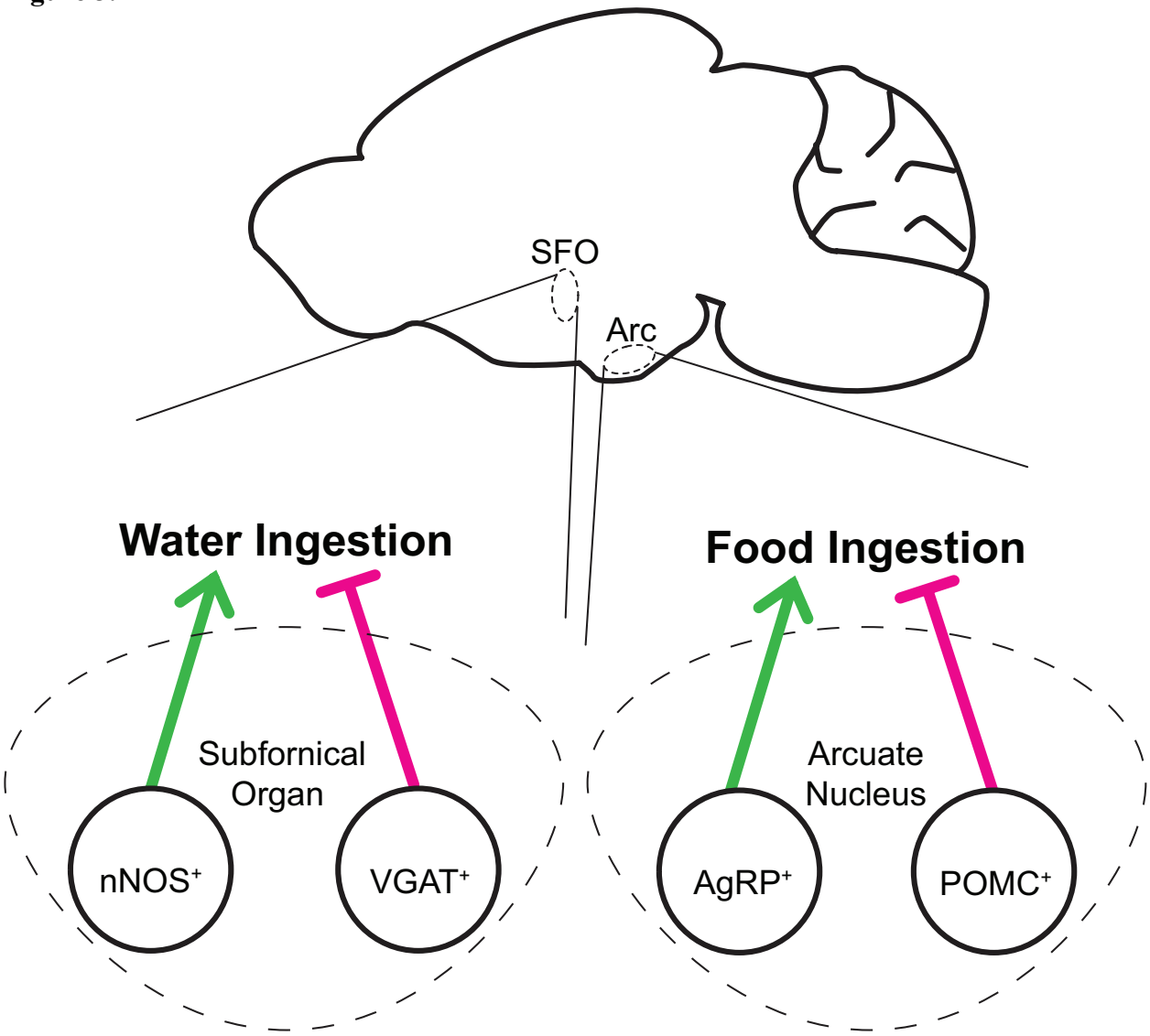

Figure 3.1 Circuit motifs for the regulation of food and water ingestion
Top: Cross sectional schematic of a mouse brain, showing relative locations of the subfornical organ (SFO) and the arcuate nucleus of the hypothalamus (Arc). Bottom: In the SFO, nNOS+ and VGAT+ neurons have opposing effects on water ingestion. nNOS+ neurons promote water ingestion, while VGAT+ neurons suppress this behavior. A similar circuit logic exists in the Arc to regulate food ingestion. Here, AgRP+ neurons promote food ingestion while POMC+ neurons suppress food ingestion.

Figure 3.2

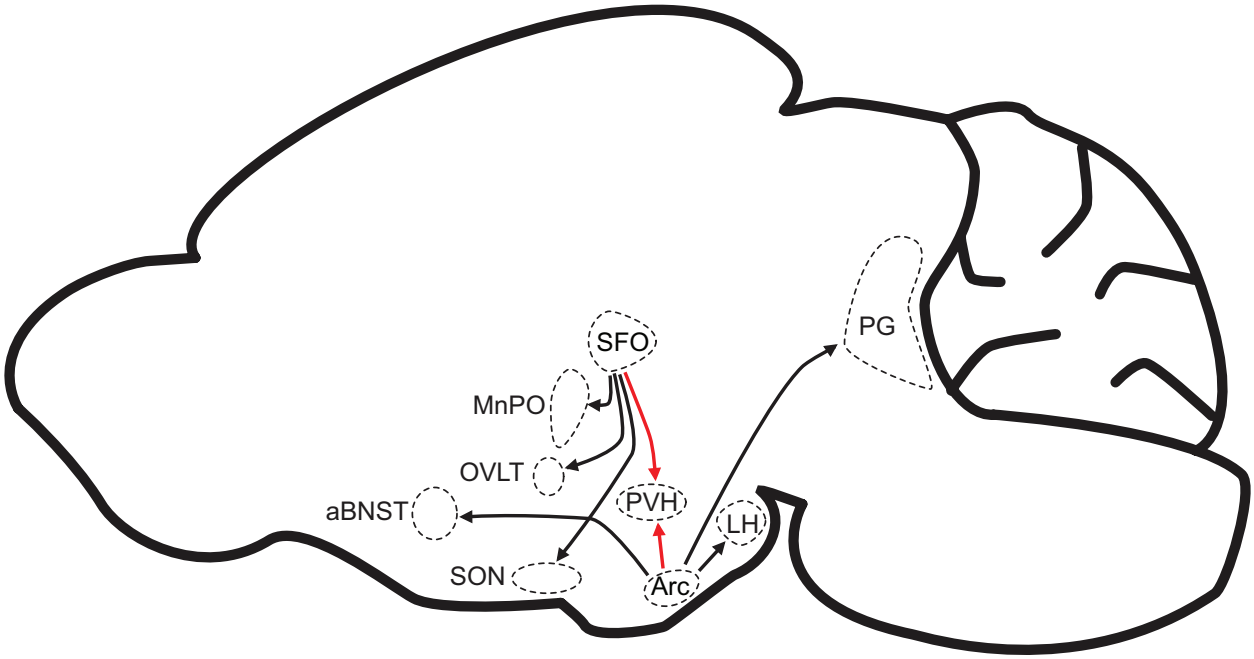

Figure 3.2 Neural connectivity among regions involved in food and water ingestion in the mouse brain
Axonal projections that link brain areas implicated in food and water ingestion are highlighted in red. SFO, subfornical organ; Arc, arcuate nucleus; PVH, paraventricular hypothalamus; LH, lateral hypothalamus; PG, periaqueductal grey; OVLT, organum vasculosum of the lamina terminalis; MnPO, median preoptic nucleus; SON, supraoptic nucleus; aBNST, anterior subdivisions of the bed nucleus of the stria terminalis.

Figure 3.3

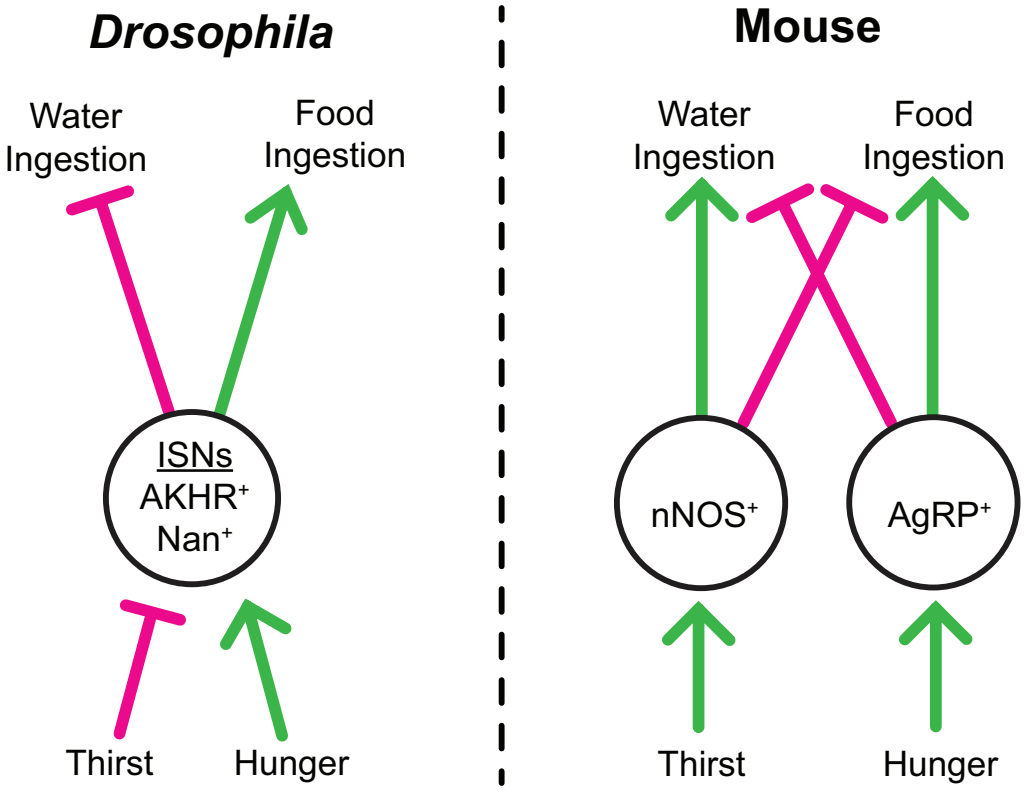

Figure 3.3 Neurons with opposing effects on food and water ingestion in *Drosophila* and mammals

In *Drosophila*, ISNs concurrently sense internal signals of both thirst (hemolymph osmolarity) and hunger (AKH) via the AKH receptor AKHR and the osmolarity sensor Nanchung (Nan). Activity in ISNs is sufficient both to promote food ingestion and inhibit water ingestion. In mammals, distinct populations in the subfornical organ (nNOS+ neurons) and arcuate nucleus of the hypothalamus (AgRP+ neurons) are specifically sensitive to internal signals of thirst and hunger, respectively. However, each of these populations is sufficient to influence both food and water ingestion, and they do this by promoting one of these behaviors and suppressing the other. Other neurons in the mammalian brain may concurrently sense signals of thirst and hunger.

Table 3.1

Table 1: Molecules proposed to signal hunger and satiety in flies and mammals

Signal	Organism	Homologs?	Proposed Site of Action	References
glucose	Mouse Human *Drosophila*	n/a	In mammals, multiple hypothalamic brain regions. In insects, the *pars intercerebralis*.	(*97, 133*)
fructose	*Drosophila*	n/a	*pars intercerebralis*	(*28*)
amino acids	Mouse *Drosophila*	n/a	In mammals, piriform cortex, although this has been debated (see (*101*)). In *Drosophila* larvae, dopaminergic neurons.	(*92, 99, 101*)
blood osmolarity	Rat *Drosophila*	n/a	In mammals, circumventricular organs. In insects, ISNs.	(*80, 134*)
cholecystokinin (CCK)	Mouse Human	Drosulfakinin	Multiple brain regions, including cortex and olfactory bulb.	(*82, 102, 135-137*)
ghrelin	Mouse Human	No invertebrate homologs characterized.	AgRP neurons in the Arcuate Nucleus of the hypothalamus, subfornical organ.	(*128, 138-140*)
leptin	Mouse Human	unpaired-2	POMC neurons in the Arcuate Nucleus of the hypothalamus.	(*111, 141*)
insulin	Mouse Human *Drosophila*	insulin-like peptides 1-8.	In insects, the *pars intercerebralis*. Broad expression of insulin receptors in the mammalian brain.	(*62, 82, 140, 142*)
glucagon-like peptide 1	Mouse	No invertebrate homologs characterized.	Vagus nerve; nucleus of the solitary tract.	(*143-146*)
corticotropin releasing hormone (CRH)	Mouse Human	diuretic hormone 44	Ventromedial hypothalamus.	(*147-149*)
urocortin	Mouse	No invertebrate homologs characterized.	Urocortin belongs to the CRH family and binds CRH receptors.	(*150*)
agouti related protein	Mouse	No invertebrate homologs characterized.	Arcuate Nucleus	(*151, 152*)
neuropeptide Y	Mouse	No invertebrate homologs characterized.	NPY-receptor is highly expressed in NPY/AgRP neurons.	(*153-156*)
Peptide YY	Mouse	No invertebrate homologs characterized.	Peptide YY binds neuropeptide Y receptor.	(*156*)
orexin (aka hypocretin)	Mouse	No invertebrate homologs characterized.	Ventromedial hypothalamus; Paraventricular hypothalamus	(*157, 158*)

Table 1: Molecules proposed to signal hunger and satiety in flies and mammals (continued)

alpha-melanocyte stimulating hormone	Mouse	No invertebrate homologs characterized.	Multiple sites of action including hypothalamus.	(*159-161*)
amylin	Mouse	No invertebrate homologs characterized.	Multiple sites of action including circumventricular organs	(*162-165*)
galanin	Mouse	No invertebrate homologs characterized.	Multiple sites of action including hypothalamus.	(*161*)
melanin-concentrating hormone	Mouse	No invertebrate homologs characterized.	Multiple sites of action including hypothalamus.	(*159, 161*)
cocaine/amphetamine-regulated transcript	Mouse	No invertebrate homologs characterized.	Receptors not yet identified	(*161, 166*)
neuromedin U	Rat	hugin	Multiple sites of action including hypo-thalamus.	(*167, 168*)
adipokinetic hormone (AKH)	*Drosophila*	glucagon	ISNs	(*40, 80*)
drosulfakinin	*Drosophila*	cholecystokinin	Not yet characterized.	(*82*)
allatostatin A	*Drosophila*	galanin	Not yet characterized.	(*64, 169*)
hugin	*Drosophila*	neuromedin U	Multiple sites of action including neuropeptide producing neurons.	(*83, 170*)
short neuropeptide F	*Drosophila*	No vertebrate homologs characterized.	Multiple sites of action including subesophegeal zone.	(*120, 171*)
leucokinin	*Drosophila*	No vertebrate homologs characterized.	Malpighian tubule, multiple central brain neurons including fan shaped body.	(*172*)
diuretic hormone 44	*Drosophila*	CRH	*pars intercerebralis*	(*21*)
CCH-amide-2	*Drosophila*	No vertebrate homologs characterized.	Not yet characterized.	(*173*)
Unpaired-2	*Drosophila*	leptin	GABAergic neurons innervating *pars intercerebralis*	(*22*)

References

1. Aristotle. (Oxford: Clarendon Press, 1908), vol. 3.
2. H. F. Judson, *The 8th Day of Creation*. (Simon and Schuster, New York, 1979).
3. U. Alon, *An Introduction to Systems Biology: Design Principles of Biological Circuits*. (Chapman and Hall, Boca Raton, 2007).
4. L. T. a. E. Zeiger, *Plant Physiology*. (Sinauer Associates, ed. 5, 2010).
5. H. K. Laualee Sherwood, and Paul Yancey, *Animal Physiology: From Genes to Organisms*. (Brooks Cole, U.S.A, ed. 2, 2012).
6. H. Modell *et al.*, A physiologist's view of homeostasis. *Adv Physiol Educ* **39**, 259-266 (2015).
7. W. Cannon, *The Wisdom of the Body*. (W.W. Norton and Co., New York, ed. 2, 1939).
8. S. J. Cooper, From Claude Bernard to Walter Cannon. Emergence of the concept of homeostasis. *Appetite* **51**, 419-427 (2008).
9. K. Lorenz, Leyhausen P., *Motivation of Human and and Animal Behavior*. (Van Nostrand Reinhold Company, New York, 1973).
10. C. Hull, *Principles of Behavior*. (D. Appleton-Century Co., New York, 1943).
11. E. Tolman, *Purposive Behavior in Animals and Men*. (The Century Co., New York, 1932).
12. D. J. Anderson, Circuit modules linking internal states and social behaviour in flies and mice. *Nat Rev Neurosci* **17**, 692-704 (2016).
13. N. Jourjine, Hunger and thirst interact to regulate ingestive behavior in flies and mammals. *Bioessays* **39**, (2017).
14. G. E. Haley, F. W. Flynn, Tachykinin neurokinin 3 receptor signaling in cholecystokinin-elicited release of oxytocin and vasopressin. *Am J Physiol Regul Integr Comp Physiol* **294**, R1760-1767 (2008).
15. C. W. Bourque, Central mechanisms of osmosensation and systemic osmoregulation. *Nature reviews* **9**, 519-531 (2008).
16. S. M. Sternson, Hypothalamic survival circuits: blueprints for purposive behaviors. *Neuron* **77**, 810-824 (2013).
17. Y. Chen, Y. C. Lin, T. W. Kuo, Z. A. Knight, Sensory detection of food rapidly modulates arcuate feeding circuits. *Cell* **160**, 829-841 (2015).
18. S. Lin *et al.*, Neural correlates of water reward in thirsty Drosophila. *Nat Neurosci* **17**, 1536-1542 (2014).
19. A. H. Pool, K. Scott, Feeding regulation in Drosophila. *Curr Opin Neurobiol* **29**, 57-63 (2014).
20. Y. Yu *et al.*, Regulation of starvation-induced hyperactivity by insulin and glucagon signaling in adult Drosophila. *Elife* **5**, (2016).
21. M. Dus *et al.*, Nutrient Sensor in the Brain Directs the Action of the Brain-Gut Axis in Drosophila. *Neuron* **87**, 139-151 (2015).
22. A. Rajan, N. Perrimon, Drosophila cytokine unpaired 2 regulates physiological homeostasis by remotely controlling insulin secretion. *Cell* **151**, 123-137 (2012).
23. D. R. Nassel, A. M. Winther, Drosophila neuropeptides in regulation of physiology and behavior. *Prog Neurobiol* **92**, 42-104 (2010).
24. J. P. Paluzzi, M. Vanderveken, M. J. O'Donnell, The heterodimeric glycoprotein hormone, GPA2/GPB5, regulates ion transport across the hindgut of the adult mosquito, Aedes aegypti. *PLoS One* **9**, e86386 (2014).

25. Y. Liu, J. Luo, M. A. Carlsson, D. R. Nässel, Serotonin and insulin-like peptides modulate leucokinin-producing neurons that affect feeding and water homeostasis in Drosophila. *Journal of Comparative Neurology* **523**, 1840-1863 (2015).
26. S. Terhzaz *et al.*, Mechanism and function of Drosophila capa GPCR: a desiccation stress-responsive receptor with functional homology to human neuromedinU receptor. *PLoS One* **7**, e29897 (2012).
27. M. Prager-Khoutorsky, C. W. Bourque, Osmosensation in vasopressin neurons: changing actin density to optimize function. *Trends in neurosciences* **33**, 76-83 (2010).
28. T. Miyamoto, J. Slone, X. Song, H. Amrein, A fructose receptor functions as a nutrient sensor in the Drosophila brain. *Cell* **151**, 1113-1125 (2012).
29. C. M. Root, K. I. Ko, A. Jafari, J. W. Wang, Presynaptic facilitation by neuropeptide signaling mediates odor-driven food search. *Cell* **145**, 133-144 (2011).
30. M. Bjordal, N. Arquier, J. Kniazeff, J. P. Pin, P. Leopold, Sensing of amino acids in a dopaminergic circuitry promotes rejection of an incomplete diet in Drosophila. *Cell* **156**, 510-521 (2014).
31. V. G. Dethier, *The Hungry Fly*. (Harvard University Press, Cambridge, MA, 1976).
32. D. M. Gohl *et al.*, A versatile in vivo system for directed dissection of gene expression patterns. *Nature methods* **8**, 231-237 (2011).
33. F. N. Hamada *et al.*, An internal thermal sensor controlling temperature preference in Drosophila. *Nature* **454**, 217-220 (2008).
34. J. D. Clyne, G. Miesenbock, Sex-specific control and tuning of the pattern generator for courtship song in Drosophila. *Cell* **133**, 354-363 (2008).
35. A. Jenett *et al.*, A GAL4-driver line resource for Drosophila neurobiology. *Cell Rep* **2**, 991-1001 (2012).
36. E. Z. Kvon *et al.*, Genome-scale functional characterization of Drosophila developmental enhancers in vivo. *Nature* **512**, 91-95 (2014).
37. D. T. Harris, B. R. Kallman, B. C. Mullaney, K. Scott, Representations of Taste Modality in the Drosophila Brain. *Neuron* **86**, 1449-1460 (2015).
38. T. W. Chen *et al.*, Ultrasensitive fluorescent proteins for imaging neuronal activity. *Nature* **499**, 295-300 (2013).
39. K. N. Bharucha, P. Tarr, S. L. Zipursky, A glucagon-like endocrine pathway in Drosophila modulates both lipid and carbohydrate homeostasis. *The Journal of experimental biology* **211**, 3103-3110 (2008).
40. G. Lee, J. H. Park, Hemolymph sugar homeostasis and starvation-induced hyperactivity affected by genetic manipulations of the adipokinetic hormone-encoding gene in Drosophila melanogaster. *Genetics* **167**, 311-323 (2004).
41. S. K. Kim, E. J. Rulifson, Conserved mechanisms of glucose sensing and regulation by Drosophila corpora cardiaca cells. *Nature* **431**, 316-320 (2004).
42. D. J. Candy, Adipokinetic hormones concentrations in the haemolymph of Schistocerca gregaria, measured by radioimmunoassay. *Insect biochemistry and molecular biology* **32**, 1361-1367 (2002).
43. P. Cameron, M. Hiroi, J. Ngai, K. Scott, The molecular basis for water taste in Drosophila. *Nature* **465**, 91-95 (2010).
44. Z. Chen, Q. Wang, Z. Wang, The amiloride-sensitive epithelial Na+ channel PPK28 is essential for drosophila gustatory water reception. *J Neurosci* **30**, 6247-6252 (2010).

45. A. Sellami, H. J. Agricola, J. A. Veenstra, Neuroendocrine cells in Drosophila melanogaster producing GPA2/GPB5, a hormone with homology to LH, FSH and TSH. *Gen Comp Endocrinol* **170**, 582-588 (2011).
46. J. Kim *et al.*, A TRPV family ion channel required for hearing in Drosophila. *Nature* **424**, 81-84 (2003).
47. L. Liu *et al.*, Drosophila hygrosensation requires the TRP channels water witch and nanchung. *Nature* **450**, 294-298 (2007).
48. Z. Gong *et al.*, Two interdependent TRPV channel subunits, inactive and Nanchung, mediate hearing in Drosophila. *J Neurosci* **24**, 9059-9066 (2004).
49. W. Zhang, Z. Yan, L. Y. Jan, Y. N. Jan, Sound response mediated by the TRP channels NOMPC, NANCHUNG, and INACTIVE in chordotonal organs of Drosophila larvae. *Proceedings of the National Academy of Sciences of the United States of America* **110**, 13612-13617 (2013).
50. W. Liedtke, D. M. Tobin, C. I. Bargmann, J. M. Friedman, Mammalian TRPV4 (VR-OAC) directs behavioral responses to osmotic and mechanical stimuli in Caenorhabditis elegans. *Proceedings of the National Academy of Sciences of the United States of America* **100 Suppl 2**, 14531-14536 (2003).
51. S. Ciura, W. Liedtke, C. W. Bourque, Hypertonicity sensing in organum vasculosum lamina terminalis neurons: a mechanical process involving TRPV1 but not TRPV4. *J Neurosci* **31**, 14669-14676 (2011).
52. H. A. Colbert, T. L. Smith, C. I. Bargmann, OSM-9, a novel protein with structural similarity to channels, is required for olfaction, mechanosensation, and olfactory adaptation in Caenorhabditis elegans. *J Neurosci* **17**, 8259-8269 (1997).
53. W. Liedtke, J. M. Friedman, Abnormal osmotic regulation in trpv4-/- mice. *Proc Natl Acad Sci U S A* **100**, 13698-13703 (2003).
54. L. Jin *et al.*, Single action potentials and subthreshold electrical events imaged in neurons with a fluorescent protein voltage probe. *Neuron* **75**, 779-785 (2012).
55. J. Na *et al.*, A Drosophila model of high sugar diet-induced cardiomyopathy. *PLoS genetics* **9**, e1003175 (2013).
56. A. Arav, B. Rubinsky, Temperature gradient osmometer and anomalies in freezing temperatures. *The American journal of physiology* **267**, R1646-1652 (1994).
57. M. A. Albers, T. J. Bradley, Osmotic regulation in adult Drosophila melanogaster during dehydration and rehydration. *The Journal of experimental biology* **207**, 2313-2321 (2004).
58. S. Limmer, A. Weiler, A. Volkenhoff, F. Babatz, C. Klambt, The Drosophila blood-brain barrier: development and function of a glial endothelium. *Front Neurosci* **8**, 365 (2014).
59. Y. G. a. M. Krausz, Regulation of food and water intake in rats as related to plasma osmolarity and volume. *Physiol Behav* **4**, 311-313 (1969).
60. E. G. Mietlicki, E. L. Nowak, D. Daniels, The effect of ghrelin on water intake during dipsogenic conditions. *Physiol Behav* **96**, 37-43 (2009).
61. C. J. Burke *et al.*, Layered reward signalling through octopamine and dopamine in Drosophila. *Nature* **492**, 433-437 (2012).
62. Y. Liu, J. Luo, M. A. Carlsson, D. R. Nässel, Serotonin and insulin-like peptides modulate leucokinin-producing neurons that affect feeding and water homeostasis in Drosophila. *J Comp Neurol* **523**, 1840-1863 (2015).

63. C. Liu *et al.*, A subset of dopamine neurons signals reward for odour memory in Drosophila. *Nature* **488**, 512-516 (2012).
64. A. C. Hergarden, T. D. Tayler, D. J. Anderson, Allatostatin-A neurons inhibit feeding behavior in adult Drosophila. *Proc Natl Acad Sci U S A* **109**, 3967-3972 (2012).
65. H. K. Inagaki *et al.*, Visualizing neuromodulation in vivo: TANGO-mapping of dopamine signaling reveals appetite control of sugar sensing. *Cell* **148**, 583-595 (2012).
66. H. K. Inagaki, K. M. Panse, D. J. Anderson, Independent, reciprocal neuromodulatory control of sweet and bitter taste sensitivity during starvation in Drosophila. *Neuron* **84**, 806-820 (2014).
67. S. Marella, K. Mann, K. Scott, Dopaminergic modulation of sucrose acceptance behavior in Drosophila. *Neuron* **73**, 941-950 (2012).
68. J. W. Wang, A. M. Wong, J. Flores, L. B. Vosshall, R. Axel, Two-photon calcium imaging reveals an odor-evoked map of activity in the fly brain. *Cell* **112**, 271-282 (2003).
69. D. G. Baskin, T. M. Hahn, M. W. Schwartz, Leptin sensitive neurons in the hypothalamus. *Horm Metab Res* **31**, 345-350 (1999).
70. M. De Ambrogi, S. Volpe, C. Tamanini, Ghrelin: central and peripheral effects of a novel peptydil hormone. *Med Sci Monit* **9**, RA217-224 (2003).
71. S. Y. Takemura *et al.*, A visual motion detection circuit suggested by Drosophila connectomics. *Nature* **500**, 175-181 (2013).
72. W. C. Lee *et al.*, Anatomy and function of an excitatory network in the visual cortex. *Nature* **532**, 370-374 (2016).
73. J. G. White, E. Southgate, J. N. Thomson, S. Brenner, The structure of the nervous system of the nematode Caenorhabditis elegans. *Philos Trans R Soc Lond B Biol Sci* **314**, 1-340 (1986).
74. E. M. Callaway, Transneuronal circuit tracing with neurotropic viruses. *Curr Opin Neurobiol* **18**, 617-623 (2008).
75. C. A. Zimmerman *et al.*, Thirst neurons anticipate the homeostatic consequences of eating and drinking. *Nature* **537**, 680-684 (2016).
76. J. N. Betley, Z. F. Cao, K. D. Ritola, S. M. Sternson, Parallel, redundant circuit organization for homeostatic control of feeding behavior. *Cell* **155**, 1337-1350 (2013).
77. Y. Mandelblat-Cerf *et al.*, Arcuate hypothalamic AgRP and putative POMC neurons show opposite changes in spiking across multiple timescales. *Elife* **4**, (2015).
78. A. S. Garfield *et al.*, Dynamic GABAergic afferent modulation of AgRP neurons. *Nat Neurosci* **19**, 1628-1635 (2016).
79. Z. Zheng *et al.*, A Complete Electron Microscopy Volume Of The Brain Of Adult Drosophila melanogaster. *bioRxiv*, (2017).
80. N. Jourjine, B. C. Mullaney, K. Mann, K. Scott, Coupled Sensing of Hunger and Thirst Signals Balances Sugar and Water Consumption. *Cell* **166**, 855-866 (2016).
81. D. R. Nassel, J. Vanden Broeck, Insulin/IGF signaling in Drosophila and other insects: factors that regulate production, release and post-release action of the insulin-like peptides. *Cell Mol Life Sci* **73**, 271-290 (2016).
82. J. A. Soderberg, M. A. Carlsson, D. R. Nassel, Insulin-Producing Cells in the Drosophila Brain also Express Satiety-Inducing Cholecystokinin-Like Peptide, Drosulfakinin. *Front Endocrinol (Lausanne)* **3**, 109 (2012).

83. R. Bader *et al.*, Genetic dissection of neural circuit anatomy underlying feeding behavior in Drosophila: distinct classes of hugin-expressing neurons. *J Comp Neurol* **502**, 848-856 (2007).
84. N. C. Klapoetke *et al.*, Independent optical excitation of distinct neural populations. *Nat Methods* **11**, 338-346 (2014).
85. M. Talay *et al.*, Transsynaptic Mapping of Second-Order Taste Neurons in Flies by trans-Tango. *Neuron* **96**, 783-795 e784 (2017).
86. C. Choi *et al.*, Autoreceptor control of peptide/neurotransmitter corelease from PDF neurons determines allocation of circadian activity in drosophila. *Cell Rep* **2**, 332-344 (2012).
87. N. X. Tritsch, A. J. Granger, B. L. Sabatini, Mechanisms and functions of GABA co-release. *Nat Rev Neurosci* **17**, 139-145 (2016).
88. J. Kim, T. P. Neufeld, Dietary sugar promotes systemic TOR activation in Drosophila through AKH-dependent selective secretion of Dilp3. *Nat Commun* **6**, 6846 (2015).
89. Y. Liu, J. Luo, M. A. Carlsson, D. R. Nässel, Serotonin and insulin-like peptides modulate leucokinin-producing neurons that affect feeding and water homeostasis in Drosophila. *Journal of Comparative Neurology* **523**, 1840-1863 (2015).
90. M. Zandawala, R. Marley, S. A. Davies, D. R. Nassel, Characterization of a set of abdominal neuroendocrine cells that regulate stress physiology using colocalized diuretic peptides in Drosophila. *Cell Mol Life Sci*, (2017).
91. S. A. Davies *et al.*, Signaling by Drosophila capa neuropeptides. *Gen Comp Endocrinol* **188**, 60-66 (2013).
92. M. Bjordal, N. Arquier, J. Kniazeff, J. P. Pin, P. Léopold, Sensing of amino acids in a dopaminergic circuitry promotes rejection of an incomplete diet in Drosophila. *Cell* **156**, 510-521 (2014).
93. E. A. Pnevmatikakis, A. Giovannucci, NoRMCorre: An online algorithm for piecewise rigid motion correction of calcium imaging data. *J Neurosci Methods* **291**, 83-94 (2017).
94. K. C. Berridge, Motivation concepts in behavioral neuroscience. *Physiol Behav* **81**, 179-209 (2004).
95. K. L. a. P. Leyhausen, *Motivation of Human and and Animal Behavior*. (Van Nostrand Reinhold Company, 1973).
96. N. Tinbergen, *The Study of Instinct*. (Clarendon Press, 1951).
97. J. Mayer, Glucostatic mechanism of regulation of food intake. 1953. *Obes Res* **4**, 493-496 (1996).
98. Y. P. Zhan, L. Liu, Y. Zhu, Taotie neurons regulate appetite in Drosophila. *Nat Commun* **7**, 13633 (2016).
99. S. Hao *et al.*, Uncharged tRNA and sensing of amino acid deficiency in mammalian piriform cortex. *Science* **307**, 1776-1778 (2005).
100. A. C. Maurin *et al.*, The GCN2 kinase biases feeding behavior to maintain amino acid homeostasis in omnivores. *Cell Metab* **1**, 273-277 (2005).
101. D. E. Leib, Z. A. Knight, Rapid Sensing of Dietary Amino Acid Deficiency Does Not Require GCN2. *Cell Rep* **16**, 2051-2052 (2016).
102. J. Gibbs, R. C. Young, G. P. Smith, Cholecystokinin elicits satiety in rats with open gastric fistulas. *Nature* **245**, 323-325 (1973).
103. G. S. Barsh, M. W. Schwartz, Genetic approaches to studying energy balance: perception and integration. *Nat Rev Genet* **3**, 589-600 (2002).

104. M. W. Schwartz, S. C. Woods, D. Porte, Jr., R. J. Seeley, D. G. Baskin, Central nervous system control of food intake. *Nature* **404**, 661-671 (2000).
105. S. C. Woods, R. J. Seeley, D. Porte, Jr., M. W. Schwartz, Signals that regulate food intake and energy homeostasis. *Science* **280**, 1378-1383 (1998).
106. B. J. R. a. E. T. Rolls, *Thirst*. (Cambridge University Press, 1982).
107. E. B. VERNEY, The antidiuretic hormone and the factors which determine its release. *Proc R Soc Lond B Biol Sci* **135**, 25-106 (1947).
108. C. Gizowski, C. Zaelzer, C. W. Bourque, Clock-driven vasopressin neurotransmission mediates anticipatory thirst prior to sleep. *Nature* **537**, 685-688 (2016).
109. R. F. Chapman, *The Insects: Structure and Function*. (Cambridge University Press, ed. 5, 2013).
110. V. G. Dethier, *The Hungry Fly: a Physiological Study of the Behavior Associated With Feeding*. (Harvard University Press, 1976).
111. Y. Mandelblat-Cerf *et al.*, Bidirectional Anticipation of Future Osmotic Challenges by Vasopressin Neurons. *Neuron* **93**, 57-65 (2017).
112. C. J. Burnett *et al.*, Hunger-Driven Motivational State Competition. *Neuron* **92**, 187-201 (2016).
113. B. G. Stanley, L. H. Ha, L. C. Spears, M. G. Dee, 2nd, Lateral hypothalamic injections of glutamate, kainic acid, D,L-alpha-amino-3-hydroxy-5-methyl-isoxazole propionic acid or N-methyl-D-aspartic acid rapidly elicit intense transient eating in rats. *Brain Res* **613**, 88-95 (1993).
114. A. W. H. a. S. W. Ranson, Hypothalamic lesions and adiposity in the rat. *Anat. Rec.* **78**, 149-172 (1940).
115. J. K. Elmquist, C. F. Elias, C. B. Saper, From lesions to leptin: hypothalamic control of food intake and body weight. *Neuron* **22**, 221-232 (1999).
116. S. Luquet, F. A. Perez, T. S. Hnasko, R. D. Palmiter, NPY/AgRP neurons are essential for feeding in adult mice but can be ablated in neonates. *Science* **310**, 683-685 (2005).
117. Y. Aponte, D. Atasoy, S. M. Sternson, AGRP neurons are sufficient to orchestrate feeding behavior rapidly and without training. *Nat Neurosci* **14**, 351-355 (2011).
118. M. J. Krashes *et al.*, Rapid, reversible activation of AgRP neurons drives feeding behavior in mice. *J Clin Invest* **121**, 1424-1428 (2011).
119. C. Zhan *et al.*, Acute and long-term suppression of feeding behavior by POMC neurons in the brainstem and hypothalamus, respectively. *J Neurosci* **33**, 3624-3632 (2013).
120. M. A. Carlsson, L. E. Enell, D. R. Nässel, Distribution of short neuropeptide F and its receptor in neuronal circuits related to feeding in larval Drosophila. *Cell Tissue Res* **353**, 511-523 (2013).
121. Y. Oka, M. Ye, C. S. Zuker, Thirst driving and suppressing signals encoded by distinct neural populations in the brain. *Nature* **520**, 349-352 (2015).
122. V. Perttunen, H. Erkkila, Humidity reaction in Drosophila melanogaster. *Nature* **169**, 78 (1952).
123. E. E. LeDue *et al.*, Starvation-Induced Depotentiation of Bitter Taste in Drosophila. *Curr Biol* **26**, 2854-2861 (2016).
124. E. Soria-Gómez *et al.*, The endocannabinoid system controls food intake via olfactory processes. *Nat Neurosci* **17**, 407-415 (2014).

125. S. Hsiao, F. Trankina, Thirst-hunger interaction. I. Effects of body-fluid restoration on food and water intake in water-deprived rats. *J Comp Physiol Psychol* **69**, 448-453 (1969).
126. S. H. a. E. R. Smutz, Thirst-reducing and hunger-inducing effects of water and saline by stomach-tubing vs. drinking in rats. *Psychobiology* **4**, (1976).
127. S. N. Thornton, Thirst and hydration: physiology and consequences of dysfunction. *Physiol Behav* **100**, 15-21 (2010).
128. A. V. Ferguson, in *Neurobiology of Body Fluid Homeostasis: Transduction and Integration,* L. A. De Luca, Jr., J. V. Menani, A. K. Johnson, Eds. (Boca Raton (FL), 2014).
129. N. Medeiros, L. Dai, A. V. Ferguson, Glucose-responsive neurons in the subfornical organ of the rat--a novel site for direct CNS monitoring of circulating glucose. *Neuroscience* **201**, 157-165 (2012).
130. A. Mimee, P. M. Smith, A. V. Ferguson, Circumventricular organs: targets for integration of circulating fluid and energy balance signals? *Physiol Behav* **121**, 96-102 (2013).
131. C. Sherington, *The Integrative Action of the Nervous System*. (Yale University Press, 1906).
132. K. J. Pulman, W. M. Fry, G. T. Cottrell, A. V. Ferguson, The subfornical organ: a central target for circulating feeding signals. *J Neurosci* **26**, 2022-2030 (2006).
133. L. Steinbusch, G. Labouebe, B. Thorens, Brain glucose sensing in homeostatic and hedonic regulation. *Trends Endocrinol Metab* **26**, 455-466 (2015).
134. Y. G. a. M. Krausz, Regulation of food and water intake in rats as related to plasma osmolarity and volume *Physiol Behav* **4**, 311-313 (1969).
135. A. Saito, H. Sankaran, I. D. Goldfine, J. A. Williams, Cholecystokinin receptors in the brain: characterization and distribution. *Science* **208**, 1155-1156 (1980).
136. L. P. Wennogle, D. J. Steel, B. Petrack, Characterization of central cholecystokinin receptors using a radioiodinated octapeptide probe. *Life Sci* **36**, 1485-1492 (1985).
137. J. Ma, L. Dankulich-Nagrudny, G. Lowe, Cholecystokinin: an excitatory modulator of mitral/tufted cells in the mouse olfactory bulb. *PLoS One* **8**, e64170 (2013).
138. M. Kojima *et al.*, Ghrelin is a growth-hormone-releasing acylated peptide from stomach. *Nature* **402**, 656-660 (1999).
139. M. Nakazato *et al.*, A role for ghrelin in the central regulation of feeding. *Nature* **409**, 194-198 (2001).
140. J. D. Kim, S. Leyva, S. Diano, Hormonal regulation of the hypothalamic melanocortin system. *Front Physiol* **5**, 480 (2014).
141. J. L. Halaas *et al.*, Weight-reducing effects of the plasma protein encoded by the obese gene. *Science* **269**, 543-546 (1995).
142. Q. Wu, Y. Zhang, J. Xu, P. Shen, Regulation of hunger-driven behaviors by neural ribosomal S6 kinase in Drosophila. *Proc Natl Acad Sci U S A* **102**, 13289-13294 (2005).
143. A. Flint, A. Raben, A. Astrup, J. J. Holst, Glucagon-like peptide 1 promotes satiety and suppresses energy intake in humans. *J Clin Invest* **101**, 515-520 (1998).
144. L. B. Knudsen, A. Secher, J. Hecksher-Sorensen, C. Pyke, Long-acting glucagon-like peptide-1 receptor agonists have direct access to and effects on pro-opiomelanocortin/cocaine- and amphetamine-stimulated transcript neurons in the mouse hypothalamus. *J Diabetes Investig* **7 Suppl 1**, 56-63 (2016).

145. M. R. Hayes, B. C. De Jonghe, S. E. Kanoski, Role of the glucagon-like-peptide-1 receptor in the control of energy balance. *Physiol Behav* **100**, 503-510 (2010).
146. E. K. Williams *et al.*, Sensory Neurons that Detect Stretch and Nutrients in the Digestive System. *Cell* **166**, 209-221 (2016).
147. S. C. Heinrichs, F. Menzaghi, E. M. Pich, R. L. Hauger, G. F. Koob, Corticotropin-releasing factor in the paraventricular nucleus modulates feeding induced by neuropeptide Y. *Brain Res* **611**, 18-24 (1993).
148. P. Chen, C. V. Hover, D. Lindberg, C. Li, Central urocortin 3 and type 2 corticotropin-releasing factor receptor in the regulation of energy homeostasis: critical involvement of the ventromedial hypothalamus. *Front Endocrinol (Lausanne)* **3**, 180 (2012).
149. D. Richard, Q. Lin, E. Timofeeva, The corticotropin-releasing factor family of peptides and CRF receptors: their roles in the regulation of energy balance. *Eur J Pharmacol* **440**, 189-197 (2002).
150. M. Spina *et al.*, Appetite-suppressing effects of urocortin, a CRF-related neuropeptide. *Science* **273**, 1561-1564 (1996).
151. M. Graham, J. R. Shutter, U. Sarmiento, I. Sarosi, K. L. Stark, Overexpression of Agrt leads to obesity in transgenic mice. *Nat Genet* **17**, 273-274 (1997).
152. D. Huszar *et al.*, Targeted disruption of the melanocortin-4 receptor results in obesity in mice. *Cell* **88**, 131-141 (1997).
153. K. Tatemoto, M. Carlquist, V. Mutt, Neuropeptide Y--a novel brain peptide with structural similarities to peptide YY and pancreatic polypeptide. *Nature* **296**, 659-660 (1982).
154. J. T. Clark, P. S. Kalra, W. R. Crowley, S. P. Kalra, Neuropeptide Y and human pancreatic polypeptide stimulate feeding behavior in rats. *Endocrinology* **115**, 427-429 (1984).
155. J. W. Sohn, Network of hypothalamic neurons that control appetite. *BMB Rep* **48**, 229-233 (2015).
156. R. L. Batterham *et al.*, Gut hormone PYY(3-36) physiologically inhibits food intake. *Nature* **418**, 650-654 (2002).
157. J. Hara *et al.*, Genetic ablation of orexin neurons in mice results in narcolepsy, hypophagia, and obesity. *Neuron* **30**, 345-354 (2001).
158. T. Sakurai, Orexins and orexin receptors: implication in feeding behavior. *Regul Pept* **85**, 25-30 (1999).
159. D. S. Ludwig *et al.*, Melanin-concentrating hormone: a functional melanocortin antagonist in the hypothalamus. *Am J Physiol* **274**, E627-633 (1998).
160. A. N. Eberle, *The Melanotropins. Chemistry, Physiology, and Mechanism of Action*. (Karger, 1988).
161. J. A. Parker, S. R. Bloom, Hypothalamic neuropeptides and the regulation of appetite. *Neuropharmacology* **63**, 18-30 (2012).
162. Z. Li, L. Kelly, M. Heiman, P. Greengard, J. M. Friedman, Hypothalamic Amylin Acts in Concert with Leptin to Regulate Food Intake. *Cell Metab* **22**, 1059-1067 (2015).
163. E. G. Mietlicki-Baase, D. R. Olivos, B. A. Jeffrey, M. R. Hayes, Cooperative interaction between leptin and amylin signaling in the ventral tegmental area for the control of food intake. *Am J Physiol Endocrinol Metab* **308**, E1116-1122 (2015).
164. J. E. Morley, J. F. Flood, Amylin decreases food intake in mice. *Peptides* **12**, 865-869 (1991).

165. E. G. Mietlicki-Baase, M. R. Hayes, Amylin activates distributed CNS nuclei to control energy balance. *Physiol Behav* **136**, 39-46 (2014).
166. P. Kristensen *et al.*, Hypothalamic CART is a new anorectic peptide regulated by leptin. *Nature* **393**, 72-76 (1998).
167. D. A. Bechtold, T. R. Ivanov, S. M. Luckman, Appetite-modifying actions of pro-neuromedin U-derived peptides. *Am J Physiol Endocrinol Metab* **297**, E545-551 (2009).
168. P. J. Brighton, P. G. Szekeres, G. B. Willars, Neuromedin U and its receptors: structure, function, and physiological roles. *Pharmacol Rev* **56**, 231-248 (2004).
169. J. Chen *et al.*, Allatostatin A Signalling in Drosophila Regulates Feeding and Sleep and Is Modulated by PDF. *PLoS Genet* **12**, e1006346 (2016).
170. P. Schlegel *et al.*, Synaptic transmission parallels neuromodulation in a central food-intake circuit. *Elife* **5**, (2016).
171. K. S. Lee, K. H. You, J. K. Choo, Y. M. Han, K. Yu, Drosophila short neuropeptide F regulates food intake and body size. *J Biol Chem* **279**, 50781-50789 (2004).
172. B. Al-Anzi *et al.*, The leucokinin pathway and its neurons regulate meal size in Drosophila. *Curr Biol* **20**, 969-978 (2010).
173. G. R. Ren *et al.*, CCHamide-2 Is an Orexigenic Brain-Gut Peptide in Drosophila. *PLoS One* **10**, e0133017 (2015).